CHALMERS
UNIVERSITY OF TECHNOLOGY

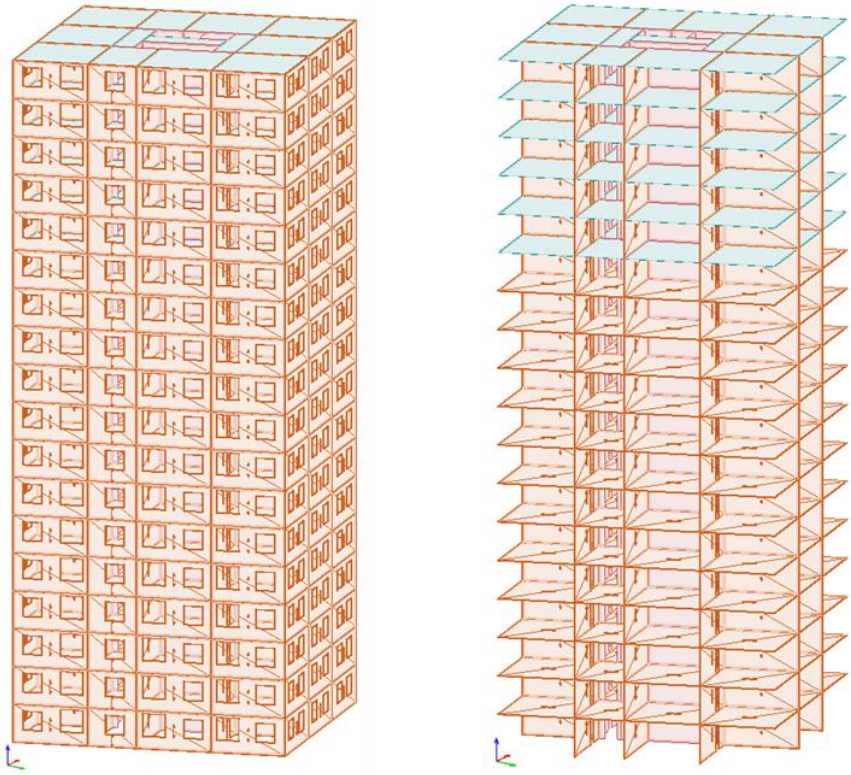

Strength of a Tower for a High-Rise Hybrid Timber Building

A study of how different parameters affect the dynamic performance of a building

Master's thesis in Structural Engineering and Building Technology

Mahmoud Alkhateb
Isak Kallmér

DEPARTMENT OF ARCHITECTURE AND CIVIL ENGINEERING

CHALMERS UNIVERSITY OF TECHNOLOGY
Gothenburg, Sweden 2024
www.chalmers.se

Master's thesis ACEX30

Strength of a Hybrid Tower for a High-Rise Timber Building

A study of how different parameters affect the dynamic performance of a building

Mahmoud Alkhateb
Isak Kallmér

CHALMERS
UNIVERSITY OF TECHNOLOGY

Department of Architecture and Civil Engineering
Division of Structural Engineering
Lightweight Structures
Chalmers University of Technology
Gothenburg, Sweden 2024

Strength of a Hybrid Tower for a High-Rise Timber Building
A study of how different parameters affect the dynamic performance of a building

Master's thesis in Structural Engineering and Building Technology

Mahmoud Alkhateb
Isak Kallmér

Supervisor: Robert Jockwer, Department of Architecture and Civil Engineering
Supervisor: Thomas Hallgren, COWI
Examiner: Robert Jockwer, Department of Architecture and Civil Engineering

Examensarbete ACEX30
Institutionen för arkitektur och samhällsbyggnadsteknik
Chalmers tekniska högskola, 2024

Department of Architecture and Civil Engineering
Division of Structural Engineering
Lightweight Structures
Chalmers University of Technology
SE-412 96 Gothenburg
Telephone +46 31 772 1000

Cover: FE-model obtained from FEM-Design software for a hybrid timber building with a concrete core and concrete slabs in the upper third of the building.

Department of Architecture and Civil Engineering
Gothenburg, Sweden 2024

Strength of a Hybrid Tower for a High-Rise Timber Building
A study of how different parameters affect the dynamic performance of a building
Master's thesis in Structural Engineering and Building Technology

Mahmoud Alkhateb
Isak Kallmér

Department of Architecture and Civil Engineering
Division of Structural Engineering
Lightweight Structures
Chalmers University of Technology

Abstract

One of the most common construction materials for tall buildings is concrete. Alternatives to concrete buildings are timber and hybrid buildings. Two main advantages of building in timber are that it is environmentally friendly and the strength-to-weight ratio is large. The main challenge is also tied to timber's lightweight nature, which significantly contributes to wind-induced accelerations. These accelerations have adverse effects on the occupants, leading to a threshold beyond which they become unacceptable. Another challenge arises from timber's inherent weakness compared to concrete, which implies that there may be a limit to the height a building can reach while maintaining reasonable dimensions.

The thesis investigates how different parameters affect the dynamic response of a tall building but also in relation to load-bearing capacity. The project was performed for a fictitious building with different structural systems. Both FE analyses and hand calculations were performed to verify the serviceability limit state criteria with a major focus on accelerations together with verifying the load-bearing capacity of the structural timber elements in a building.

The investigations showed that the dynamic performance of the building increased when the amount of concrete increased. The increase also resulted in an increased utilization ratio in the ultimate limit state. Based on the results, it was concluded that in most cases, it was the acceleration criterion that was the most critical in the design of a timber hybrid building. The main parameters determining the dynamic performance are the stiffness of the building and the equivalent mass. An increase in mass and possibly also the stiffness of the building will decrease the acceleration of the building. For example, thicker wall elements will contribute to larger mass and stiffness. The structural system with walls and slabs performed dynamically better than a beam and column system with less mass and stiffness, which becomes more prone to wind-induced vibrations.

Keywords: Hybrid building, Tall Hybrid Timber Building, CLT, Glulam, Structural Dynamcis, Wind Dynamcis, Finite Element Analysis, Acceleration, ULS, SLS.

Hållfastheten av höga hybridbyggnader i trä
En studie av hur olika parametrar påverkar den dynamiska prestandan av en byggnad.
Examensarbete inom Konstruktionsteknik och Byggnadsteknologi

Mahmoud Alkhateb
Isak Kallmér

Institutionen för arkitektur och samhällsbyggnadsteknik
Avdelningen för Konstruktionsteknik
Lättviktskonstruktioner
Chalmers tekniska högskola

Sammanfattning

Idag är det vanligaste byggnadsmaterialet i stomsystem för höga hus betong. Ett alternativ till betonghus är träbyggnader och hybridbyggnader. Att bygga i trä har flera fördelar. Två av dessa är att trä har en låg vikt i förhållande till bärförmåga och har miljömässiga fördelar. De utmaningar med att bygga högre hus i mer trä är att det lätta materialet bidrar också till stora accelrationer för höga hus som initieras av vinden. Dessa accelerationer påverkar kroppen negativt och därav måste accelrationen befinna sig innom gräns. En annan utmaning är att trä har en lägre bärförmåga jämfört med betong, vilket betyder att det kan finnas en gräns i hur hög en byggnad kan bli med rimliga dimensioner.

Examensarbetet utreder hur olika parametrar påverkar en byggnads respons för vinddynamik samt hur dess respons står i relation till bärförmågan. Projektet genomfördes för en fiktiv byggnad med olika stomsystem. FEM analyser och handberäkningar genomfördes för att verifiera accelrationskravet samt bärförmågan för de bärande elementen i trä.

Utredningarna visade att en ökad andel betong för den aktuella byggnaden förbättrade den dynamiska responsen. Det resulterade också i en ökande utnyttjandegrad i brottgränstillstånd. Baserat på resultaten kunde slutsatsen dras att det mest kritiska designkravet var accelration i de flesta fall. De paramentrar som främst avgör byggnadens dynamiska respons var ekvivalent massa och styvhet. Större massa och styvhet förbättrar accelrationerna för en byggnad. Exempelvis bidrar större bärande element till ökad massa och möjligen också styvhet. Ett stomsystem med bärande väggar och plattor visar sig vara ett bättre system än ett balk och pelare system utifrån ett vinddynamiskt system då ett balk och pelare system har lägre massa och styvhet.

Nyckelord: Hybridbyggnad, Höga byggnader, Träkonstruktioner, Vinddynamik, Korslimmat trä, Finita Element-analyser, Accelrationer, Brottgränstillstånd, Bruksgränstillstånd.

Acknowledgements

This master thesis project has been carried out from January to June 2024 at the division of Structural Engineering at Chalmers University of Technology in collaboration with COWI in Gothenburg.

We would like to express our gratitude to our supervisor, Thomas Hallgren, at COWI. He has been very supportive throughout the thesis, provided us with very useful advice, and suggested the topic. We alo want to thank Adam Jonsson and Thomas Andersson for their support in the software FEM-Design.

We also want to thank our examiner and supervisor, Associate Professor Robert Jockwer at Chalmers, for organizing the study trip to a hybrid timber building in Gothenburg, giving advice during meetings, and continuously providing feedback throughout the thesis.

Mahmoud Alkhateb and Isak Kallmér, Gothenburg, June 2024

Notations

Roman upper-case letters

A_i	Cross-sectional area for bracing member i
A_{ref}	Reference area of the structure
B^2	Background response
$\mathbf{C}$	Damping matrix
E_i	Modulus of elasticity of bracing member i
F	Kárman's wind energy spectrum
H	Horizontal force
I_i	Moment of inertia for bracing member i
$I_v(z)$	Turbulence intensity
$\mathbf{K}$	Stiffness matrix
$\mathbf{M}$	Mass matrix
R^2	Resonance frequency
S_{bi}	Bending stiffness of wall i
S_{si}	Shear stiffness of wall i
S_t	Global torsional stiffness
S_{xi}	Stiffness of bracing member i in x-direction
S_{yi}	Stiffness of bracing member i in y-direction
T	Reference time
T_a	Time period
W_e	Wind pressure acting on external surfaces
$\ddot{X}_{max}$	Acceleration

Roman lower-case letters

a_i	Distance from arbitrary position to the center of bracing unit i in x-direction
b	Cross-dimension which is perpendicular to the wind direction
b_i	Distance from arbitrary position to the center of bracing unit i in y-direction
c	Viscous damping coefficient
$c_o(z)$	Topography factor
c_f	Force coefficient

$c_{f,0}$	Force coefficient without free-end flow
c_o	Orthography factor
c_{pe}	Pressure coefficient for external pressure
c_r	Roughness factor
$c_s c_d$	Structural factor
e	Eccentricity
f	Frequency
f_c	Damping force
$f(t)$	External force
h	Height of the structure
h_{ref}	Reference height of 10 m
k	Stiffness
k_b	Factor that considers bending and is dependent on load case
k_p	Peak factor
k_r	Terrain factor
k_s	Factor that considers shear and is dependent on load case
l_i	Length of a shear wall for bracing member i
m	Mass
m_e	Equivalent mass
$n_{1,x}$	Fundamental frequency
q_b	Reference mean (basic) velocity pressure
q_p	Peak wind pressure
t	Time
u	Displacement
$\dot{u}(t)$	Velocity
$\ddot{u}$	Acceleration
$\hat{\mathbf{u}}$	Amplitude vector
v	Up-crossing frequency
v_b	Basic wind velocity dependent on region
v_m	Characteristic mean wind velocity
x_i	Distance between the rotational center of the building in x-direction for bracing i
y_c	Non-dimensional frequency
y_i	Distance between the rotational center of the building in x-direction for bracing i
z	Height over the ground surface
z_0	Roughness length
$z_{0,II}$	Reference height set to 0.05 m
z_{max}	Maximum height
z_{min}	Minimum height
z_s	Reference height

Greek letters

α	Positive scalar factor, alpha
β	Positive scalar factor, beta
δ_a	aerodynamic decrement of damping
δ_s	Structural damping expressed by the logarithmic decrement
ξ	Viscous damping ratio
ξ_1	Damping ratio at first natural frequency
ξ_k	Viscous damping ratio at k:th eigenmode
ρ	Air density
$\sigma_{\ddot{X}}(z)$	Standard deviation of acceleration
ϕ	Eigenvector
$\phi_{1,x}$	Mode shape function
ϕ_b	Size factor with respect to the width of the structure
ϕ_h	Size factor with respect to the height of the structure
ϕ_k	The k:th eigenvector
ψ_λ	Reduction factor for elements with end effects
ψ_r	Reduction factor for a square section with rounded corners
ω	Circular or angular natural eigenfrequency

Abbreviations

BSV	Boverket's Handbook for Snow and Wind Actions
CLT	Cross Laminated timber
DOF	Degree of Freedom
EC	Eurocode
EKS	Boverket's Application of the European Construction Standards
EWP	Engineered Woord Products
FE	Finite Element
FRP	Fiber-Reinforced Polymer
GLT	Glue Laminated Timber
LVL	Laminated Veneer Lumber
MDOF	Multiple Degrees of Freedom
MUF	Melamine-Urea-Formadentyl
SDOF	Single Degree of Freedom
SLS	Serviceability Limit State
ULS	Ultimate Limit State
WRI	World Resources Institute

Contents

List of Figures

List of Tables

1
Introduction

This chapter introduces the topic of the thesis. The chapter begins with the background of the project and is followed by the problem description, aim and objective, limitations, method and ends with ethical, ecological and social aspects.

1.1 Background

The population living on earth increases every year. Many cities have plans to densify the urban environment and therefore the need for high-rise buildings has grown. In the last couple of decades, knowledge about climate change has increased which means that the need for new solutions to lower the carbon footprint of structures has risen. Timber has environmental benefits compared to other construction materials and has therefore grown in popularity. A type of structure called hybrid structure is one that combines two different materials in order to utilize the benefit of each material. Hybrid structures have better structural performance with regard to wind than pure timber structures. One example of a hybrid structure is one with a core made of concrete, while other elements such as columns, beams and floor elements are made of timber. The progress achieved in hybrid technologies, which involve combining various structural materials, is facilitating the potential for constructing taller buildings with timber as one of the primary structural materials. Hybrid buildings become an alternative to other structural systems, such as prefabricated concrete buildings (Iqbal, 2021).

1.2 Problem Description

Hybrid structures show positive effects with regard to lowered climate impact and enhancing structural performance of buildings by utilizing the most of each material when combined with each other. Timber has a high strength-to-weight ratio, is considered as an environmentally friendly material and has a high degree of prefabrication. Concrete complements timber by having a good resistance against lateral forces. Although hybrid structures are a good solution due to the mentioned effects of combining different building materials, there are still some challenging issues with hybrid structures that need to be considered. One possible issue to evaluate is the overall strength of a building which has a lightweight structure and also the ability to withstand wind horizontal loads as it becomes the design load for a certain height of the building. Another possible challenge to consider in the design of tall hybrid buildings, is the design of connections. The choice of connections will influence the

total structural response of the building. Previous study (Dahlén & Niemi-Impola, 2023) have shown that comfort criteria with regard to wind dynamics can be fulfilled. In the mentioned studies the building's strength with regard to wind dynamics have not been explored.

As different materials are used, their properties influence the overall behaviour of the structure. Timber and concrete exhibit time-dependent response which is associated with creep and shrinkage. These two phenomena affect the total deformation of the structural elements and they are highly affected by the environmental conditions resembled by the relative humidity. Another issue to consider is the dimensions of some structural elements such as wall thickness and column size which can be to some extent unrealistic which emphasises the need for taking into account the economical aspects and also the manufacturing method of such elements.

When the height of a building increases, the wind loads will increase and the dynamic behavior of a building can be the determining load case. The dynamic response of a tall building is therefore important to study. Timber has a lower density and stiffness compared to other construction materials and is therefore more sensitive to wind loads.

1.3 Aim and Objectives

The main objective of the thesis is to get a better understanding of how concrete and timber interact with each other in a hybrid structure. It aims to increase knowledge in the design of buildings with a focus on wind dynamics and how it affects tall hybrid buildings. The thesis will include a parametric study where knowledge about how changes in different parameters will affect the performance of a hybrid structure. The primary objective is to ascertain the maximum height attainable for a hybrid structure, with a particular focus on wind dynamics in the ultimate limit state. The primary load-bearing structure for vertical and horizontal loads will be assessed.

1.4 Limitations

The scope of the thesis work is limited to control the overall strength of the structural bearing system of the building and the dynamic response to wind loads acting on the high-rise building. With regard to connection details, only a few high-performance connections will be studied in a simplified manner. Secondary load-bearing systems will be disregarded. One example of these systems are floor elements, which are considered to be strong enough. The analysis carried out in this report will be performed on one specific building with fixed size and spans, located in an urban environment. Another limitation is that it is assumed that the building is constructed on top of a stiff foundation. Long-term effects will not be considered in this report as major focus is on wind loads which are considered to be short-term.

1.5 Method

The first part of the project involves conducting an in-depth review of the existing literature concerning the dynamic behaviors exhibited by high-rise hybrid structures and the corresponding design strategies employed to address such behaviors. Additionally, currently implemented hybrid structures will be assessed. A parametric study will be conducted with finite element analysis, where different parameters are changed. This process will span various building heights, building configurations and material usage, enabling an exploration of how alterations in parameters influence the dynamic response of the building. Some analytical calculations will be conducted to verify the results from the numerical analysis. The main design load considered will be the wind load, with a primary focus on the Ultimate Limit State (ULS) criteria. While Serviceability Limit State (SLS) will be examined in a more simplified manner with a primary focus on the comfort criteria related to maximum allowed acceleration in the building.

1.6 Ethical, Ecological and Social Aspects

The most common construction material is concrete. In the manufacturing process of cement, large amounts of carbon dioxide are emitted into the atmosphere. The emissions contribute to the issue of global warming. Other construction materials emit less carbon dioxide in the manufacturing process in relation to volume compared to concrete. One of these materials is timber. Incorporating more timber into the structural system could reduce the ecological footprint of a building. Besides the ecological benefits of timber, the material itself will store carbon dioxide until the demolition of a building.

High-rise hybrid buildings can contribute to densification. According to Cavicchia (2021) densification has many positive effects. Some of them are reduction of pollution, better service such as schools and supermarkets, better and more reliable public transport, easier to find jobs, social connections will improve and increased preservation of natural land. There are also some disadvantages such as increased health issues due to noise and increased pollution from traffic.

Another aspect to consider is forestry. If the demand for timber increases, the felling of trees will also rise. The consequence of increased harvesting could be a decrease in biodiversity (Latterini et al., 2023). An increased biodiversity will increase the amount of ecological services. Examples of ecological services are photosynthesis and decomposition. Managing forests in a good way is the key to sustainable forestry.

2
Theory

This chapter contains the theory needed to understand the structural behavior of timber and wind dynamics. These are later used to decide on appropriate building configurations and verify the FE model.

2.1 Timber

Constructing timber houses has a long tradition in Sweden (Kallmén, 2022). It is a part of the Swedish cultural heritage and the oldest wooden house dates back to the 13th century. In 1888 construction of timber buildings was limited to two floors by the building authority due to fire reasons. When Sweden joined the European Union, building timber buildings with more than two floors became legal. To ensure the fire safety of buildings, new regulations were adopted from EU. After 1994 the construction of timber buildings has therefore increased for every year.

2.1.1 Mechanical Properties of Timber

Timber is an anisotropic material with different strength in different directions (Swedish Wood, 2022). This is due to that the timber fibers are connected with lignin. The strength parallel to the wood fibers is larger compared to the strength in the perpendicular direction. When defining strength in wood there are three main directions; longitudinal, tangential, and radial. The directions are defined in Figure 2.1.

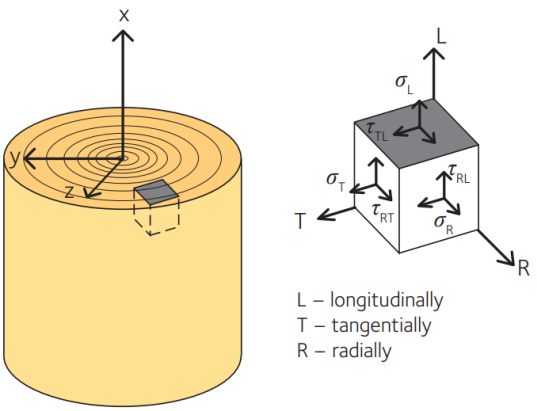

Figure 2.1: Strength for different directions for wood (Swedish Wood, 2022).

The strength of timber can differ depending on imperfections, climate conditions, load and size (Swedish Wood, 2022). One example of imperfections in wood is knots. The effect of knots can result in large stress concentrations around the knots. It is therefore difficult to know the strength of wood without testing. Moisture does also have a large impact on the material's strength. A lower moisture content will lead to greater strength. In most cases, the strength increase with a lowered moisture content can be described with a linear relationship. If the moisture content increases to the saturation point the strength will not further decrease with an increasing moisture content. The effect of moisture content will also vary between direction, loading type and duration. An example is if the moisture content is increased with 1 % the strength in compression will decrease with 5 % and 2.5 % loaded in tension in the perpendicular direction. This example is not valid for all moisture contents and could be applied for moisture contents between 8 % - 20 %. Temperature can also impact the strength and stiffness of the material. However, in most cases, the temperature will not influence the strength. With temperatures above 95 °C the material will deteriorate for short-term loads. The load duration will impact the strength of wood. Previous laboratory testing of bending capacity has shown that the strength of wood will decrease with time. After a year of loading the strength has decreased to 60 % of the original strength with short-term loading. The size of a timber specimen has a large impact on strength. A larger specimen will have a lower strength due to the fact that larger specimens are more prone to have weaknesses such as knots in the specimen.

2.1.2 Structural Timber

For many years the structural timber used in buildings was sawn timber (Swedish Wood, 2022). The largest size of these products in Sweden is a length of 5.5 meters and a height of 245 millimeters. In order to produce larger elements, engineered wood products (EWP) were invented. The first was glued laminated timber which was invented in the 19th century. The invention was followed by many EWP in the 20th century.

2.1.2.1 Glue Laminated Timber

Glue laminated timber is made out of sawn and planed construction timber boards which are 45 mm thick and maximum 215 mm wide (Swedish Wood, 2022). The boards are glued together with adhesives to make a beam. An example of a GLT beam can be observed in Figure 2.2. The most common adhesive is called Melamine-Urea-Formadentyl (MUF). The beam can be wider by gluing two boards together. The product can contain higher quality boards at the top and bottom of the beam as higher stresses will be achieved in bending. They can be curved. The fibers should be in a parallel direction to the length of the boards. The beams can be constructed with an infinite length as they can be glued together with finger joints. The moisture content when manufacturing GLT should be between 6 %-15 % and the variation between the boards should be less than 5 %. When comparing the strength of sawn timber and GLT, the GLT does not have a higher strength, but the variation of strength is smaller due to that imperfections for the whole beam are

being spread out as it consists of several glued boards. The quality of these boards differ and therefore boards will be classified with a strength class ranging from GL22 - GL32. The numbers refer to strength in bending parallel to the grain. There are also some supplementary letters to the bending strength such as c, which stands for combined, h, is homogeneous and s, means re-sawn.

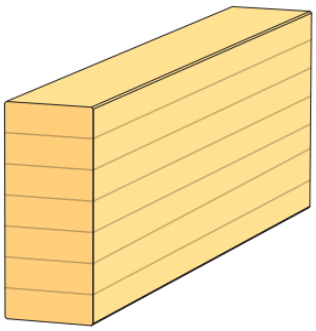

Figure 2.2: An example of a GLT beam. (Swedish Wood, 2022)

There are two main types of grading structural timber elements (Swedish Wood, 2022). The oldest one is called visual grading where the size of imperfections such as knots are measured. Larger and more imperfections will result in a lower grading. Historically, humans were grading visually and now there are scanning machines that can perform this task. The largest uncertainty with visual grading is that the method only takes surface imperfections into account and not the imperfections inside the specimen. The other type of grading is machine grading. The most common machine grading is the static flat-wise bending where the boards go through rollers. The load and displacement are measured in a three-point bending test to determine the modulus of elasticity. The method can be observed in Figure 2.3.

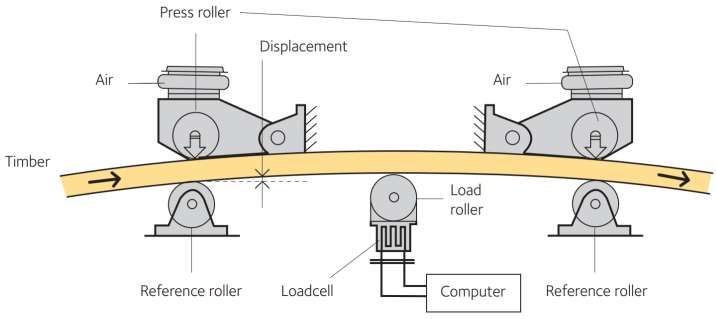

Figure 2.3: Static flat-wise bending test (Swedish Wood, 2022).

2.1.2.2 Cross-Laminated Timber

Cross-laminated timber (CLT) elements are typically used for floor or wall elements (Swedish Wood, 2022). They are made of sawn boards arranged in multiple layers, with each layer's fiber direction perpendicular to that of the adjacent layers.

These layers are then glued together to form the final CLT element. The panel will therefore be strong in two directions. Generally, the size limit is determined by the manufacturing facility and shipping limits. Normal size limits are a thickness between 0.5 m to 3 meters, a maximum width of three meters and a maximum length of 24 meters. The common number of layers is typically 3, 5, and 7. These numbers are uneven due to that the fiber direction of the top and bottom layers should be in the same direction because higher strength in the main loading direction could be achieved that way. An example of a three-layered CLT element can be observed in Figure 2.4. One advantage of CLT is the ability to pre-fabricate large elements in factories and then easily assemble them on-site

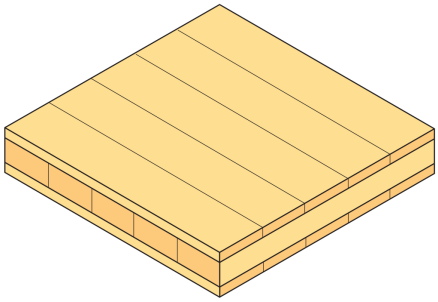

Figure 2.4: Example of a CLT element (Swedish Wood, 2022).

2.1.2.3 Laminated Veneer Lumber

Another EWP is called laminated veneer lumber (LVL) (Swedish Wood, 2022). In the manufacturing of LVL, thin layers that are several millimeters thick are peeled from logs. These layers are glued together with the fibers in the same direction to make a board that is between 2 and 9 cm thick. The width of the board can be up to 3 m and the maximum length is 24 meters. The benefits are similar to GLT in the way that the variation of strength is smaller as the imperfections are spread out. The boards are often used in floor structures.

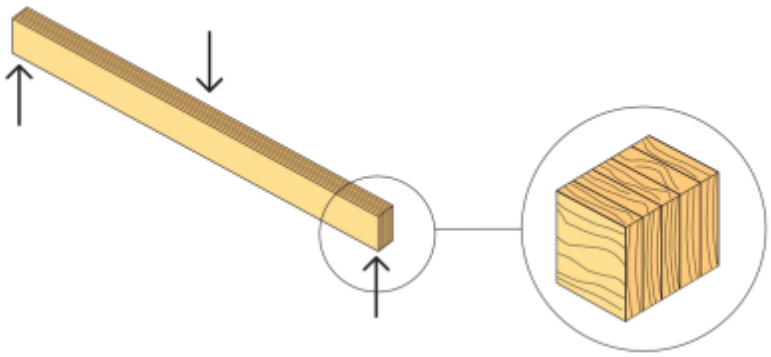

Figure 2.5: Example of an LVL (Swedish Wood, 2022).

2.2 Concrete

Concrete stands as the most extensively employed building material globally (Gagg, 2014). Comprising a blend of components, including cement, sand, aggregates, and water, concrete can be formed. Concrete can be further enhanced by the addition of admixtures. These additions serve to improve either the fresh or hardened properties of the concrete, allowing for the achievement of specific desired characteristics (Al-Emrani et al., 2013). The term 'cement' is a general term that can be used to describe all binder materials (Gagg, 2014). The increased amount of cement in the mix often generates higher strength in the concrete. The World Resources Institute (WRI) reports in an analysis, Barcelo et al. (2014) that the cement industry represent 3.8 % of the global greenhouse gas emissions and around 5 % of the global carbon dioxide emissions.

Concrete is recognized for its low tensile strength, being significantly lower than its compressive strength. The tensile strength in concrete, therefore, can be measured to only around 10 % of the compressive strength. As a result, it requires reinforcement from other materials that can offer higher tensile resistance. Due to its low tensile strength, even under moderate loading conditions, concrete is prone to cracking. This entails a significant concern as cracking not only diminishes the stiffness of the structural element but also impacts its durability, particularly in terms of corrosion of steel reinforcement (Al-Emrani et al., 2013).

Embedded steel bars, serving as reinforcement, are often utilized to maintain force equilibrium during the cracked stage of a concrete structural element. Other reinforcing methods, such as utilizing fiber-reinforced polymers (FRP), can be employed. Fiber-reinforced polymers (FRP) feature a high strength-to-weight and stiffness-to-weight ratios, corrosion resistance and high durability (Van Den Einde et al., 2003).

One other technical solution to address the issue of concrete cracking is by prestressing the structural concrete element. Prestressing involves introducing compressive forces, creating compressive stresses within the element. As external loads are applied, the compressive stresses decrease, leading to the occurrence of tensile stresses at higher load levels compared to regular reinforced concrete elements. Thus, the crack formation is delayed (Al-Emrani et al., 2013).

2.3 Horizontal Stabilization

Lateral loads acting on a building will cause deformation. Through the internal forces of the horizontal loads, equilibrium must be obtained (Engström, n.d.). The deformations are commonly divided into two categories; translational deformation and rotational deformation. If the centre of lateral loads acts in the rotational centre in each direction the transational deformation will only contribute to deformation, but if that is not the case the rotational deformation will also act on the building.

The rotational centre depends on both the stiffness and shape of the bracing. The rotational centre can be calculated through Equation 2.1. All of the equations in this subsection are sourced from Engström (n.d.). The loads are also divided into two directions, denoted here as x- and y-direction. One important assumption is that the bracing is assumed to have the same stiffness along the whole height of a building.

$$x_t = \frac{\Sigma(a_i S_{yi})}{\Sigma S_{yi}} \qquad y_t = \frac{\Sigma(b_i S_{xi})}{\Sigma S_{xi}} \tag{2.1}$$

Where:

- S_{xi} is the stiffness of bracing member i in x-direction,
- S_{yi} is the stiffness of bracing member i in y-direction,
- a_i and b_i are defined in Figure 2.6 where the point P is an arbitrary position.

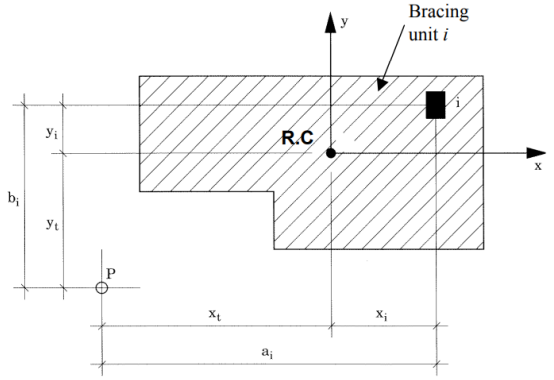

Figure 2.6: Rotational Centre (Engström, n.d.).

The lateral loads from translation can be calculated with Equation 2.2 for each bracing in their respective direction.

$$H_{xi} = H_x \frac{S_{xi}}{\Sigma S_{xi}} \qquad H_{yi} = H_y \frac{S_{yi}}{\Sigma S_{yi}} \tag{2.2}$$

The total lateral loads from both translation and rotation for each bracing and direction can be found in Equation 2.3.

$$H_{xi} = H_x \frac{S_{xi}}{\Sigma S_{xi}} + T \frac{S_{xi} \cdot y_i}{S_T} \qquad H_{yi} = H_y \frac{S_{yi}}{\Sigma S_{yi}} + T \frac{S_{yi} \cdot x_i}{S_T} \tag{2.3}$$

Where:

- $T = H \cdot e$, H is the horizontal force and e is the eccentricity defined in Figure 2.7,
- x_i and y_i are defined in Figure 2.6,
- S_t is the global torsional stiffness.

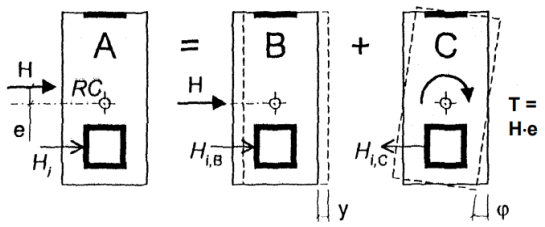

Figure 2.7: Load resultant (Engström, n.d.).

The global torsional stiffness is described in Equation 2.4 where the rotation center is assumed to be in the middle of the coordinate system.

$$S_T = \Sigma(S_{xi} \cdot y_i^2) + \Sigma(S_{yi} \cdot x_i^2) \tag{2.4}$$

The stiffness for each bracing unit is divided into shear and bending stiffness. The total stiffness of a shear wall can be calculated through Equation 2.5.

Where:

- S_{si} is the shear stiffness of wall i,
- S_{bi} is the bending stiffness of wall i.

$$\frac{1}{S_i} = \frac{1}{S_{si}} + \frac{1}{S_{bi}} \tag{2.5}$$

A general expression for both bending- and shear stiffnesses can be observed in Equation 2.6.

$$S_{si} = k_s \frac{E_i \cdot A_i}{l_i} \quad S_{bi} = k_b \frac{E_i \cdot I_i}{l_i^3} \tag{2.6}$$

Where:

- k_s and k_b are factors that are dependent on load case. Figure 2.8 shows the factors for some commonly used cases,
- E_i is the modulus of elasticity of bracing member i,
- I_i is the moment of inertia for bracing member i,
- A_i is the cross-sectional area for bracing member i,
- l_i is the length of a shear wall for bracing member i.

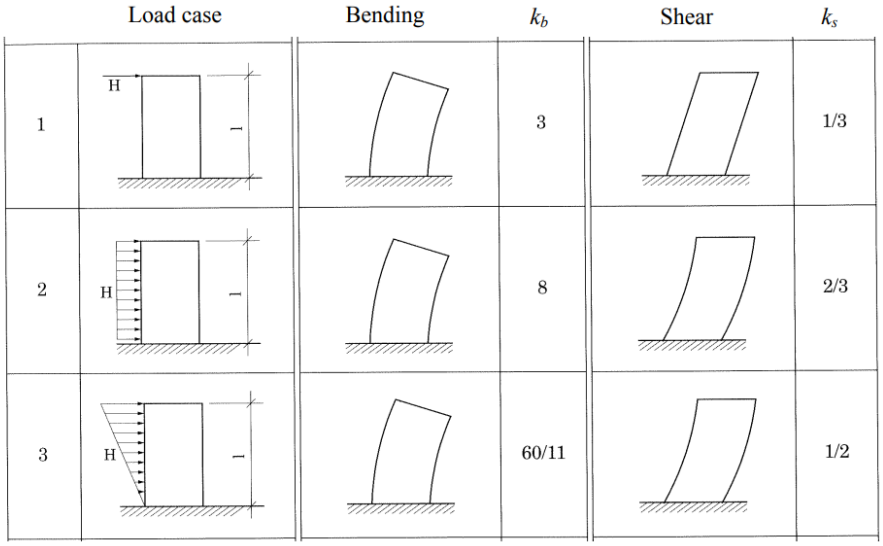

Figure 2.8: Load case factors (Engström, n.d.).

2.4 Connections in Tall Timber Building

Different types of connections have different properties and depend on the use case and design of the connection (Swedish Wood, 2019). A common way to connect CLT elements is through screws or other steel components. Different connections have different types of failure modes and the designer has many possibilities to control the failure mode. One common type of connection is between slab and wall. One easy way to connect the elements is by using long screws where the slab is placed on top of a wall element and screws are vertically drilled into the panels. Then a wall is placed on top and diagonal screws are inserted. To ensure anchorage and to make sure that the screws are not fully penetrated, the screws need to be inserted carefully. Another way is to instead of using the diagonal screws to use angle brackets. An advantage of brackets is the possibility of achieving a larger shear resistance. Other ways include installing steel rods into the wall and slab element or using steel plates and dowels. These connections can also be made in a different manner as when incorporating a slab between two walls the loads need to go through the slab where it is loaded perpendicular to the grain. A way to avoid the challenge is to place the slab on top of a steel plate which is screwed into the wall. Examples of these connections can be found in Figure 2.9.

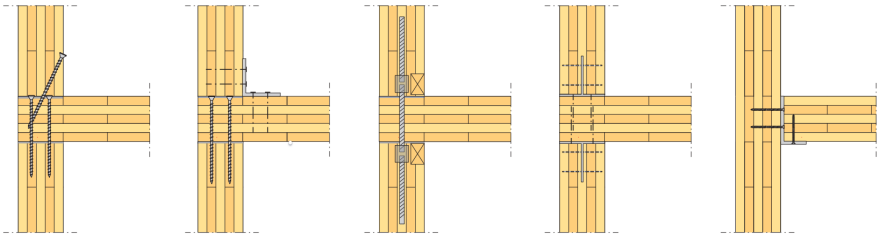

Figure 2.9: Examples of slab to wall connection (Swedish Wood, 2019).

For high-rise timber buildings some connections can be difficult to design (Tapia & Aicher, 2023). These connections include column-to-CLT plate connections with additional bracing. There are two major design challenges. The first challenge is high stress and shear concentrations in the CLT close to the connection. CLT has low capacity in rolling shear which is a third of the resistance compared to shear parallel to the grain. The other challenge is to transfer large forces between columns. The connection commonly has a steel plate between the timber members as the strength perpendicular to the grain is low. The plate will further increase the tensile stress concentration for the CLT-to-column connection. Some solutions can cope with the problem such as reinforced CLT. Two types of CLT and column connections can be seen in Figure 2.10. As the popularity of tall timber buildings is increasing new types of high-performance connections are being developed. One of them is a column-to-column connection that only contains timber components and glue by utilizing different EWPs. Due to new techniques with robot cutting the connection in Figure 2.11 can be fabricated.

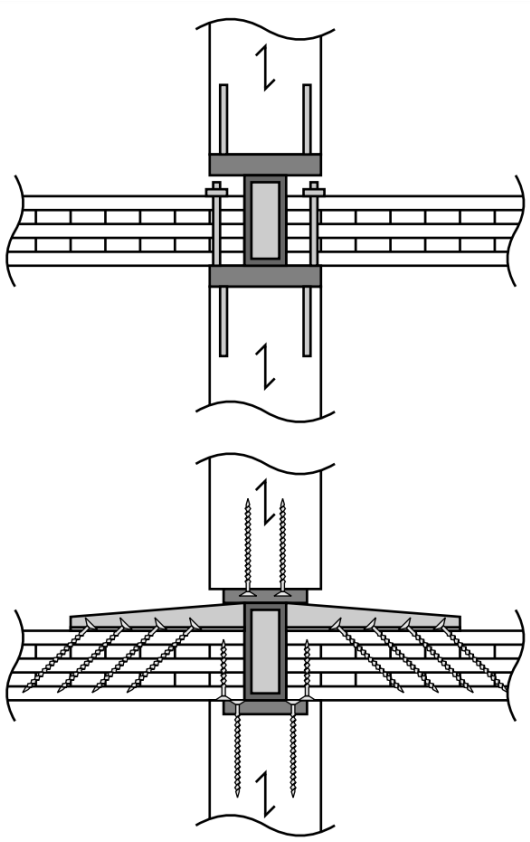

Figure 2.10: Examples of timber connections (Tapia & Aicher, 2023).

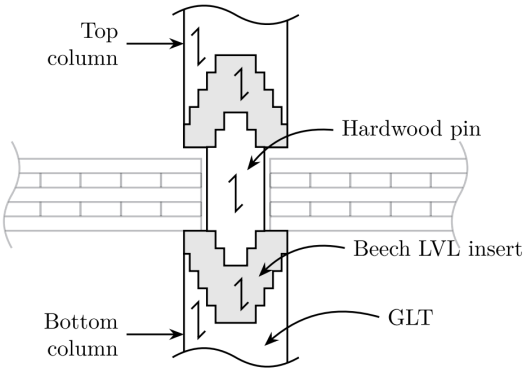

Figure 2.11: Example of an EWP connection (Tapia & Aicher, 2023).

2.5 Structural Systems of Timber Buildings

Single-family houses in timber have been commonly constructed in the Nordic countries throughout the years (Swedish Wood, 2022). In 1995 the construction of apartment buildings with platform systems in timber started to become popular. Shortly after, the construction of prefabricated systems increased. The construction of timber buildings in Europe is mainly concentrated in the Nordic countries and German-speaking countries.

The structural systems of a timber building can be simplified into three main categories of geometry (Swedish Wood, 2022). One of them is a panel system which contains plane elements. Two examples of these types are floor and walls. They can be constructed with both solid and frame structures. The width of these elements can be up to 1.8 meters wide and typical spans are between 8 and 10 meters. Another category is the modular systems where whole modules are prefabricated in factories. The modules do not only contain structural elements but also installations such as ventilation and all work regarding floor, ceiling and walls can be made in a factory. Due to limitations in transportation, large spans cannot be achieved. The third category is a post and beam system where larger beams and columns are used to construct a frame structure. This type of structure is commonly used for commercial, industrial buildings and other types of buildings where large spans are required such as aquatic centers and hockey arenas. The beams and columns are often considered as simply supported. Additional structural elements need to be considered such as bracing and shear walls. Examples of the three main categories are in Figure 2.12 to Figure 2.14.

There is another category system that the industry uses where structural elements are divided into an open system and a closed system (Swedish Wood, 2022). The open system consists of elements and dimensions that are standard which multiple companies can produce. The closed system is the opposite where companies can create their designs and products.

Figure 2.12: Example of a panel system (Swedish Wood, 2019).

Figure 2.13: Example of a modular system (Swedish Wood, 2022).

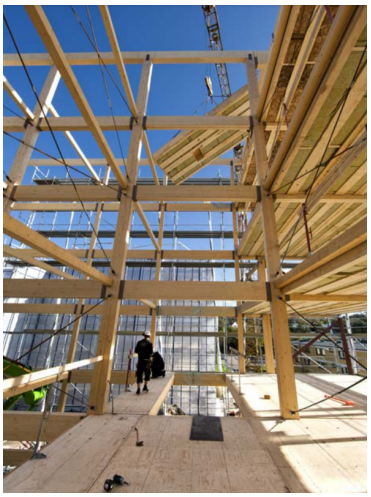

Figure 2.14: Example of a post and beam system (Swedish Wood, 2022).

2.6 Structural Systems of Timber-Concrete Hybrid Buildings

The structural systems in this section contain systems with separate elements for concrete and timber and not systems where composite elements are used. Larsson (2023) performed an interview study on buildings that were completed or under construction in 2020 in Sweden through interviews with the ones responsible of the planning and construction for the projects. The aim was to categorize timber-concrete hybrid buildings. He decided on four categories which are presented below.

The first system has the first floor elements in concrete and the rest of the elements in timber. These types of buildings are commonly used in residential buildings. One benefit is that the first floors can have another floor plans compared to the first floors. Another advantage is the added weight at the bottom of the building. The added weight will counteract the uplift when lateral loads act on the building. The first system can be observed in Figure 2.15.

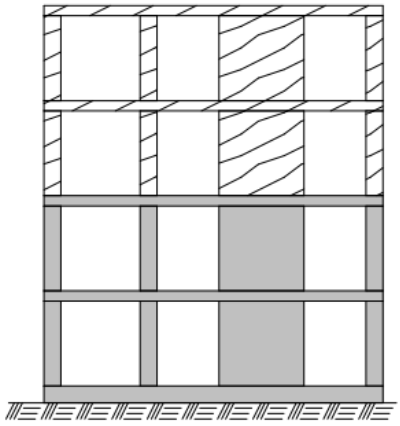

System type 1:
A timber structure in CLT/GLT on top of a concrete structure

Figure 2.15: Timber-concrete hybrid system 1 (Larsson, 2023).

The second system is a post-beam system where beams and columns are made out of timber. This type of system is commonly used for office buildings. The system creates an open floor plan. It means that the floor plan is flexible and if the operations change in the building the floor plan can adapt. The shear walls are made out of concrete as the material has a higher strength compared to CLT walls. The shear walls often create a core where elevators and staircases can be placed. The hybrid system can be seen in Figure 2.16.

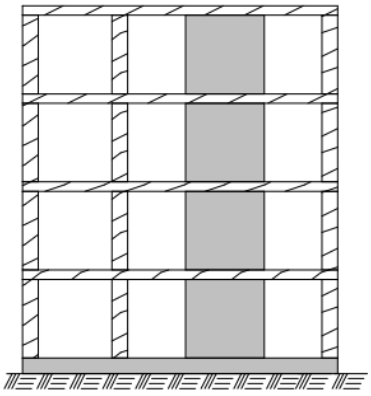

System type 2:
Post beam system in timber with CLT slabs and walls in concrete

Figure 2.16: Timber-concrete hybrid system 2 (Larsson, 2023).

The third system is commonly used in either schools or for offices that need larger spans. CLT floor elements do not have the capacity for longer span lengths. Therefore prestressed hollow core elements are used instead. Floor structures are supported with timber beams and columns. Structural elements that resist lateral loads

are trusses in timber or steel, but could also be steel bracing units. The system can be observed in Figure 2.17.

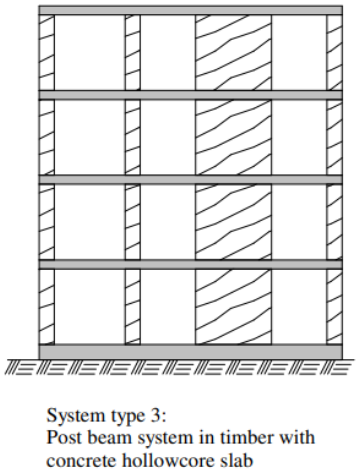

Figure 2.17: Timber-concrete hybrid system 3 (Larsson, 2023).

The fourth system is commonly used in high-rise buildings such as Sara Kulturhus and Mjøstårnet. The buildings are mainly built with timber elements, but the top floors are concrete elements. A benefit is the added mass which makes the building perform better with regard to wind dynamics. These buildings are in some cases considered timber buildings, but as the structural system of the building contain concrete it is here considered as a hybrid building. The system is shown in Figure 2.18.

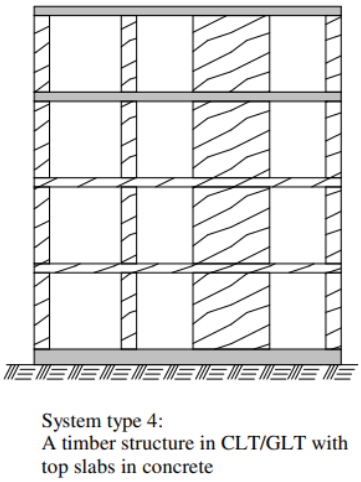

Figure 2.18: Timber-concrete hybrid system 4 (Larsson, 2023).

2.7 Structural Dynamics

The design of buildings necessitates careful consideration of various types of actions, as outlined in design codes and standards. A fundamental distinction is made

between two categories of actions: static and dynamic. Static actions, classified as time-independent, do not induce significant acceleration in the structure or its elements. Conversely, dynamic actions are time-dependent and lead to noticeable structural accelerations. This classification is predicated on how structures respond to these forces (Kappos, 2001).

Although in most civil engineering applications the loads applied on structures are based on the assumption of static loads, there are instances where exceptions arise, necessitating a clear differentiation between static and dynamic loads. Structures may encounter dynamic loading, also referred to as time or frequency varying loading. There are numerous situations when dynamic loading needs to be considered. Dynamic loads can originate from various sources such as wind gusts, earthquakes, or ocean wave motions, blast pressure on a structure, loads from machines and the response of a bridge to moving vehicles or people. In the case of tall slender buildings, the dynamic effects from wind loads might govern the design.

In Eurocode 1 (SS-EN 1991-1-1, 2002), a method is presented to address dynamic actions by employing a dynamic magnification factor. On the other hand, if actions are deemed to result in substantial accelerations of the structure or its elements, such actions should be classified as dynamic. In such instances, dynamic analysis must be employed to thoroughly consider and address these dynamic actions. Tall timber structures possess a reduced weight compared to conventional high-rise buildings, making them more susceptible to wind-induced excitations (Landel, 2022).

2.7.1 Dynamic Modelling with Force, Mass and Stiffness

In the dynamic analysis procedure, it is essential to establish a mechanical model that can accurately describe the physical problem (Tedesco et al., 2000). Then, the dynamic response of a structure can be modelled by first discretizing the structure into smaller elements with a defined number of nodes and each node has motion variables. These variables are known as *degrees of freedom* (dofs) and are used to describe displacement, rotation, etc. In theory, all structures inherently have an unlimited number of degrees of freedom (Craig Jr & Benzley, 1982). The simplest dynamic model is represented by a *single degree of freedom* (SDOF) system, where mass, stiffness, and force are indicated as illustrated in Figure 2.19. This analytical SDOF model serves as an approximation of a structure and is particularly useful for simplified dynamic analyses, especially in the context of high-rise buildings (Landel, 2022).

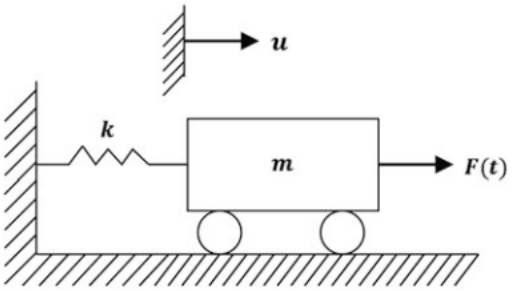

Figure 2.19: A model for a SDOF mass-spring system with mass m, stiffness k, displacement *u(t)* and force *f(t)*.

D'Alembert's principle of dynamic equilibrium provides a convenient approach for formulating the equations of motion in a simple single degree of freedom (SDOF) and multiple degrees of freedom (MDOF) systems (Mario & Young, 2019). Essentially, this principle applies Newton's second law of motion to the system. According to Newton's second law, the rate of change in momentum is directly proportional to the applied force and takes place along the force's line of action. In the case of a constant mass, the rate of change of momentum equals the product of the mass and its acceleration. By using Newton's second law of motion together with Hooke's law for spring force (assuming a linear spring), the structural dynamic equation of the SDOF system can be obtained as in Equation 2.7:

$$m\ddot{u} + ku = f(t) \tag{2.7}$$

where u is the displacement,$\ddot{u}$ is the acceleration, which is the second derivative of time of the displacement u, k is the stiffness, m is the mass and *f(t)* is an external force acting on the system.

In principle, all structures possess an infinite number of degrees of freedom (dofs), allowing for the construction of models with multiple degrees of freedom (MDOF). Consequently, a multi-storey building can be effectively described using an MDOF model (Landel, 2022). Figure 2.20 illustrates a 4-storey building that is modelled with a 4-dofs spring system as illustrated in Figure 2.21.

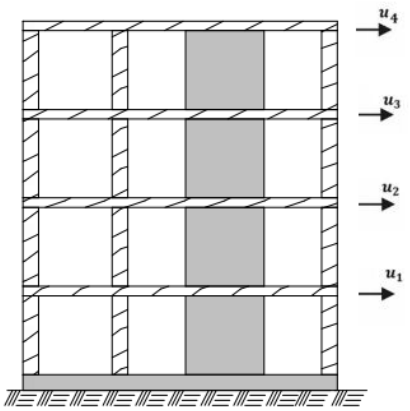

Figure 2.20: A 4-storey building to be modelled with a mass-spring system, adapted from (Larsson, 2023)

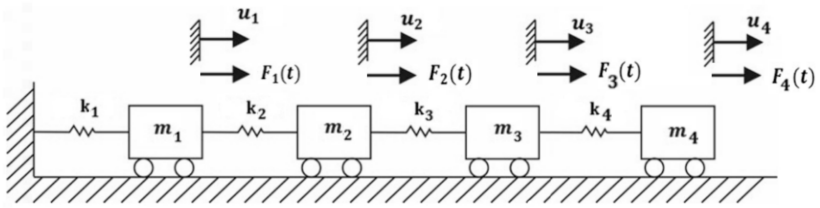

Figure 2.21: A model for a 4-dofs mass-spring system with mass m, stiffness k and displacement $u(t)$.

To establish the force equilibrium of the model shown in Figure 2.21, a free-body diagram is constructed for the 4-degree-of-freedom mass-spring system.

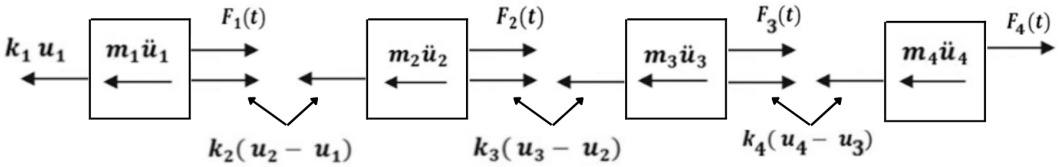

Figure 2.22: A free-body diagram of the 4-dofs mass-spring system.

Considering the free-body diagram of the 4-dofs model in Figure 2.22, the law of motion depicted in the Equation 2.7 can be formulated for each element considering force equilibrium:

$$\begin{aligned} &m_1\ddot{u}_1 + (k_1 + k_2)u_1 - k_2u_2 = f_1(t) \\ &m_2\ddot{u}_2 - k_2u_1 + (k_2 + k_3)u_2 - k_3u_3 = f_2(t) \\ &m_3\ddot{u}_3 - k_3u_2 + (k_3 + k_4)u_3 - k_4u_4 = f_3(t) \\ &m_4\ddot{u}_4 - k_4u_3 + k_4u_4 = f_4(t) \end{aligned} \tag{2.8}$$

On matrix form, the system of equations in 2.8 can be expressed as in 2.9:

$$\begin{bmatrix} m_1 & 0 & 0 & 0 \\ 0 & m_2 & 0 & 0 \\ 0 & 0 & m_3 & 0 \\ 0 & 0 & 0 & m_3 \end{bmatrix} \begin{bmatrix} \ddot{u}_1 \\ \ddot{u}_2 \\ \ddot{u}_3 \\ \ddot{u}_4 \end{bmatrix} + \begin{bmatrix} k_1 + k_2 & -k_2 & 0 & 0 \\ -k_2 & k_2 + k_3 & k_3 & 0 \\ 0 & k_3 & k_3 + k_4 & -k_4 \\ 0 & 0 & -k_4 & k_4 \end{bmatrix} \begin{bmatrix} u_1 \\ u_2 \\ u_3 \\ u_4 \end{bmatrix} = \begin{bmatrix} f_1(t) \\ f_2(t) \\ f_3(t) \\ f_4(t) \end{bmatrix} \tag{2.9}$$

Which can be further written on a symbolic matrix form as follows in Equation 2.10:

$$\mathbf{M}\ddot{\mathbf{u}}(t) + \mathbf{K}\mathbf{u}(t) = \mathbf{f}(t) \tag{2.10}$$

Where $\mathbf{M}$ is the mass matrix, $\mathbf{K}$ is the stiffness matrix, $\mathbf{u}$ is the displacement vector, $\ddot{\mathbf{u}}$ is the acceleration vector (which is the second time derivative of the vector $\mathbf{u}$) and the $\mathbf{f}$ is the force vector.

2.7.2 Eigenmodes and Eigenfrequencies

Within the field of dynamics, there is a clear distinction made in the analysis between the so called *free vibration and forced vibration.* In the context of free vibration, the system initiates motion due to an initial disturbance from its static equilibrium state. Subsequently, it is permitted to move without the influence of additional external forces. The ensuing motion is solely determined by the inherent properties of the structure. Notably, the natural frequency of oscillation is predominantly dictated by the mass and stiffness of the system (Williams, 2016). This is a special case of the system described in Figure 2.19. Consequently, the system vibrates freely while no external forces act on it. Therefore *f(t)* is set to zero in Equation 2.7. The structural dynamic equation in 2.10 will then equate to zero and can be solved to determine the eigenfrequencies of the system as shown in Equation 2.11 below:

$$\mathbf{M}\ddot{\mathbf{u}}(t) + \mathbf{K}\mathbf{u}(t) = \mathbf{0} \tag{2.11}$$

In the field of vibration engineering, a crucial assumption is made in the analysis, dependent on the nature of oscillation, wherein it is considered to be subjected to harmonic excitation (Abrahamsson, 2019). A freely vibrating system has generally a harmonic motion which can be described by a periodic sinusoidal displacement with time.

As seen in the Equation 2.11, it is a type of linear second-order differential equation due to the presence of the displacement $\mathbf{u}$ together with its second derivative $\ddot{\mathbf{u}}$. The solution to the second-order differential equation is the displacement which is sinusoidal in time with an amplitude $\hat{\mathbf{u}}$ expressed by the following equation:

$$\mathbf{u}(t) = \hat{\mathbf{u}} \ \sin \omega t \tag{2.12}$$

Now, by taking the derivative of 2.12 two times as illustrated in 2.13 and inserting the result together with 2.12 into 2.11 the following expression illustrated in Equation 2.14 is obtained:

$$\ddot{\mathbf{u}}(t) = -\hat{\mathbf{u}}\ \omega^2 \sin \omega t \tag{2.13}$$

$$[\mathbf{K} - \omega^2 \mathbf{M}]\ \hat{\mathbf{u}}\ \sin \omega t = \mathbf{0} \tag{2.14}$$

If this equation is to hold true at any given time, it will have a non-trivial solution as follows by Equation 2.15:

$$\det\left[\mathbf{K} - \omega^2 \mathbf{M}\right] = \mathbf{0} \tag{2.15}$$

The solution to the eigenvalue problem is defined as the eigenvalue ω_k^2, $k = 1, 2, 3, ...,$ n and the associated eigenvector ϕ_k. Where k refers to a specific eigenmode shape and n is the number of dofs of the system. The eigenvector ϕ_k is then used in equation 2.14:

$$[\mathbf{K} - \omega^2 \mathbf{M}]\phi_k = \mathbf{0} \tag{2.16}$$

By multiplying Equation 2.16 with the inverse of the mass matrix $\mathbf{M}^{-1}$, the following expression is obtained:

$$[\mathbf{M}^{-1}\mathbf{K} - \omega^2 \mathbf{M}^{-1}\mathbf{M}]\phi_k = \mathbf{0} \tag{2.17}$$

Which can be rewritten by substituting for the identity matrix $\mathbf{I} = \mathbf{M}^{-1}\mathbf{M}$ in Equation 2.17:

$$[\mathbf{M}^{-1}\mathbf{K} - \omega^2 \mathbf{I}]\phi_k = \mathbf{0} \tag{2.18}$$

Now, with the acquired expression in 2.18 being similar to the conventional formulation of the standard eigenvalue problem used in mathematics with eigenvalues and eigenvectors for a matrix $\mathbf{A}$.

$$[\mathbf{A} - \lambda \mathbf{I}]\mathbf{x} = \mathbf{0} \tag{2.19}$$

The eigenvalue problem in 2.18 can be solved for the eigenvalues ω_k^2 of the system. Taking the positive square root of ω_k^2, provides the following expression which represents the system's natural frequencies, also called the system's resonance frequencies:

$$\omega_k = \sqrt{\omega_k^2} \quad [rad/s] \tag{2.20}$$

As observed by the expression in 2.20, the term ω_k is sometimes also referred to as the *circular or angular natural frequency*, and it has the unit radians per second. The systems eigenfrequency can also be defined as a number of oscillation cycles per second given by the following expression 2.21:

$$f = \frac{\omega_k}{2\pi} \quad [1/s]\ or\ [Hz] \tag{2.21}$$

The time period is usually expressed as the time it takes to complete a single cycle and therefore it has the unit second per cycle of simply seconds, which is expressed in Equation 2.22.

$$T = \frac{1}{f} = \frac{2\pi}{\omega_k} \quad [s] \tag{2.22}$$

2.7.3 Effect of Added Mass and Added Stiffness

The mass and stiffness of a structure has a substantial importance in the dynamic response of a structure and they are coupled with the eigenfrequency of that structure. A useful tool in the theory of free vibration is Rayleigh's quotient expressed in 2.23.

$$\omega^2 = \frac{\phi^T \mathbf{K} \phi}{\phi^T \mathbf{M} \phi} \tag{2.23}$$

Rayleigh's theorem on added mass or stiffness explains the effect of adjusting the mass or stiffness in a system on the eigenvalue ω^2 of that system. Let ΔM be the added mass to be imposed on the system. This will then affect the system's eigenvalue as follows in 2.24:

$$\omega^2 = \frac{\mathbf{u}^T \mathbf{K} \mathbf{u}}{\mathbf{u}^T [\mathbf{M} + \Delta \mathbf{M}] \mathbf{u}} = \frac{\mathbf{u}^T \mathbf{K} \mathbf{u}}{\mathbf{u}^T \mathbf{M} \mathbf{u} + \mathbf{u}^T \Delta \mathbf{M} \mathbf{u}} \leq \frac{\mathbf{u}^T \mathbf{K} \mathbf{u}}{\mathbf{u}^T \mathbf{M} \mathbf{u}} \tag{2.24}$$

The system's eigenvalues either stay or decrease. Let ΔK be the added mass to be imposed on the system. This will then affect the system's eigenvalue as follows in 2.25:

$$\omega^2 = \frac{\mathbf{u}^T [\mathbf{K} + \Delta \mathbf{K}] \mathbf{u}}{\mathbf{u}^T \mathbf{M} \mathbf{u}} = \frac{\mathbf{u}^T \mathbf{K} \mathbf{u}}{\mathbf{u}^T \mathbf{M} \mathbf{u}} + \frac{\mathbf{u}^T \Delta \mathbf{K} \mathbf{u}}{\mathbf{u}^T \mathbf{M} \mathbf{u}} \geq \frac{\mathbf{u}^T \mathbf{K} \mathbf{u}}{\mathbf{u}^T \mathbf{M} \mathbf{u}} \tag{2.25}$$

Consequently, the system's eigenvalues either stay or increase.

2.7.4 Damping of Structural Systems

An important characteristic in structural dynamics is related to the ability of a structure to reduce the dynamic responses by dissipating or in other words, losing energy and this is indicated by its damping. High damping values in a building are crucial to mitigate occupant discomfort during strong winds. Additionally, for safety considerations during earthquakes, damping becomes a critical parameter to prevent disproportionate collapse of the entire structure. One such a way of damping is called *viscous damping* and it refers to the damping force f_c being proportional to the velocity $\dot{u}(t)$, illustrated by the Equation 2.26. Viscous damping is popular in the field of structural dynamics.

The SDOF system presented in Figure 2.19 is characterized as undamped because it doesn't involve any energy dissipation. Such an idealized system, once it is excited, it will vibrate freely and indefinitely without the influence of external forces (Williams, 2016). In practice, it is evident that vibrations naturally diminish over time unless sustained by an external force. The decay of motion occurs due to the involvement of internal mechanisms that extract energy from the system which is described by the damping characteristics of a system.

In many applications in real life, damping occurs in different ways such as friction between sliding surfaces, often called *Coulomb damping*, energy loss in lubricating fluids in-between moving or rotating components which is referred to as *Viscous damping* and the energy loss in materials subjected to cyclic loading causing internal friction in the hysteresis loop which is referred to *Hysteretic damping* or sometimes also as *Structural damping* (Williams, 2016). Figure 2.23 illustrates a model for a damped SDOF spring system.

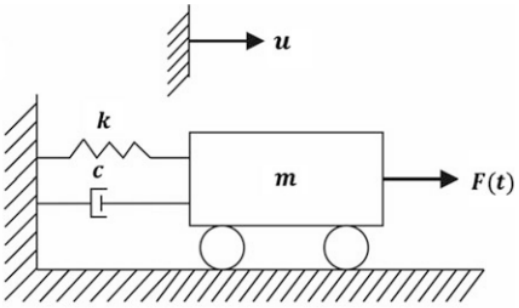

Figure 2.23: A model for a damped SDOF mass-spring system with mass m, stiffness k, viscous damper c, displacement $u(t)$ and force $f(t)$.

The damping force f_c is presented in following Equation 2.26, where c describes the viscous damping coefficient in unit [Ns/m] and $\dot{u}(t)$ is the velocity which is the first time derivative of the displacement u.

$$f_c = c\dot{u}(t) \tag{2.26}$$

Newton's second law of motion presented in Equation 2.7 can be formulated for the damped SDOF mass-spring system above as shown in Equation 2.27.

$$m\ddot{u} + c\dot{u}(t) + ku = f(t) \tag{2.27}$$

The structural dynamic equation of a damped MDOF system can then be written as in 2.28:

$$\mathbf{M}\ddot{\mathbf{u}}(t) + \mathbf{C}\dot{\mathbf{u}}(t) + \mathbf{K}\mathbf{u}(t) = \mathbf{f}(t) \tag{2.28}$$

Damping is both frequency and mode dependent with regard to its mechanism and also its magnitude. The viscous damping ratio is defined by expression in 2.29:

$$\xi = \frac{c}{2\sqrt{km}} \tag{2.29}$$

The damping matrix can be constructed on a global level by the equation 2.30.

$$\mathbf{C} = \alpha\mathbf{K} + \beta\mathbf{M} \tag{2.30}$$

Where α and β are coefficients that serve as positive scalar factors, providing a two-factor flexibility in the modelling of damping. They can be calculated from 2.31.

$$\xi_k = \frac{1}{2}\left(\frac{\alpha}{\omega_k} + \beta\omega_k\right) \tag{2.31}$$

2.8 Wind Dynamics

New lightweight materials in combination with taller buildings and optimization in design have caused dynamic responses for buildings to increase (Smith & Coull, 1991). In some cases, the dynamic stresses can be larger compared to the static stresses. The wind forces cause sinusoidal vibrations in the structure. The vibrations can both be caused by winds along the structure and cross-winds. The winds result in rotation around the vertical axis. The extent of the displacement depends on several factors which include material properties, the geometry of the structure and the wind velocity and direction. In some cases, the cross-wind action can govern the design of the building.

2.8.1 Human Response to Movements in Tall Buildings

From the perspective of an occupant, a tall building should not move horizontally (Smith & Coull, 1991). The movement of a building can have a negative impact on humans. Two examples of these are anxiety and acute nausea. Larger movements have a larger impact. If the movements cause large accelerations that the comfort criteria is no longer fulfilled, the buildings could become undesirable to live in or to work at, which can be a problem for the owner of the building. It is therefore important not to just design for ULS.

Many different factors contribute to how humans tolerate and precipitate motions of a swaying building (Saemundsson, 2007). Some examples of psychological effects are presented further in this section.

- The effect is dependent on the individuals, where everyone will experience motions and vibrations in different ways.
- A gender-specific effect and different genders will experience motions differently. Women are often more sensitive.
- Age-related effect. Children are more sensitive to motions compared to older people.
- A body-related effect where depending on orientation the motion is precipitated differently. A human who experiences a side-to-side motion is less sensitive than a person exposed to a forward-backward motion. The individual's body type will also have an influence.
- Effect related to the expectancy of movement. If a person knows that the building is moving, they would be more sensitive to movements.
- An effect that considers walking or other movements inside the building. A moving person can tolerate more movements compared to a still person.
- An effect which is dependent on different types of clues. When looking outdoors one may see that the outside moves compared to the inside.
- Another effect is the hearing. The winds can make one think that the building is swaying.

Another category of effects is physiological effects which are presented in this section (Saemundsson, 2007). The swaying of the building can be felt in a sense of balance. A person who is exposed to swaying can feel acceleration, but could also feel motion sickness. When touching a vibrating object the whole body can feel it. When a building is moving, objects that are hanging such as lamps might move freely. Different levels of perception are described in Table 2.1.

Table 2.1: Perception levels (Abu-zidan et al., 2022)

Level	Acceleration [m/s^2]	Effect
1	< 0.05	Humans cannot perceive motion.
2	0.05 - 0.1	Sensitive people can perceive motion, and hanging objects may move slightly.
3	0.1 - 0.25	Majority of people will perceive motion. May affect desk work, and long-term exposure may produce motion sickness.
4	0.25 - 0.4	Desk work becomes difficult or almost impossible, but ambulation is till possible.
5	0.4 - 0.5	People strongly perceive motion and walking naturally is difficult. Standing people may lose balance.
6	0.5 - 0.6	Most people cannot tolerate motion and are unable to walk naturally.
7	0.6 - 0.7	People cannot walk or tolerate motion.
8	> 0.85	Objects begin to fall, and people may be injured.

2.8.2 Wind Field

The wind profile varies with the height of a structure above the surface of earth and is also dependent on the terrain category which is characterized by different *roughness length* z_0 for different terrain category, as illustrated in Figure 2.24. Various phenomena contribute to the dynamic response of structures coming from wind, including buffeting, vortex shedding, galloping, and flutter (Mendis et al., 2007). Slender structures are prone to experiencing dynamic responses aligned with the

wind direction, primarily due to turbulence buffeting. Transverse or cross-wind responses are more likely to be triggered by vortex shedding or galloping but can also result from excitation caused by turbulence buffeting. Flutter is a coupled motion, often involving a combination of bending and torsion, and has the potential to result in instability. However, in many cases for building structures flutter and galloping are not considered as an issue.

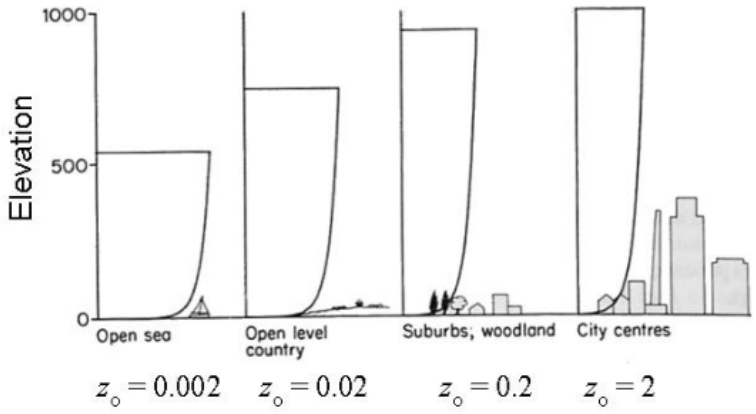

Figure 2.24: Mean wind profiles for different terrains (Mendis et al., 2007).

Wind acting on a building can generate significant, fluctuating forces on the structure's facade, resulting in vibrations in both rectilinear and torsional modes. The building's response is typically assessed in the along-wind direction, cross-wind direction, and torsional response. These responses are illustrated in Figure 2.25 below.

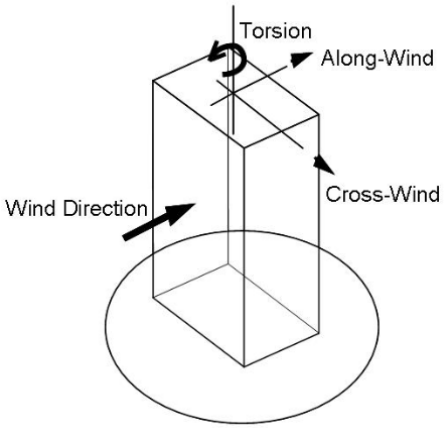

Figure 2.25: Wind response directions. (Mendis et al., 2007).

2.8.3 Vortex Shedding Phenomena

In a steady flow of air, forces on a structure can vary due to friction between the air and surfaces. Unless the structure is highly streamlined with low flow velocity, these forces undergo fluctuations, leading to the shedding of vortices alternately

from one side to the other. This process generates alternating low-pressure zones on the downwind side, giving rise to the phenomenon of *Vortex Shedding* (Strømmen, 2010) which illustrated in Figure 2.26. The primary source of crosswind excitation, often associated with vortex shedding, is prevalent in tall buildings, which, being bluff bodies rather than streamlined, cause the flow to separate from the structure's surface rather than following its contour.

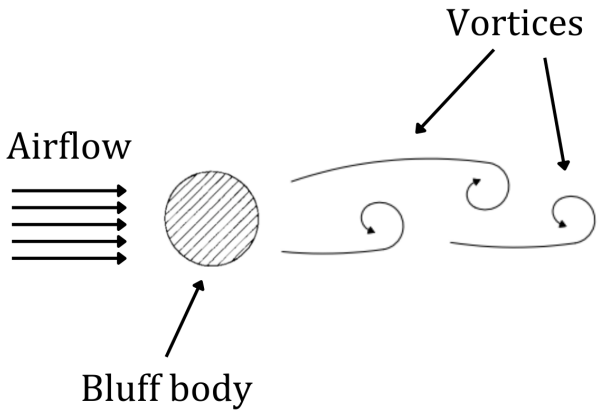

Figure 2.26: Vortex shedding behind a bluff body.

2.8.4 Structural Response Related to Wind

To describe the wind loads historical data about wind velocity and climate (Smith & Coull, 1991) can be provided by the Swedish Meteorological and Hydrological Institute. Other aspects also contribute to the understanding of wind. Some of these are wind turbulence properties, wind velocity variation, and interactional forces between the turbulent boundary layer of the building and its response to aerodynamics.

There are some characteristics of a structure that will determine if a dynamic analysis is needed (Smith & Coull, 1991). Those are mainly the resonance frequencies for the first couple of normal modes of vibration and geometry of the building. For small buildings, the facade will be exposed to the whole spectrum of frequencies caused by the first boundary of turbulence and the turbulence the building will generate.

In tall buildings, smaller gusts will only act on parts of the building (Smith & Coull, 1991). For hybrid structures with large amounts of timber, the building will be more flexible compared to a concrete building. Flexible lightweight buildings do have lower natural frequencies compared to more rigid buildings such as concrete buildings. The frequency of the wind force has a large impact on the building's structural response. When the building is exposed to wind forces acting below the resonance frequencies the building's response will follow the forces. When the wind forces follow the same frequency as the natural frequency of the building the acceleration can be large. The accelerations will cause deflection which can be larger than the deflection for the static scenario. In these cases, the dynamic stresses can also become larger than the static scenario. When the frequency of the forces increases the acceleration will decrease. The dynamic effect of deflections and stresses needs

to be considered in the design process.

2.8.5 Wind Tunnel Tests

The testing of wind tunnels originated in Copenhagen in 1893 where a model of a structure was tested (Cermak, 1977). In 1933 a model of the Empire State Building was tested and some wind pressures were measured. The tests then had a uniform wind velocity for the entire height of the tunnel. No trials regarding turbulence were performed at that time.

Sometimes, the analytical determination of wind loads does not capture the actual response of a building (Mendis et al., 2007). The associated building may have an unusual shape or flexibility. Accurate wind forces can be obtained through testing. Testing buildings in wind tunnels has become popular. The tunnel testing can result in lower wind loads compared to the building code and material costs can be decreased.

There are generally two different categories of wind tunnel tests (Mendis et al., 2007). The first category is to determine the wind load effect acting on the structure in order to design the structural elements. The other category is to model the dynamic wind flow close to the building. This is important if, for example, one wants to know how cyclists or pedestrians are affected by the winds. The complex aerodynamics are modeled with simple building structures. The simple models can be used as the displacement is simplified to a vertical line for the fundamental mode.

When there are buildings close to the planned new building cross-winds may occur and need to be considered (Mendis et al., 2007). As a rule of thumb, structures closer than ten times the width of the planned building should be considered. If there are plans for future buildings in the area they should also be considered. The buildings are placed on top of a rotating board to model the wind from different directions. The floor in the wind tunnel has a pattern that makes the surface uneven to simulate the landscape terrain.

2.9 Standards

The Swedish National Annex (EKS) regulates the design of a building in Sweden (Boverket, 2021). Concerning dynamic analysis and wind loads, there are some limitations to consider. The appendices include the determination of the structural factor C_sC_d, which is used to calculate the structural response of a building. EKS has its own method to calculate C_sC_d that originates from BSV 97 (Boverket, 1997). The EC (SS-EN 1991-1-4, 2005) also has some limitations concerning wind load, where for example only the first mode of vibration can be considered, and if torsional vibrations need to be studied the standard cannot be used. The dynamic loads should be used in the design of structural elements. The building's acceleration also

needs to be investigated using the EKS and SS-ISO 10137 (2008) which contain recommendations regarding allowable accelerations for a building.

2.9.1 Wind Calculations in Ultimate Limit State

The process of determining wind forces involves complying with various standards such as Eurocode 1 (SS-EN 1991-1-4, 2005) and the Swedish National Annex, EKS 12 (Boverket, 2021). These regulations provide guidelines for building design with respect to wind actions. They encompass crucial aspects such as reference wind velocity, terrain category, and also include several equations, tables, and empirical values for consideration.

2.9.1.1 Reference Wind Velocity

The Swedish National Annex EKS 12, illustrates the values of the reference wind velocity v_b in [m/s] on a map of Sweden, highlighting different regions in the country with specific reference wind velocity values (Boverket, 2021). The reference wind velocity v_b is ranging between 21-26 m/s as can be seen in Figure 2.27 below.

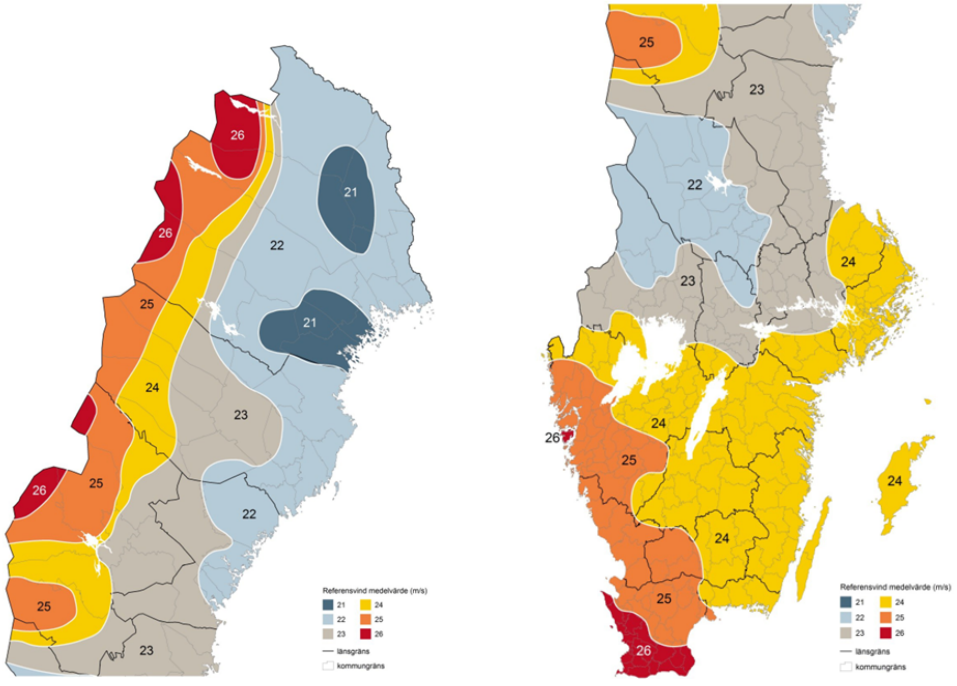

(a) Northern part of Sweden **(b)** Southern part of Sweden

Figure 2.27: The reference wind velocity v_b in [m/s] for different regions in Sweden, (Boverket, 2021)

The reference wind velocity v_b is being determined as a mean wind velocity accounted for 10 minutes at a height of 10 meters above the ground with a roughness length of $z_0 = 0.05$ and a repetition time of 50 years.

2.9.1.2 Terrain Category and Exposure Factor

In Eurocode 1, (SS-EN 1991-1-4, 2005), five different terrain categories are specified and they outline regulations concerning orographic effects, encompassing aspects such as displacement height, variations in roughness, the impact of the landscape, and the influence of nearby structures. Each terrain type is assigned a value for *roughness length* z_0 as shown in Table 2.2 below.

Table 2.2: Terrain categories and terrain parameters (SS-EN 1991-1-4, 2005)

Terrain category		z_0 m	z_{min} m
0	Sea or coastal area exposed to the open sea	0,003	1
I	Lakes or flat and horizontal area with negligible vegetation and without obstacles	0,01	1
II	Area with low vegetation such as grass and isolated obstacles (trees, buildings) with separations of at least 20 obstacle heights	0,05	2
III	Area with regular cover of vegetation or buildings or with isolated obstacles with separations of maximum 20 obstacle heights (such as villages, suburban terrain, permanent forest)	0,3	5
IV	Area in which at least 15 % of the surface is covered with buildings and their average height exceeds 15 m	1,0	10

Furthermore, Eurocode 1, (SS-EN 1991-1-4, 2005), introduces a term called *exposure factor* $c_e(z)$ which varies based on different heights and terrain categories as illustrated in Figure 2.28.

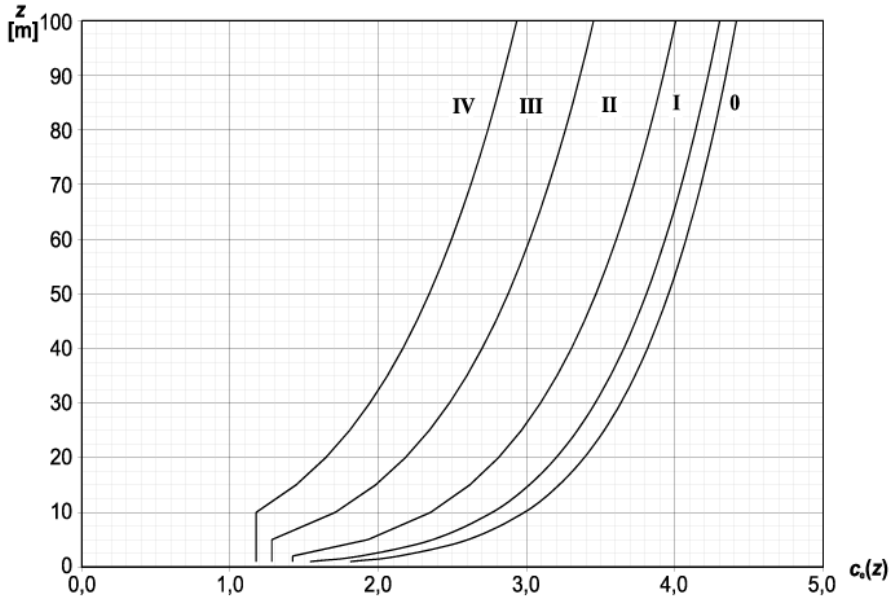

Figure 2.28: Exposure factor $c_e(z)$ depending on the height and terrain category.

2.9.1.3 Wind Pressure in EKS 12

The regulations outlining the method for calculating wind pressure can be found in the Swedish National Annex EKS 12 (Boverket, 2021). The expression 2.32 for determining the characteristic peak wind pressure $q_p(z)$ is presented as illustrated below.

$$q_p(z) = [1 + 2 \cdot k_p \cdot I_v(z)] \cdot \left[k_r \cdot \ln \frac{z}{z_0} \cdot c_o(z)\right]^2 \cdot q_b \tag{2.32}$$

Where:

- k_p is a peak factor, defined by Equation 2.36,
- $I_v(z)$ is turbulence intensity at height z, defined by Equation 2.35,
- k_r is a terrain factor, defined in Equation 2.45,
- z_0 is a roughness length, given by Table 2.2,
- $c_o(z)$ is a topography factor according to Annex A.3,
- q_b is the reference mean (basic) velocity pressure, defined in Equation 2.34,
- z is the height over the ground surface.

In cases where there is no need to consider the topography and eigenfrequency of the building, the characteristic peak wind pressure $q_p(z)$ can calculated by using Equation 2.33.

$$q_p(z) = c_e(z) \cdot q_b \tag{2.33}$$

Where:

- $c_e(z)$ is the exposure factor dependent on height and terrain category defined in Figure 2.28.

$$q_b = \frac{1}{2} \cdot \rho \cdot v_b^2 \tag{2.34}$$

Where:

- v_b is the basic wind velocity dependent on region, in Gothenburg $v_b = 25\ m/s$,
- ρ is the air density, which depends on the altitude, temperature and barometric pressure.

$$I_v(z) = \frac{1}{c_0(z) \cdot \ln\left(\frac{z}{z_0}\right)} \tag{2.35}$$

For buildings that do not require consideration of the building's eigenfrequency, the peak factor k_p can be set to 3.0. However, for buildings where dynamic effects on the wind peak pressure are substantial, the peak factor k_p should be calculated as expressed in 2.36.

$$k_p = \sqrt{2\ln(vT)} + \frac{0.6}{\sqrt{2\ln(vT)}} \tag{2.36}$$

Where $T = 600$ *seconds* which is the reference time for the mean wind velocity and v is the so called *up-crossing frequency* defined in 2.37.

$$v = n_{1,x} \frac{R}{\sqrt{B^2 + R^2}} \tag{2.37}$$

The fundamental flexural frequency $n_{1,x}$ is calculated based on the mass and stiffness of the multi-storey building. It is obtained though the analysis of the structure with FE-modelling in later stage.

$$n_{1,x} = \frac{46}{h} \quad [Hz] \tag{2.38}$$

The factor B^2 is the background response factor defined in Equation 2.39 and R^2 is the resonance response defined in Equation 2.40.

$$B^2 = exp\left[-0.05\left(\frac{h}{h_{ref}}\right) + \left(1 - \frac{b}{h}\right)\left(0.04 + 0.01\left(\frac{h}{h_{ref}}\right)\right)\right] \tag{2.39}$$

Where:

- h is the height of the structure,
- b is the cross-dimension which is perpendicular to the wind direction,
- h_{ref} is a reference height of 10 m.

$$R^2 = \frac{2\pi\ F\ \phi_b\ \phi_h}{\delta_s + \delta_a} \tag{2.40}$$

Where:

- F here is describing Kárman's wind energy spectrum defined in 2.41,
- ϕ_b is a size factor with respect to the width of the structure defined in 2.49,
- ϕ_h is also a size factor but with respect to the height of the structure defined in 2.48,
- δ_s is the structural damping expressed by the logarithmic decrement,
- δ_a is the aerodynamic decrement of damping.

$$F = \frac{4\ y_c}{(1 + 70.8\ y_c^2)^{\frac{5}{6}}} \tag{2.41}$$

The non-dimensional frequency y_c is given by Equation 2.42.

$$y_C = \frac{150\ n_{1,x}}{v_m(h)} \tag{2.42}$$

In Eurocode 1, (SS-EN 1991-1-4, 2005), a definition is made of $v_m(z)$ as the characteristic mean wind velocity at a height z above the ground, expressed by Equation 2.43 as follows.

$$v_m(z) = c_r(z) \cdot c_o(z) \cdot v_b \tag{2.43}$$

Where:

- c_o is set to 1.0 and it is a orography factor,
- c_r is the roughness factor.

$$\begin{aligned} c_r(z) &= k_r \cdot \left(\frac{z}{z_0}\right) \quad for \quad z_{min} \leq z \leq z_{max} \\ c_r(z) &= c_r\left(z_{min}\right) \quad for \quad z \leq z_{min} \end{aligned} \tag{2.44}$$

Where:

- k_r is a terrain factor depending on the roughness length z_0.

$$k_r = 0.19 \cdot \left(\frac{z_0}{z_{0,II}}\right)^{0.07} \tag{2.45}$$

Where:

- z_{min} is the minimum height defined in Table 2.2,
- $z_{0,II}$ is set to 0.05 m (terrain category II in Table 2.2),
- z_{max} is a maximum height to be taken as 200 m.

$$\delta_s \approx 2\pi \cdot \xi_1 \tag{2.46}$$

ξ_1 is the critical damping ratio at first natural frequency.

$$\delta_a = \frac{c_f \cdot \rho \cdot v_m(z_s)}{2 \cdot n_{1,x} \cdot m_e} \tag{2.47}$$

Where:

- c_f is the force coefficient for wind action in the direction, defined in 2.53,
- m_e is the equivalent mass of the structure.

$$\phi_h = \frac{1}{1 + \frac{2n_{1,x}h}{v_m(h)}} \tag{2.48}$$

$$\phi_b = \frac{1}{1 + \frac{3{,}2n_{1,x}b}{v_m(h)}} \tag{2.49}$$

According to Eurocode 1, (SS-EN 1991-1-4, 2005), Part 1-4 Wind Actions, the wind pressure acting on external surfaces, W_e is calculated from 2.50.

$$W_e = q_p(z_e) \cdot c_{pe} \tag{2.50}$$

Where c_{pe} is the pressure coefficient for the external pressure, given in (SS-EN 1991-1-4, 2005), Part 1-4 Wind Actions section 7. By employing Equation 2.51, wind forces F_w acting on a structure or structural component can be determined.

$$F_w = c_s c_d \cdot c_f \cdot q_p(z_e) A_{ref} \tag{2.51}$$

Where:

- $c_s c_d$ is the structural factor,
- c_f is the force coefficient for the structure or structural element,
- A_{ref} is the reference area of the structure or structural element.

The structural factor $c_s c_d$ is provided in EKS 12 as presented in the equation 2.52 below.

$$c_s c_d = \frac{1 + 2k_p I_v(z_s)\sqrt{B^2 + R^2}}{1 + 6I_v(z_s)} \tag{2.52}$$

The force coefficient can be calculated with Equation 2.53 (SS-EN 1991-1-4, 2005).

$$c_f = c_{f,0} \cdot \psi_r \cdot \psi_\lambda \tag{2.53}$$

Where:

- $c_{f,0}$ is the force coefficient without free-end flow. The coefficient is dependent on the geometry of the building,
- ψ_r is a reduction factor for a square section with rounded corners,
- ψ_λ is a reduction factor for elements with end effects. The factor can be calculated by using interpolation in Table 7.16 and Figure 7.36 (SS-EN 1991-1-4, 2005).

2.9.2 SLS

For the service limit state, the main criterion that needs to be fulfilled is acceleration. SS-ISO 10137 (2008) describes the limit for buildings. The acceleration for the building is defined in Equation 2.54.

$$\ddot{X}_{max}(z) = k_p \cdot \sigma_{\ddot{X}}(z) \tag{2.54}$$

Where:

- k_p is the peak factor defined in Subsection 2.9.1.3,
- $\sigma_{\ddot{X}}(z)$ is the standard deviation of acceleration and is defined in Equation 2.55.

$$\sigma_{\ddot{X}}(z) = \frac{3 \cdot I_v(h) \cdot R \cdot q_m(h) \cdot b \cdot c_f \cdot \phi_{1,x}(z)}{m} \tag{2.55}$$

Where:

- b, c_f, $I_v(h)$ and R are defined in Subsection 2.9.1.3,
- m is the equivalent mass,
- $\phi_{1,x}(z)$ is the mode shape function,
- $q_m(h)$ is the wind velocity pressure.

The mode shape function can be evaluated with Equation 2.56. Note that the function depends on the structure's boundary conditions. For the chosen building Equation 2.56 is suitable due to the building acting as a cantilever.

$$\phi_{1,x}(z) = \left(\frac{z}{h}\right)^{1.5} \tag{2.56}$$

Where:

- z and h are defined in Subsection 2.9.1.3.

The equivalent mass can be calculated with Equation 2.57 and should be equal to one or less. When the mass is the same for every floor the equivalent mass can be considered as the same as the mass of the building. In SS-EN 1991-1-4 (2005) the equivalent mass can be approximated as the average mass of the top 1/3 floors in the building. The approximation assumes a building that acts as a cantilever.

$$m_e = \frac{\int_0^l m(s) \cdot \phi_{1,x}^2(s) ds}{\int_0^l \phi_{1,x}^2(s) ds} \tag{2.57}$$

Where:

- m is the structural mass,
- $\phi_{1,x}(s)$ is the mode shape function defined in Equation 2.56.

The velocity pressure can be calculated with Equation 2.58.

$$q_m = 0.5 \cdot \rho \cdot v_{T_a}^2 \tag{2.58}$$

Where:

- ρ is the air density. SS-EN 1991-1-4 (2005) recommends a value of 1.25 kg/m^3,
- $v_{T_a}^2$ is the wind velocity. The limitation for accelerations (SS-ISO 10137, 2008) are given for one-year period and therefore should the wind velocity be for one year.

The wind speed from Subsection 2.9.1.1 is based on a 50-year period and needs to be calculated to a one-year velocity. where Equation 2.59 can be used. The main problem in the equation is T_a where if one inputs a one year time period the equation would not operate. The time period should be taken as two years to achieve the one-year wind speed.

$$v_{T_a} = 0.75 \cdot v_{50} \cdot \sqrt{1 - 0.2 \cdot ln\left(1 - \frac{1}{T_a}\right)} \tag{2.59}$$

Where:

- v_{50} is the wind velocity over a 50-year time period,
- T_a is the time period.

In SS-ISO 10137 (2008) Annex D there are recommendations for wind-induced oscillations in office and residential buildings. The limits are set with regard to satisfying regular human living conditions and as mentioned before it is based on a one-year period of acceleration. The allowable acceleration is dependent on the usage of the building. The limit for a residential building is 2/3 of an office building and can be observed in Figure 2.29.

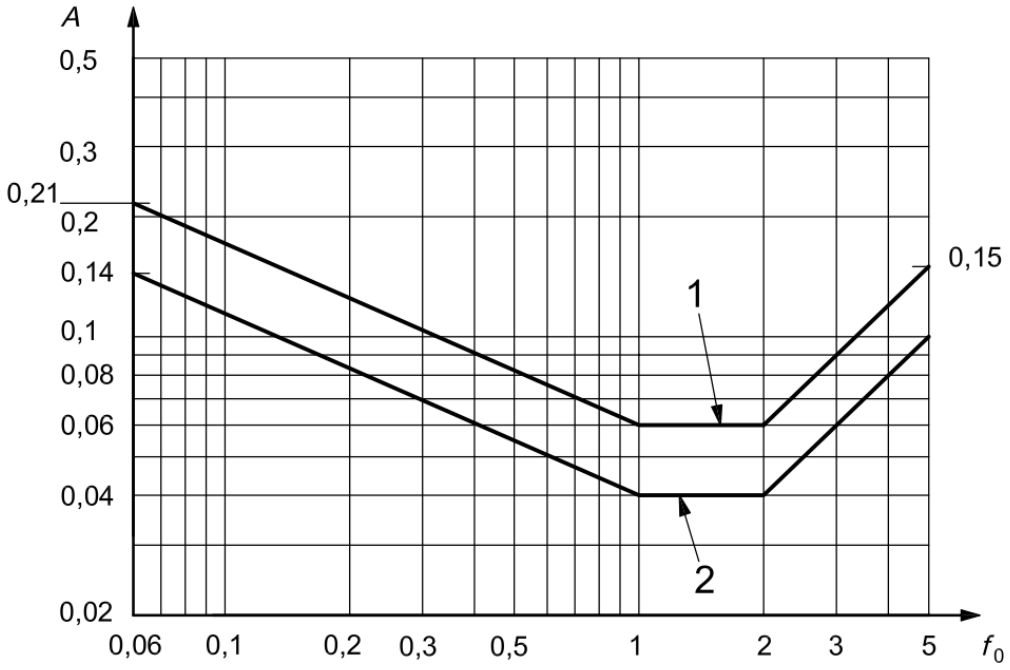

Figure 2.29: Allowable peak acceleration with regard to the fundamental frequency of the building.

As illustrated by Figure 2.29 above, there are two curves indicating the allowable peak acceleration values as a function of the fundamental eigenfrequency of the building. It's noteworthy that for a residential building with an eigenfrequency ranging from 1 to 2 Hz, the maximum allowable acceleration is 0.04 m/s². Conversely, for an office building with a fundamental eigenfrequency within the same range, the permissible maximum acceleration is higher, specifically 0.06 m/s².

3
Modelling

The chapter starts by presenting an overview of the different structural systems used later in the analyses. It is followed by a description of the different loads applied on the building. The model in the program is then explained, and a convergence study is performed. The models are verified to verify the building's behavior. Lastly, an overview of the analysis procedure is explained.

3.1 Layout of the Residential Building

The first structure to be modeled is a residential tower building with dimensions of 21.8 meters in length and 21.8 meters in width. It functions as a residential building with a storey height of 3 meters. There are plans for six different apartments on each floor. The hybrid building's primary structural system is a wall-slab system, complemented by a rigid concrete core at the building's center. Shafts for the elevators, staircase, and installations are situated at the core. CLT panels with an orthotropic material model are utilized for wall and slab plates. The load-bearing direction of the slabs aligns with the shorter span of the slab. An illustration of the layout of the floor plan is presented in Figure 3.1.

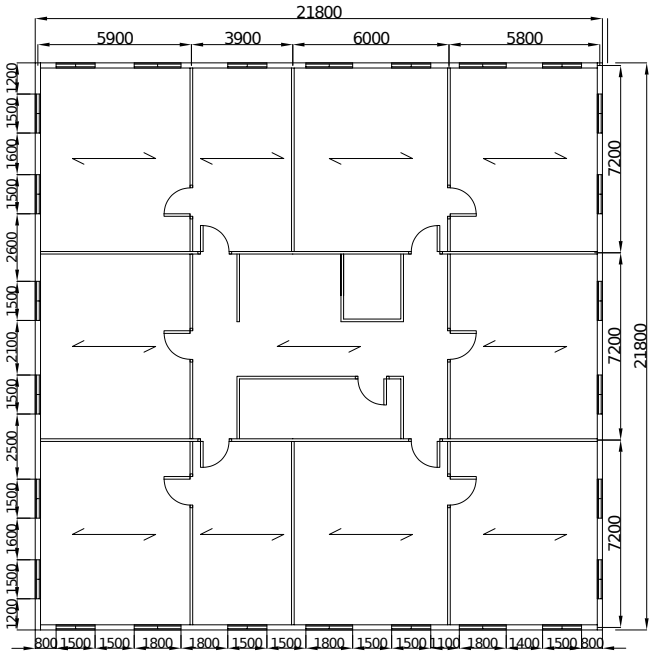

Figure 3.1: Layout of the floor plan of the building with dimensions in [mm].

The building is located in the city of Gothenburg and therefore terrain category III is assumed. The mean wind velocity is measured for Gothenburg to be at 25 m/s. The building is assumed to be built on a stiff concrete foundation.

3.2 Layout of the Office Building

The second structure to be modeled is an office tower building with approximately the same dimensions as the residential building, with 22.07 meters in length and 21.90 meters in width. It functions as an office building with a storey height of 3.5 meters. In order to make the floor plan flexible and open a structural system comprising a glulam timber beam-column system is employed. The structural system is also complemented by a rigid concrete core located at the building's center. Shafts for the elevators, staircase and installations are situated in the core. CLT panels with an orthotropic material model are utilized for slab plates on each floor.

The load-bearing direction of the slabs aligns with the direction perpendicular to the beams span length. An illustration of the layout of the floor plan is presented in Figure 3.2. Beams are generally supported on columns but only four beams on each floor have one edge supported by concrete walls in the core instead.

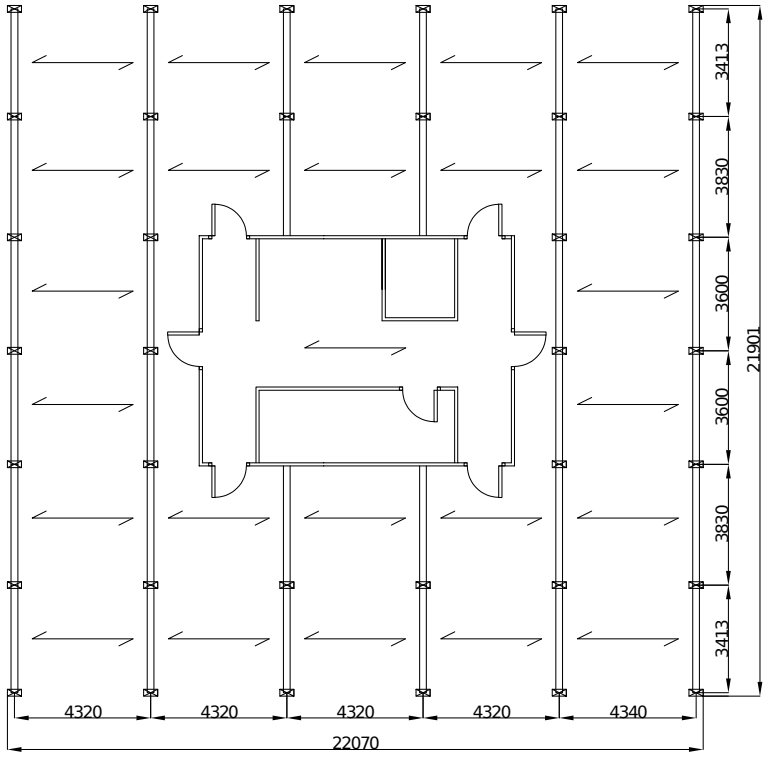

Figure 3.2: Layout of the floor plan of the office building with dimensions in [mm].

3.3 Loads

The vertical loads used in modelling of the buildings are self-weight, live loads and snow loads. The live load for a residential building was applied with a value of 2 kN/m^2 and for an office building the corresponding live load was 2.5 kN/m^2. The snow load map from EKS 12 (Boverket, 2021) was used and then snow shape coefficient for a flat roof was adopted to determine the characteristic snow load on the roof. Thus, the resulting snow load value is 1.2 kN/m^2.

To apply the horizontal wind loads, a few methods were considered. First, by applying the peak wind pressure to the whole structure. The building will be tall which would overestimate the pressure at the lower levels. Second, by using a method proposed by Eurocode, SS-EN 1991-1-4 (2005) which also is conservative. A third method was to adopt the wind pressure with a logarithmic function in the FEM software. Therefore, an approximation of the logarithmic function of the wind was made analytically and then used in the software FEM-Design. Thus, the peak pressure of each floor was adopted for the whole facade of each floor, see Figure 3.3.

The wind pressure for each floor depends on the natural frequency and the equivalent mass in EKS 12 (Boverket, 2021). The pressure would, therefore, change for every iteration as these parameters are changed. In earlier versions of EKS (Boverket, 2021), the peak factor k_p, which is used for calculating the wind pressure q_p, was a constant value of 3. However, in later versions of EKS, this peak factor k_p is dependent on the fundamental frequency and equivalent mass of the building. The largest difference between the wind pressure of the EKS 10 and that of the updated one was a factor of 1.13 for a tested building. The wind pressure from EKS 10 was, therefore, multiplied by a factor in the load combination of 1.15. This factor could change depending on the material and geometry of the building. The different wind pressures for a building can be observed in Figure 3.3. Besides this factor, the wind pressure is also multiplied with $c_s c_d$, which also will change with natural frequency and equivalent mass.

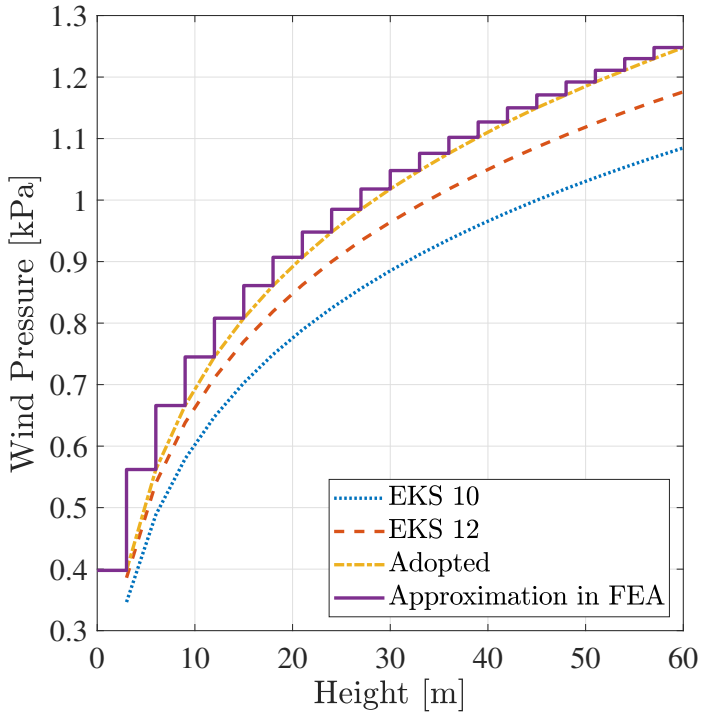

Figure 3.3: Wind pressure at different heights.

3.4 The Finite Element Model of the Residential Building

A finite element (FE) model has been created for the structural analysis of the building, employing the FEM-Design software. Timber plates are utilized for the CLT panels within the slabs and walls. The orientation of the slabs is such that the main load-bearing direction aligns with the shorter length of the slabs, because of the higher stiffness in this direction which will attract more load. An illustration is presented in Figure 3.4. The analysis of the model is performed with shell elements and different element sizes are used to establish a convergence of the analyzed parameters.

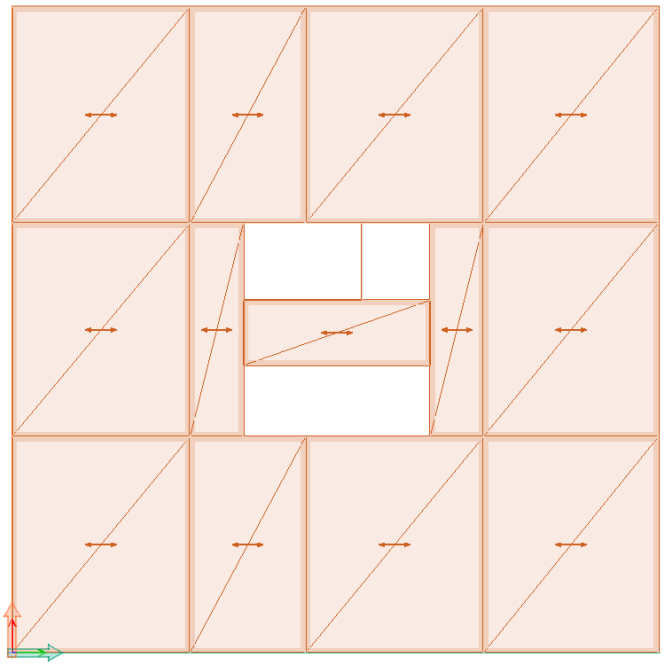

Figure 3.4: The main load-bearing direction of the slabs.

In Figure 3.5 below, an illustration depicts a single floor with both outer and inner walls. The illustration includes cut-outs in the walls representing windows and doors. Some windows are sized at 1.5 x 1.5 m^2 and others at 1.8 x 1.8 m^2, while doors measure 1.0 x 2.0 m^2. All windows are placed at a height of 1 m above each floor level. The main load-bearing direction of the walls aligns with the vertical direction, which can be seen in Figure 3.5.

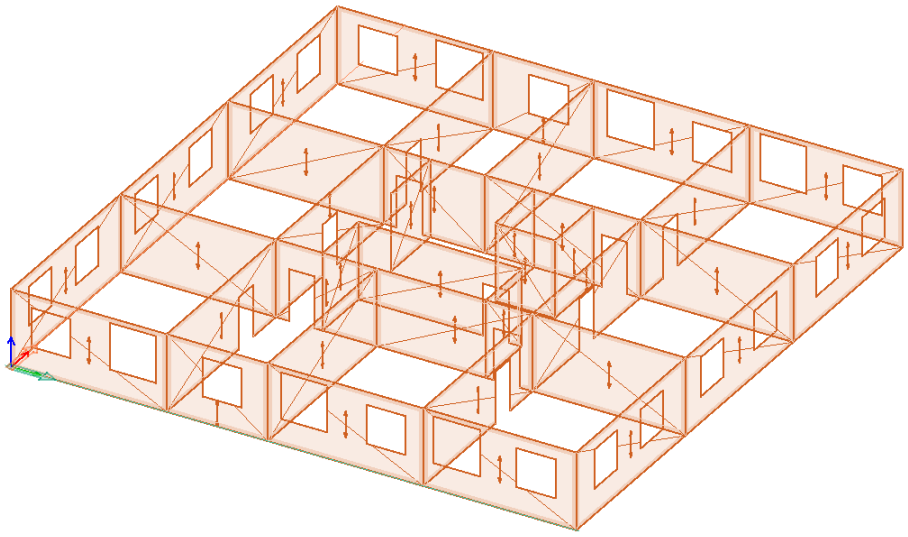

Figure 3.5: The main load-bearing direction of the walls.

The entire FE model, which is depicted of Figure 3.6 was created by using CLT-panels provided in the FEM-Design software, employing a linear-elastic material

model. Connections between the walls of the first floor and the foundation are considered stiff, allowing for moment transfer to the foundation. Conversely, all other connections in the building are assumed to be hinged, which on the contrary do not have the possibility for moment transfer in these connections.

Covers were utilized to seal cut-outs in the facade where windows are located. This is essential to accurately apply the wind load on each facade and floor. All different load cases were applied in the building model and analysis of the FE model was done to verify mesh convergence and that the results of the analysis are reliable.

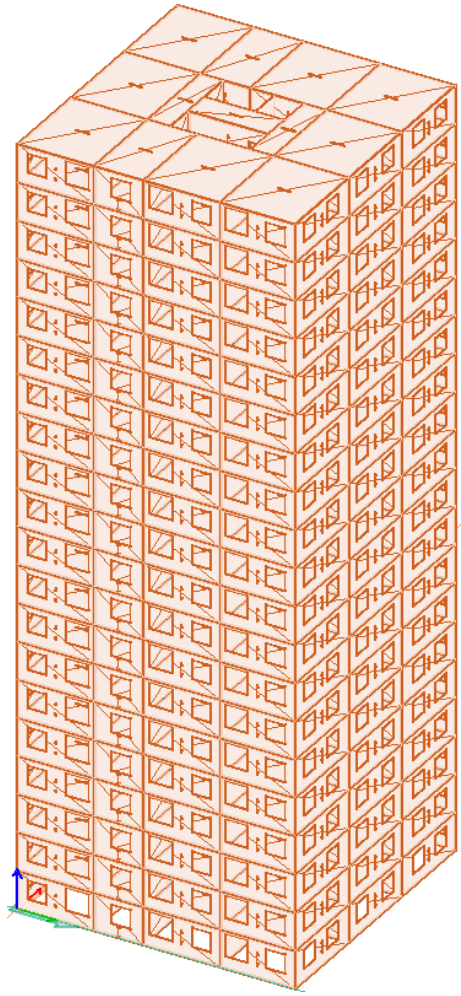

Figure 3.6: FE model of the 20-storey residential building in FEM-Design.

3.5 The Finite Element Model of the Office Building

Another finite element model has been created for the structural analysis of the office building. Timber plates are utilized for the CLT panels within the slabs. The orientation of the slabs is such that the load-bearing direction of the slabs aligns

with the direction perpendicular to the beams span length. An illustration for a single floor from the FE model is presented in Figure 3.7. The analysis of the model is performed with shell-elements for slabs and core walls, while beam-elements were used for columns and beams. Different element sizes are used to establish a convergence of the analyzed parameters.

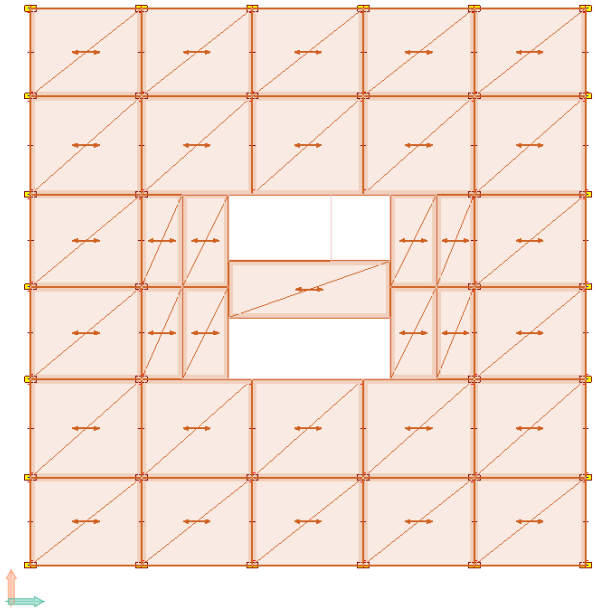

Figure 3.7: The layout and main load-bearing direction of the slabs.

Glulam timber beams and columns comprise the structural system of this model. The building features a concrete core extending its entire height, constructed with concrete walls. Figure 3.8 presents a model for the structural system on a single floor.

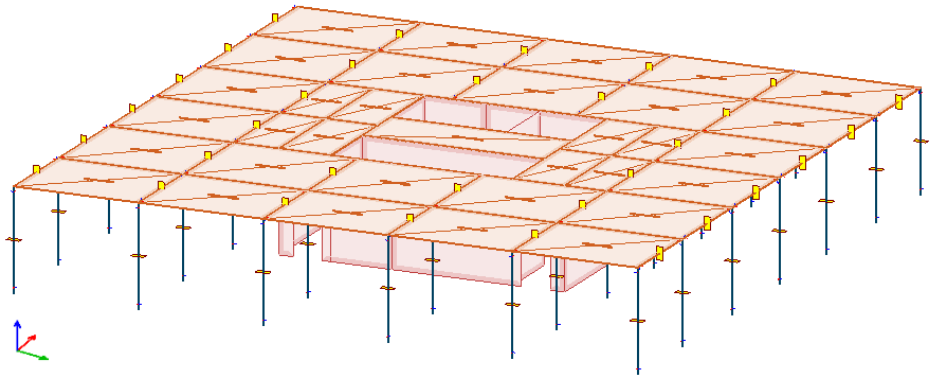

Figure 3.8: The main load-bearing elements in one floor of the office building.

Several assumptions were made in the modeling of the office building. Firstly, it is assumed that the building is constructed on a stiff foundation. Consequently, the

columns on the first floor are considered to be fixed at one end, implying a rigid connection between these columns and the foundation. For all subsequent floors above the first, the columns are modeled as simply supported, featuring hinged connections at both ends. Similarly, all beams in the model are assumed to be simply supported, with hinged connections at both ends. Figure 3.9 illustrates the complete finite element (FE) model of the office building, encompassing 20 storeys.

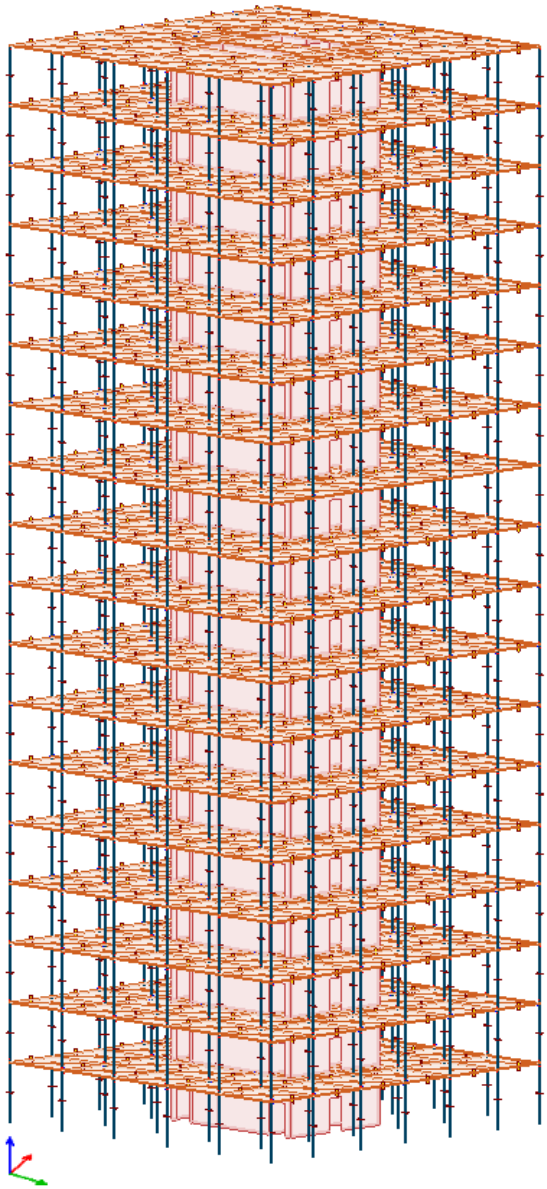

Figure 3.9: FE model of the 20-storey office building in FEM-Design.

3.6 Convergence Study

The building studied for the convergence analysis is a 20-storey CLT building. The material and geometry used for walls and floor elements are five-layer panels with

a thickness of 180 mm. This study has two main purposes. The first is to validate the results. A too-coarse mesh will lead to inaccurate results. A finer mesh will have more accurate results but the analysis can take a longer time and after a certain mesh size the results will not change significantly. As many analyses will be performed, the calculation time is crucial and the convergence study can save a lot of time. The other purpose is related to verifying the behavior of the structural elements in the building. The convergence study was performed where the seed size of the surface elements was decreased until convergence was reached for several parameters. The convergence analysis was based on the following:

1. An average moment perpendicular to the main load-bearing direction in the middle of a facade wall on the first floor.
2. Maximum moment in the middle of the facade wall.
3. An average moment perpendicular to the main load-bearing direction in the middle of a CLT-slab element on the first floor.
4. Maximum moment in the middle of the floor element.
5. An average shear force perpendicular to the main load-bearing direction a half of a meter from the edge of a CLT-element on the first floor.
6. Maximum shear force a half meter from an edge in the load-bearing direction.
7. An average value of in-plane shear forces in an internal shear wall inside the core, half a meter from the top of the wall perpendicular to the main load direction on the first floor.
8. Maximum in-plane shear forces in an internal shear wall inside the core in the middle of the wall on the first floor.
9. An average of compression forces in an internal shear wall inside the core in the middle of the wall perpendicular to the main load direction on the first floor.
10. Maximum compression forces in an internal shear wall inside the core in the middle of the wall on the first floor.
11. Fundamental frequency of the building.

A new mesh convergence study has been conducted, incorporating a design with CLT panels in the finite element model (FE-model). The investigation maintains the same seed size for elements as in previous studies. In this iteration, an additional parameter is examined concerning the maximum in-plane shear force within the internal shear walls inside the core.

12. Maximum in-plane shear forces in an internal shear wall inside the core at the sixth floor above a door opening.

The results from the mesh convergence study are illustrated in Figure 3.10 below. Detailed values for each mesh size used in the analyses can be found in Appendix A.1. Based on these graphs, it was decided that an average seed size of 0.4 m would be appropriate and all the analyses in the following chapter would use the chosen

element size.

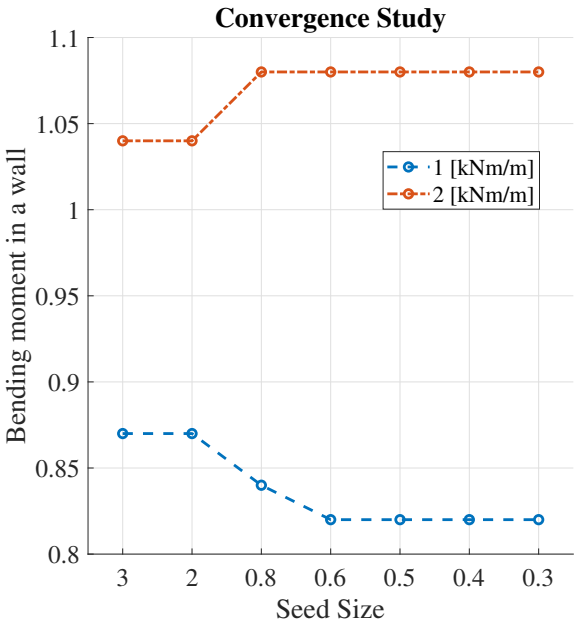

(a) Bending moment in a wall

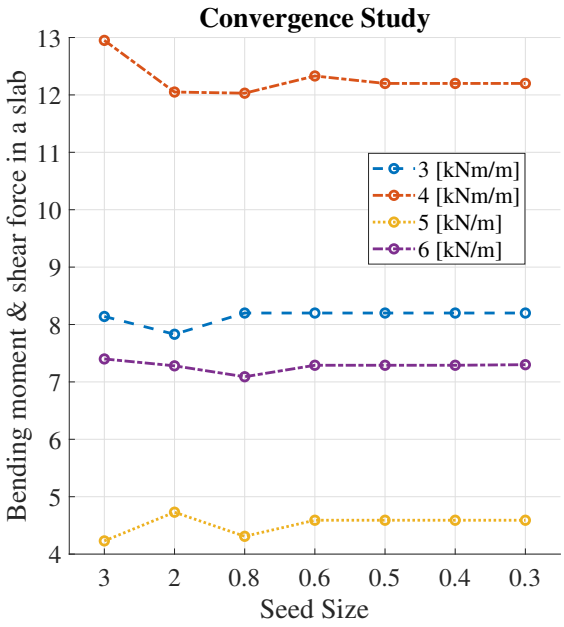

(b) Bending moment & shear force in a slab

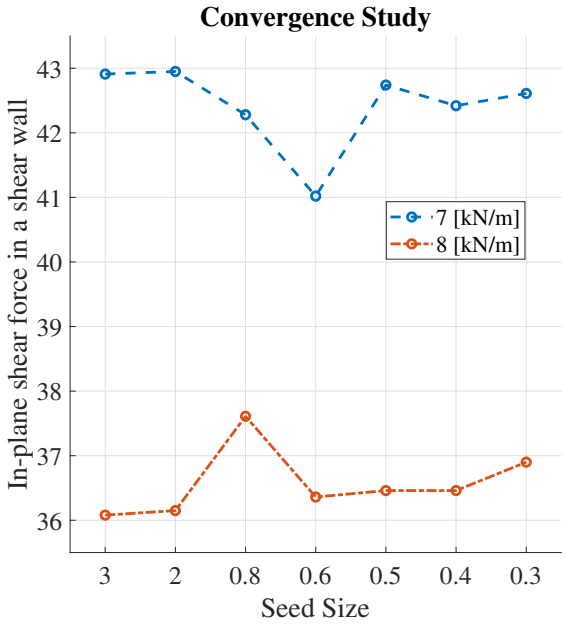

(c) In-plane shear force in a shear wall

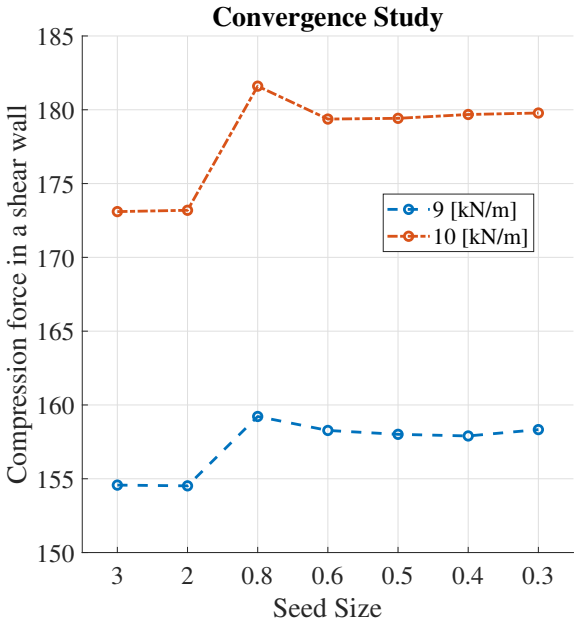

(d) Compression force in a wall

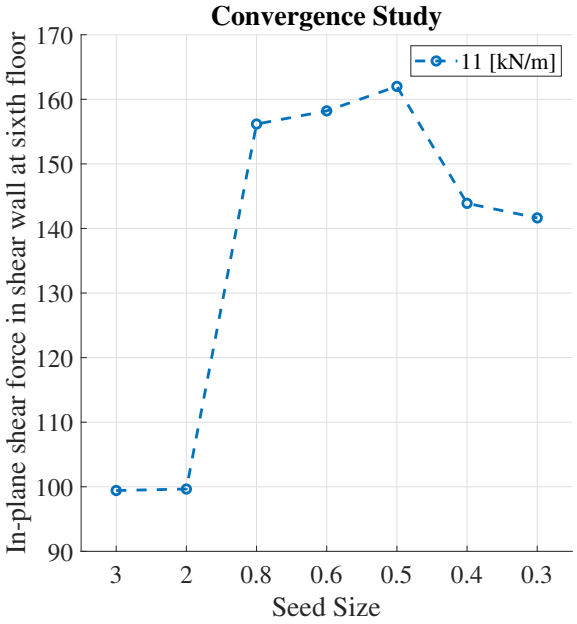

(e) In-plane shear force in a shear wall at sixth floor

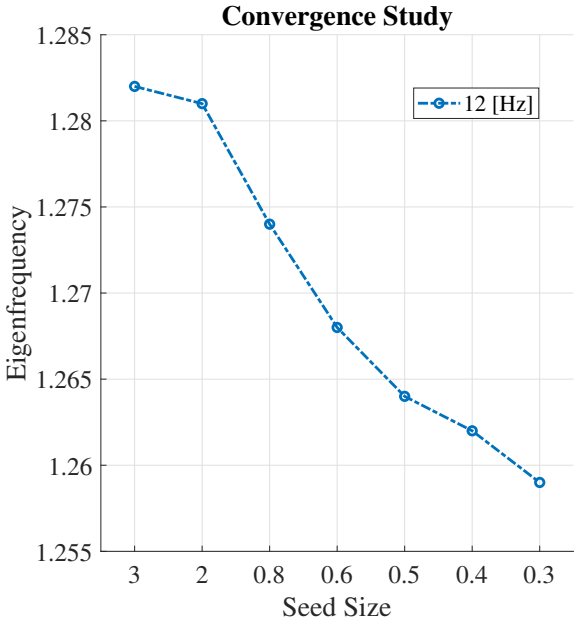

(f) Eigenfrequency

Figure 3.10: Convergence analysis

3.7 Verification of the First FE Model

To ensure that the behavior of the model corresponds to the intended behavior, a verification was performed. First, two finite element models were created independently of each other to compare different analyses between the models. The first verification concerns the dynamic behavior of the structure. The different mode shapes were important to compare between the models. The first modes of a tall building were global ones where the first two shapes were transitional movements and the third was a rotational movement. If the first mode shape had been a local, it could have been an indication that structural elements are not connected or supports may not have been correctly applied. The eigenfrequencies between the models corresponded to each other and the structural masses of the different models were also similar. An illustration of the first three vibrational mode shapes are presented in Figure 3.11.

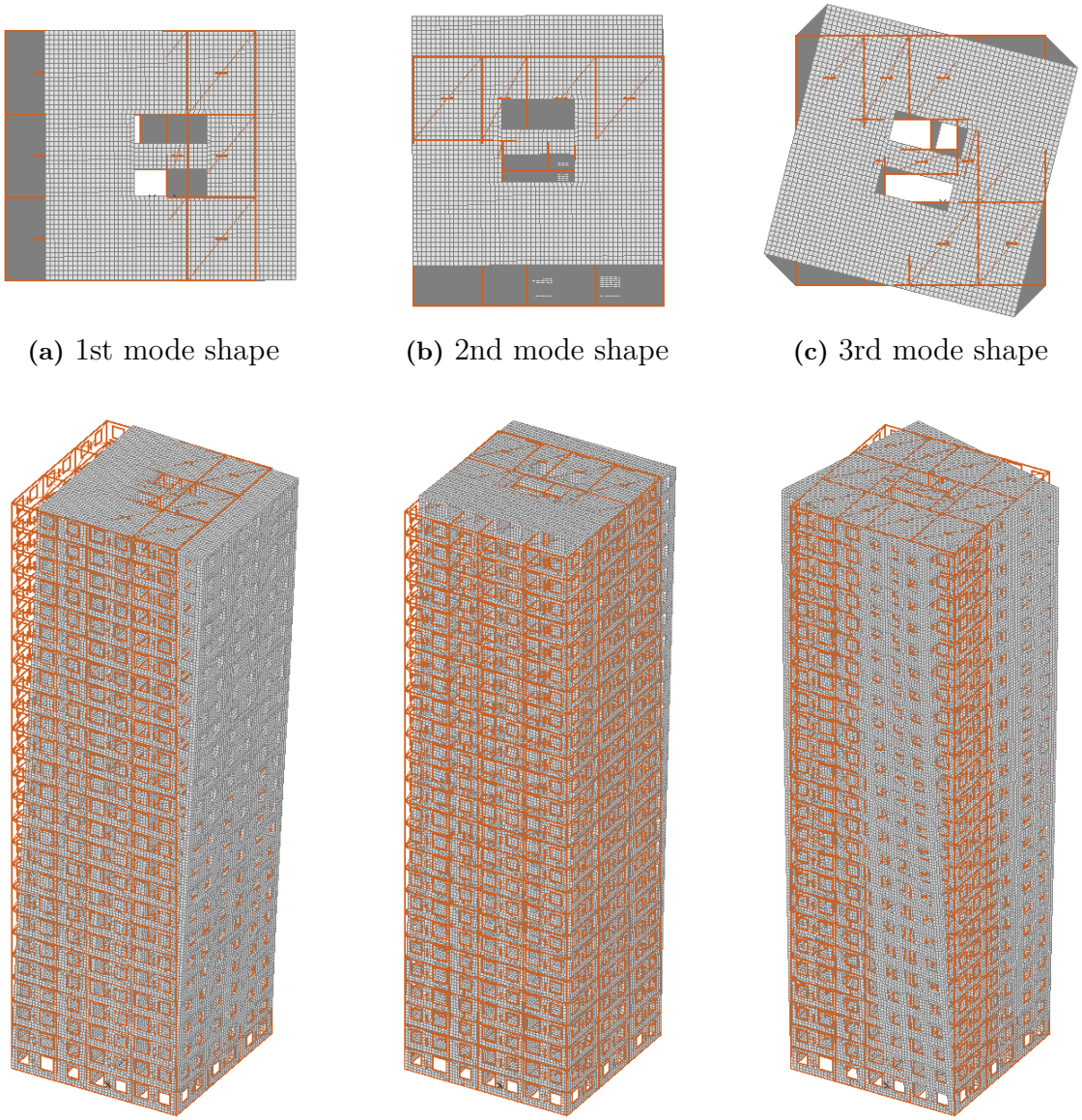

(a) 1st mode shape **(b)** 2nd mode shape **(c)** 3rd mode shape

(d) 1st mode shape **(e)** 2nd mode shape **(f)** 3rd mode shape

Figure 3.11: Illustration of the first global vibration mode shapes.

A comparison of many parameters between the two different models was performed. These include compression, bending moments, and shear forces. These parameters are the same as the convergence study in Section 3.6. The difference between the models where approximately 1-2 percent, which is acceptable.

The FEM program contains CLT elements from different manufacturers with material properties. Eurocode verifications and other design checks can be performed quickly in the program. These verifications have been performed by hand with the CLT Handbook (Swedish Wood, 2019). There is one design verification that is described in the handbook but not in the FE-program, which is shear between layers, which will not be considered in the design due to small shear forces parallel

to the main load direction and will not govern the design. To verify the design checks performed in the FE-software, a model with one wall was created which the results from were compared with hand calculations. Large wind loads contribute to in-plane shear forces and should also be considered. The walls should not be exposed to larger bending moments as almost no loads are applied in the direction that is perpendicular to the length and width of the panel. The self-weight and live loads would contribute to compression forces in the wall. In summary, compression, tension, and in-plane shear verification in the FE software were compared with the hand calculations.

3.8 Verification of the Second FE Model

To verify the structural behavior of the new FE-model, a dynamic eigenfrequency analysis was conducted. This analysis is a crucial step in assessing how the structure responds to dynamic loads and identifying its natural vibrational characteristics. The eigenfrequency analysis reveals the mode shapes of vibration, which are fundamental for understanding the dynamic behavior of the structure.

Illustrations of the first three global vibrational mode shapes extracted from the analysis results are presented in Figure 3.12. These mode shapes represent distinct patterns of movement that the structure exhibits when subjected to vibration.

The first two mode shapes predominantly exhibit translational motion along different axes within the plane of the building. Translation in this context refers to movement where all points in the structure move parallel to each other, akin to shifting or sliding. Each mode shape may emphasize movement along a specific axis, such as lateral or vertical translation, depending on the structural configuration and loading conditions.

Conversely, the third vibrational mode shape tends to exhibit torsional or rotational motion. Rotation implies a spinning or pivoting movement around a central axis. In this mode, the structure rotates about its center as a reference point, indicating a different type of dynamic response compared to translational motion.

Understanding these vibrational mode shapes is essential for evaluating the structural performance and identifying potential areas of concern. By analyzing the dominant modes of vibration, it is possible to assess how the structure responds to dynamic forces and optimize its design to enhance performance, stability, and safety.

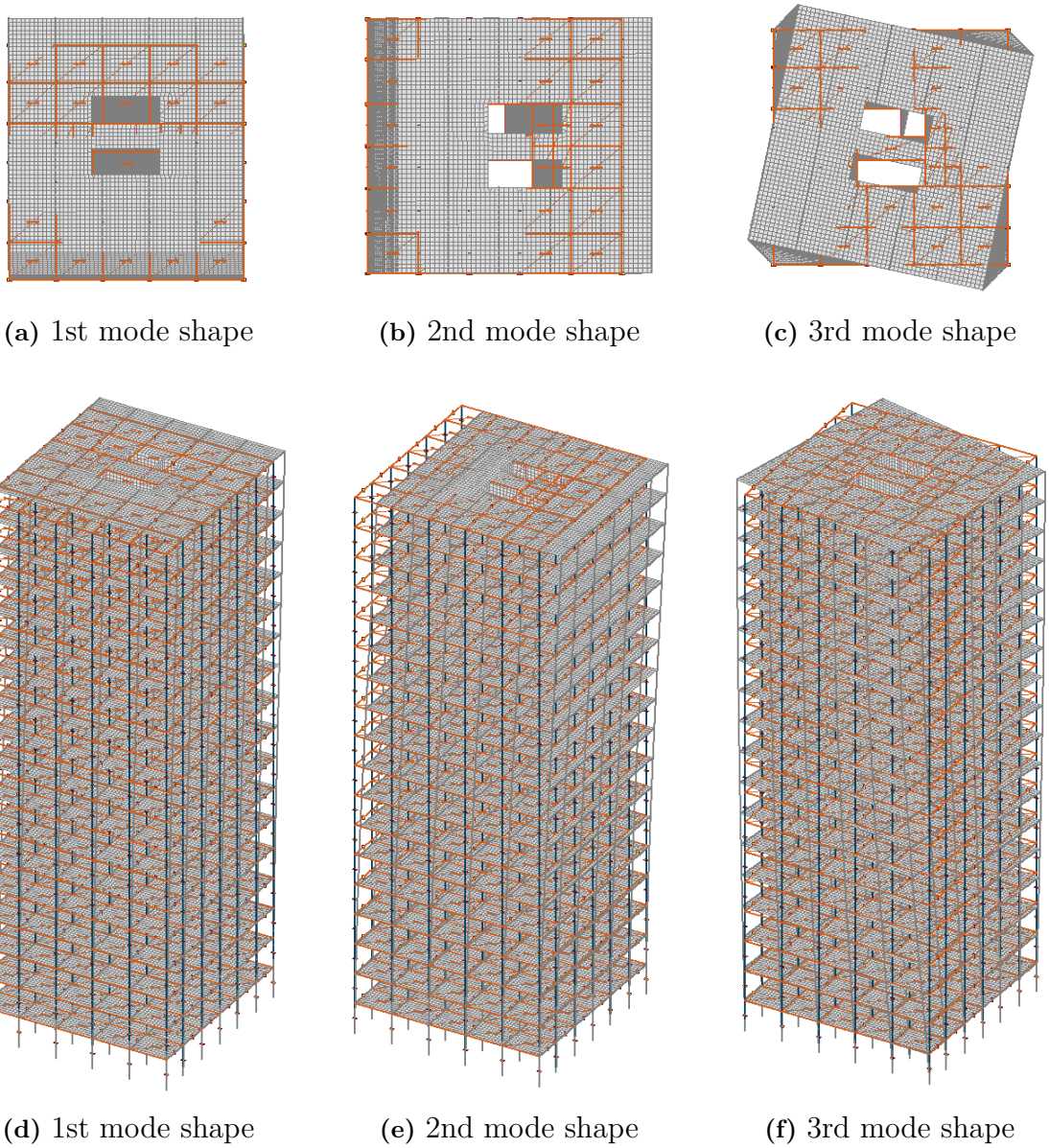

(a) 1st mode shape **(b)** 2nd mode shape **(c)** 3rd mode shape

(d) 1st mode shape **(e)** 2nd mode shape **(f)** 3rd mode shape

Figure 3.12: Illustration of the first global vibration mode shapes.

3.9 Analysis Procedure

The analysis is divided into several steps. First, a preliminary sizing was performed and then an eigenfrequency analysis was executed on a chosen height to observe the mode shape of the building, to achieve the fundamental frequency of the building, and to get the structural mass. These outputs were inserted into a calculation sheet that calculated the maximum acceleration and was compared with the limitations in the standard SS-ISO 10137 (2008). If the criteria were fulfilled, the building's height was increased, the thickness of concrete slabs or walls could be increased or decreased and the analysis was then performed again. When the criterion is fulfilled

the procedure will move into a ULS stage.

In the ULS stage, a dynamic wind analysis was performed for the building. The first step was by using the calculated fundamental frequency and mass a dynamic structural factor $c_s c_d$ was calculated together with a changed pressure coefficient. These were implemented as a load factor in the FE program. The design verifications were then applied to all structural elements. If the design did not fulfill the requirement, the chosen paramenter's value was adjusted, and the analysis should be performed again until all the requirements are fulfilled. If the requirement was fulfilled, a parameter of the building would change, and additional analyses was performed. A more detailed procedure for all types of buildings is explained in the following chapter. A flow chart that summarizes how the analysis procedure is being carried out is presented in Figure 3.13.

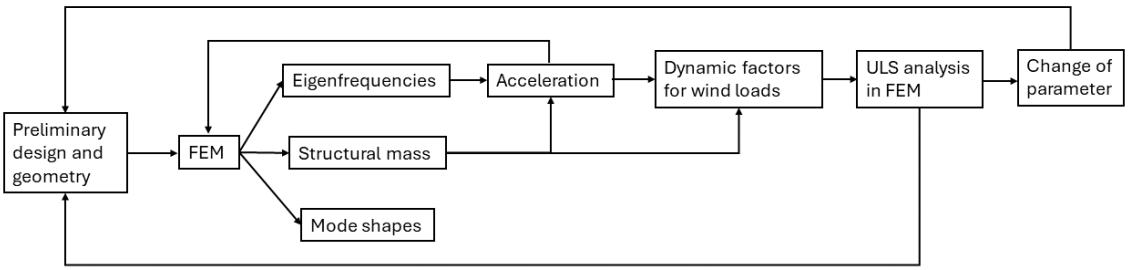

Figure 3.13: Analysis procedure

4
Analysis

Various analyses were conducted on different types of buildings, using the two finite element models introduced in the previous chapter. These analyses follow a systematic procedure, enabling the isolation of individual parameters. This facilitates the study of how changing specific parameters affects the behavior of the building.

4.1 Dynamic Analysis of Hybrid Timber Building

The analysis of the building begins by verifying the comfort requirements, which are associated with the maximum acceleration experienced within the structure. Various heights of the building were examined during the analysis. Different materials were also used for the structural load-bearing elements with different cross-sectional dimensions. If the Serviceability Limit State (SLS) criteria are not met but the Ultimate Limit State (ULS) criteria are fulfilled, in some cases the analysis proceeds to determine at what building heights and structural dimensions the ULS criteria are no longer satisfied. This procedure is carried out in a parametric study.

4.2 Parametric Study

Certain reference parameters must be specified to conduct the parametric study. These parameters will serve as guidelines for the analyses conducted on the building. Initially, the building under examination was entirely constructed of timber. The analyses focus on determining the maximum achievable building height while meeting the serviceability limit state, by assessing the maximum acceleration within the building together with confirming the highest utilization ratio in the structural elements to verify that the load-carrying capacity of those elements and whether they are higher than the design load values in the ultimate limit state.

Subsequently, a hybrid building was introduced, incorporating both timber and concrete structural elements. Various configurations were explored, altering the quantity and placement of concrete within the building. In the procedure of a parametric study, different case studies are conducted according to the following:

- Pure timber building.
- Hybrid building with a concrete core
- External and internal concrete walls and slabs on first floors.
- Incorporating concrete slabs on the upper floors.

The flowchart depicted in Figure 4.1 outlines the overall structure of the parametric study, which includes various building types, materials and compositions.

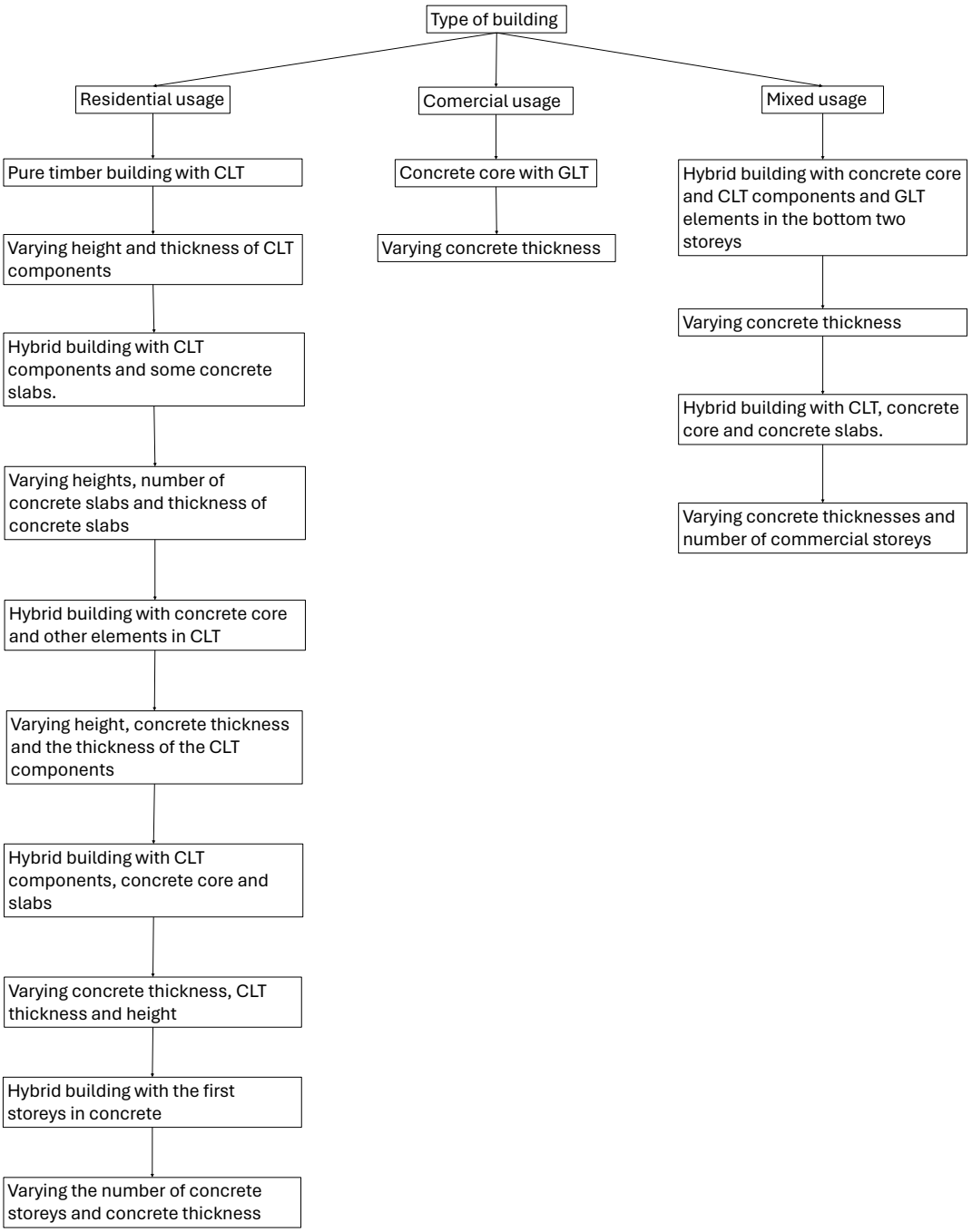

Figure 4.1: Summary of the parametric study

In the analyses, two different compositions of CLT panels were considered. The first type is labeled as 'panel type 180-5s,' indicating a 5-layer panel with a total thickness of 180 mm. The second type, denoted as 'panel type 280-7s', refers to a 7-layer panel with a total thickness of 280 mm. Details of these compositions are provided in Table 4.1 and Table 4.2 respectively.

Table 4.1: Panel properties for CLT elements of panel type 180-5s.

No. of layer	Material	Thickness [mm]	θ [°]	ρ [kg/m³]
1	C24	30	0	420
2	C14	45	90	350
3	C24	30	0	420
4	C14	45	90	350
5	C24	30	0	420

Table 4.2: Panel properties for CLT elements of panel type 280-7s.

No. of layer	Material	Thickness [mm]	θ [°]	ρ [kg/m³]
1	C24	40	0	420
2	C14	40	90	350
3	C24	40	0	420
4	C14	40	90	350
5	C24	40	0	420
6	C14	40	90	350
7	C24	40	0	420

Mechanical properties of CLT elements of panel type 180-5s and panel type 280-7s are presented in Table 4.3 and Table 4.4 respectively. All of the elasticity and shear modulus values are given in the tables in the unit MPa.

Table 4.3: Mechanical properties for panel type 180-5s.

No. of layer	$E_{0,mean}$	$E_{90,mean}$	v_{xy}	$G_{xy,mean}$	$G_{xz,mean}$	$G_{yz,mean}$
1	11000	0	0.00	690	690	69
2	7000	0	0.00	440	440	44
3	11000	0	0.00	690	690	69
4	7000	0	0.00	440	440	44
5	11000	0	0.00	690	690	69

Table 4.4: Mechanical properties for panel type 280-7s.

No. of layer	$E_{0,mean}$	$E_{90,mean}$	v_{xy}	$G_{xy,mean}$	$G_{xz,mean}$	$G_{yz,mean}$
1	11000	0	0.00	690	690	69
2	7000	0	0.00	440	440	44
3	11000	0	0.00	690	690	69
4	7000	0	0.00	440	440	44
5	11000	0	0.00	690	690	69
6	7000	0	0.00	440	440	44
7	11000	0	0.00	690	690	69

In the analysis of hybrid timber buildings incorporating concrete cores and slabs, a concrete class of C35/45 is employed. The mechanical properties for this concrete class are outlined in Table 4.5.

Table 4.5: Mechanical properties for concrete elements with concrete class C35/45.

f_{ck} [MPa]	f_{cm} [MPa]	f_{ctm} [MPa]	$f_{ctk,0.05}$ [MPa]	$f_{ctk,0.95}$ [MPa]	E_{cm} [MPa]	v [-]	ρ [kN/m^3]
35	43	3.2	2.2	4.2	34	0.2	25

4.3 Timber Building with CLT Components

The initial building model utilized timber exclusively, incorporating Cross-Laminated Timber (CLT) elements. Both the CLT wall and slab elements consisted of 5 layers, amounting to a total thickness of 180 mm. At the height at where the building does not fulfill the comfort criteria, the ULS capacity was tested. The thickness of the load-bearing elements for the building was then increased to observe how the added mass and stiffness affected the dynamic response of the building. The accelerations should decrease for the thicker elements and the ULS performance should improve as the stresses in the larger elements should decrease. The height of the building could therefore be increased. The analysis started with a 10-storey building and then increased with one floor for every SLS analysis for the 5-layer panels. The SLS analyses for the 7-layer panels started at the height where the 5-layer elements did not fulfill the comfort criteria.

Another analysis of the pure timber building was to see at which height the building would fail in the Ultimate Limit State. The comfort criteria in this analysis were disregarded. In this way, it could become clear if the building would fail in ULS. The analysis started at the height where the SLS analysis failed and increased by one floor until the utilization ratio for an element became over 100 %. The analysis was performed on the thinner 5-layer 180 mm thick elements. An illustration of the analyzed building from the FE-software is presented in Figure 4.2.

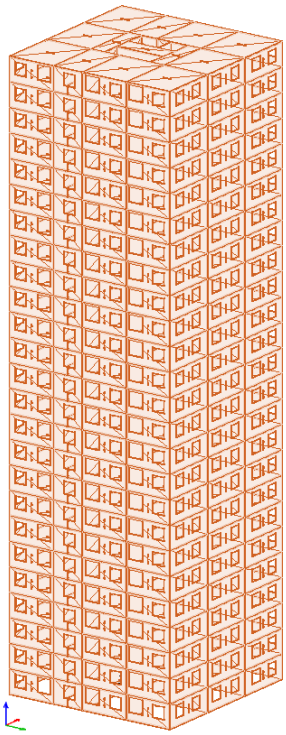

Figure 4.2: Timber building with CLT components of panel type 180-5s.

4.4 Hybrid Timber Building with Concrete Floor Elements

To improve the dynamic performance of a building one could increase the mass of the building as the acceleration is dependent on the equivalent mass. In SS-EN 1991-1-4 (2005) the equivalent mass can be approximated as the mass of the top third part per meter in height. To achieve a positive effect in decreased acceleration the added mass in this case concrete slabs should be placed on the top third part. Another positive effect could be the decrease in fundamental frequency of the building with added weight. A lower fundamental frequency can allow larger accelerations according to SS-ISO 10137 (2008), however a decrease in just the fundamental frequency also results in larger accelerations.

The first analysis was performed on the pure timber building that did not fulfill the comfort criteria to observe at which concrete thickness the criteria could be met. Only the slabs at the top were replaced with concrete elements. Another analysis was performed on a taller 20-storey building with slabs at the top third of the building being made out of concrete. The concrete thickness was gradually increased until the comfort criterion was met. The ULS was then tested to observe if it would govern the design of the building and to observe how the utilization ratio of the timber walls would increase due to the added load from the mass of the concrete slabs. The analyses were performed for both the thinner 180 mm and the thicker 280 mm CLT elements. An illustration of the analyzed hybrid timber building is

presented in Figure 4.3.

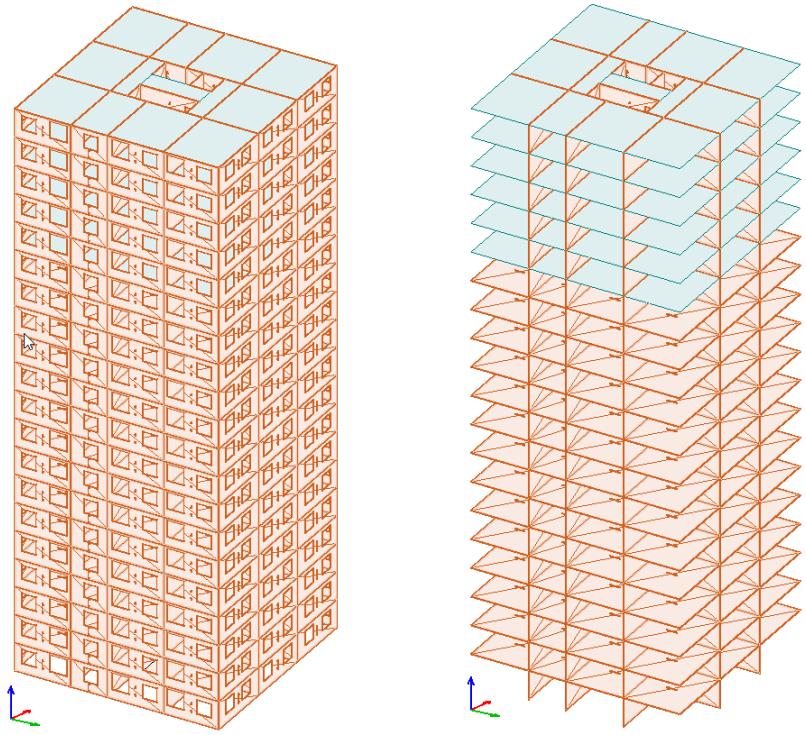

Figure 4.3: Hybrid timber building with concrete slabs on the top floors.

4.5 Hybrid Timber Building with Concrete Core

Another way to improve the dynamic performance of the building is to beside increasing the mass, also to increase the stiffness of the building. In general, two main properties that have an impact on the dynamic performance of the building are the fundamental frequency and the equivalent mass. The added weight of concrete on the upper third and increased stiffness for the whole building would contribute to better dynamic performance.

In the first analysis, a building of 20 storeys was modeled and the thickness was gradually increased from 300 mm and 5-layers CLT elements was used until the comfort criteria were fulfilled. The building was then analysed in ULS for the 300 mm thick concrete core and the thickness at where the acceleration criteria are met to observe the increase or decrease in utilization ratio. The procedure was then performed for the thicker 280 mm thick CLT elements to see how much the concrete thickness could be decreased with the added mass and stiffness. This analysis was also performed for an increased height of 25 floors to observe how the acceleration and utilization ratio changes with increased height. An illustration of the analyzed hybrid timber building with concrete core extending along the buildings height is presented in Figure 4.4.

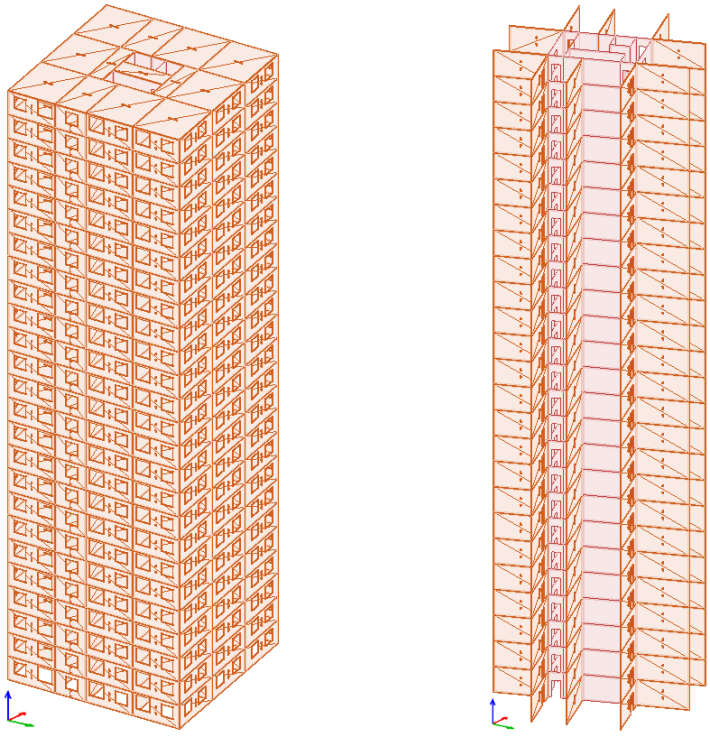

Figure 4.4: Hybrid timber building with concrete core extending along the buildings height.

4.6 Hybrid Timber Building with Concrete Core and Concrete Floors

Another hybrid structure type combines elements of the two previous designs. In this structure, the top third of the slabs and the core are constructed using concrete. This combination has a dual effect where the added mass from the concrete slabs increases the overall equivalent mass, while the core enhances both mass and stiffness. Consequently, this configuration leads to reduced accelerations.

The analysis was divided into several steps. First, a 20 storey building was analyzed with 180 mm thick CLT elements. The analysis started with a concrete thickness of 200 mm and was then increased until the comfort criteria were achieved. An Ultimate Limit state analysis was then performed with the 200 mm thick concrete slabs and the thickness at where the comfort criteria were met.

A 25-storey building was modeled with a varied concrete thickness starting from 200 mm and increased until the comfort criteria were satisfied and a ULS analysis was performed at the concrete thickness of 200 mm and the concrete thickness at where the accelerations were acceptable. The analyses was performed for both the 280 mm thick CLT elements and the 180 mm thick.

A 30- and 35- storey building with a thickness of the CLT elements of 280 mm was

then analyzed to observe how the added height would affect the accelerations of the building and how the utilization ratios in ULS would change. Initially, the concrete thickness was set at a level where the acceleration met acceptable standards for the previous height. Subsequently, the concrete thickness was incrementally augmented until comfort criteria were met, and thereafter, ULS analysis was performed for the first SLS analysis and the one that first fulfilled the comfort criteria.

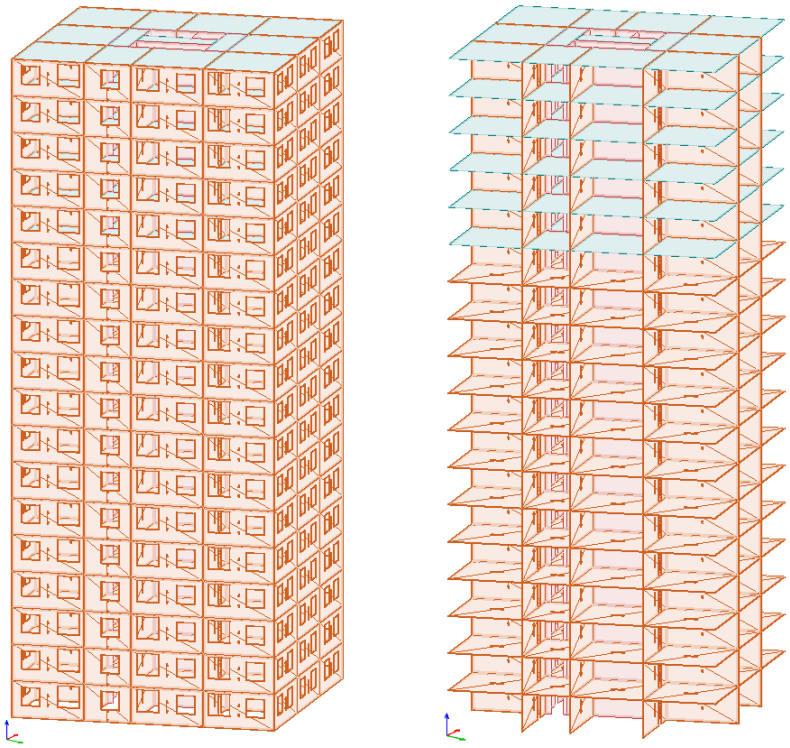

Figure 4.5: Hybrid timber building with concrete floors at upper part of building and a concrete core extending along the buildings height.

4.7 Hybrid Timber Building with the First Two Floors in Concrete

Many tall buildings often have their first floors as basements or for other usage in the building. Therefore a 20-storey building was modelled with 18 storeys made out of timber and two storeys made of concrete with the same floor plan. The concrete thickness was in the first analysis 200 mm and in the second 400 mm to observe the difference. SLS analyses were performed with the 5-layer CLT elements. This change could affect the stiffness of the building, but the equivalent mass will remain unaffected, as the concrete is situated in the lower two-thirds of the structure.

4.8 Hybrid Timber Building with Multiple Floors in Concrete

New analyses have been conducted on the hybrid timber building, involving modifications to several floors to incorporate concrete construction. Previously, only two floors were constructed with concrete. However, the latest adjustments entail integrating concrete walls and slabs into the first 8 floors at the base of the building. Despite these changes, the overall floor plan and floor height remain unchanged. Specifically, the analyses were performed on a 25-storey building, with the initial 8 storeys at the bottom featuring concrete construction, while the remaining 17 storeys consist of both timber and concrete. Figure 4.6 gives an illustration of the building from the FE-model.

Above these 8 concrete floors, a hybrid system was implemented, comprising concrete walls in the core of the building and CLT timber elements in other walls and slabs. The CLT timber elements featured a constant panel type of 280-7s, indicating seven CLT layers with a total panel thickness of 280 mm. For the analyses that were conducted, the thickness of all concrete elements, including walls and slabs, were varied to check the response of the building both in SLS and ULS. The starting concrete element thickness was set to 250 mm which was further increased to a value of 400 mm for which the comfort criteria were met.

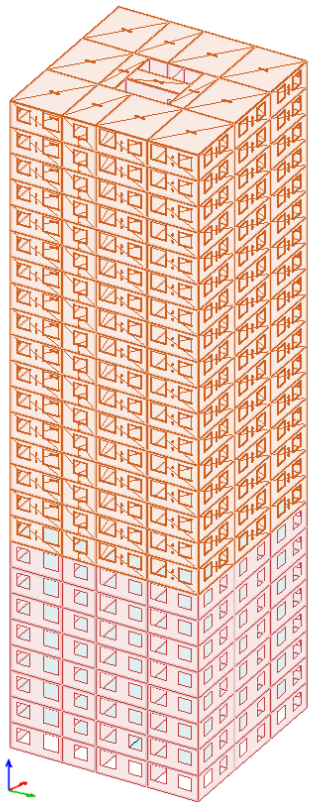

Figure 4.6: Hybrid timber building with a concrete core extending along the buildings height and 8 storeys made entirely of concrete at the bottom.

4.9 Hybrid Timber Building with Commercial Areas

The acceleration criterion is different for different types of buildings and depends on the usage of the building (SS-ISO 10137, 2008). Residential usage of a building has a lower acceleration limit than commercial usage. The profile of the acceleration with respect to height increases logarithmically with height. If the top floors had commercial usage, one could build taller or reduce the concrete thickness.

First, the top five storeys were set to commercial. A 30 storey building with the top third having concrete slabs and the rest having CLT slabs was modeled. These slabs are combined with a concrete core. The thickness of the CLT elements was 280 mm. The thickness of the concrete started at 200 mm and was increased until the comfort criterion for both commercial and residential usage was fulfilled. A ULS analysis was then performed for both the 200 mm and the first that had acceptable accelerations.

Then models with 35 and 40 storeys were analyzed with 280 mm thick CLT elements with the concrete thickness that did fulfill the acceleration criterion for the previously analyzed height. A ULS analysis was then performed for the first and last SLS analysis. The different heights and concrete thicknesses could afterwards be compared with each other and compared with the earlier analyses with a concrete core and slabs.

In earlier analyses for this subsection, the top five storeys were assumed to have commercial areas. The 40-storey building was adopted, and the number of commercial stories was varied for the building with first 200 mm thick concrete elements and was then increased with 100 mm to 500 mm. First the building had a single commercial storey. The number of commercial storeys increased by two for each analysis to a 13 commercial storey buildings. The analyses were performed to observe how the proportion of different usages of a building affects the accelerations and the allowed accelerations.

4.10 Reinforcing Critical Areas

Previous ULS analyses have shown that in tall buildings, the ULS failing criteria is local compression close to the concrete wall. To improve the local capacity, GLT columns were installed. In the 7-layer CLT wall, only 4 layers would be activated in compression as the fiber direction is alternating for every layer. The capacity would be larger for the GLT beam as all layers could be utilized. The analysis was performed for the cases where the earlier ULS analysis had a utilization ratio of more than 100 %. The columns chosen were 280 x 140 mm and 180 x 140 mm with strength class GL30c. The dimensions were chosen so that the columns would have the same thickness as the connecting CLT wall.

The type of building chosen for the analyses depends on the results of the earlier analyses. If an analysis had a ULS utilization ratio greater than 100 %, parts of the wall close to the concrete wall were replaced with GLT columns on the first floor to observe if the GLT column has the capacity to withstand the loads in ULS. The most important reason to perform the analyses was to see if the utilization ratio for the CLT elements becomes less than one and could therefore this be a practical solution. Figure 4.7 indicates the areas marked with circles, where CLT walls are reinforced with GLT columns at the corners adjacent to concrete core walls.

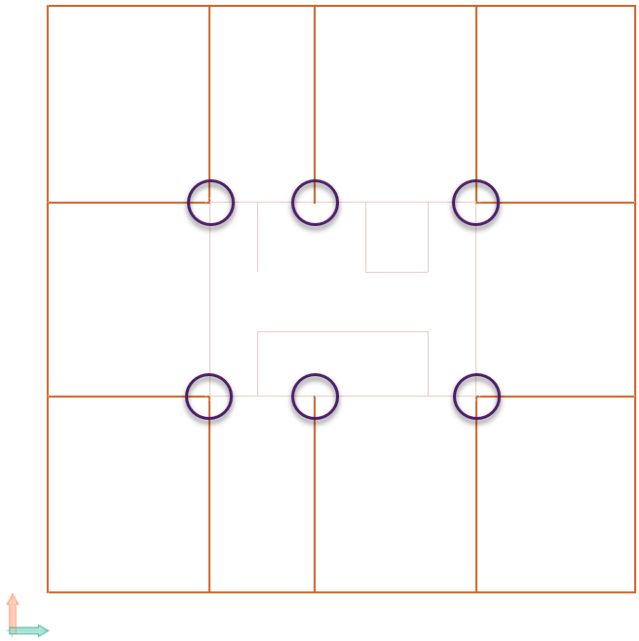

Figure 4.7: CLT walls at corners are reinforced with glulam timber columns as illustrated with circle signs.

4.11 Comparison Between ULS and SLS

In previous analysis, it can be observed that if the fundamental frequency of a building is between one and two hertz the increase in required concrete thickness to fulfill the required accelerations for an increased height can be larger compared to when the fundamental frequency is between zero and one hertz. One reason is the difference in allowed accelerations. The acceleration limit decreases logarithmically with an increased fundamental frequency to one hertz. The purpose of the analysis is to observe how the ULS together with SLS changes with increasing height for a hybrid building.

The chosen hybrid building has a concrete core and concrete slabs on the top third of the building, with a thickness of 300 mm. The 7-layer CLT elements were used. This combination was chosen as earlier analyses have shown that the height of 20 storeys shows a fundamental frequency of one hertz and that the building would fulfill the

acceleration criteria to 25 storeys. Comprehensive analyses were conducted for both ULS and SLS for heights ranging from 14 to 26 storeys with an additional analysis conducted following a two-storey height increase.

4.12 Hybrid building with Changed Structural System at the Lower Two Storeys

In buildings, it is common to have commercial spaces on the first floors. These areas often necessitate a more adaptable floor plan, typically achieved through a column and beam system. Compared to a wall and slab system, this approach entails lower mass and stiffness. Consequently, it may result in decreased performance in terms of comfort criteria.

A building of 20 storeys with the two first storeys containing the column and beam system was modeled. The height of these storeys was increased from 3 meters to 3.5 meters due to the larger height of the floor structure that both contain beams and CLT slabs. The columns and beams were placed directly under the CLT walls in the storey above. The CLT elements for the analysis contained 7-layer. The beam had the dimensions of 215 x 450 mm and the columns were the size of 215 x 405 mm. Both had the strength class of GL30h. The concrete included in the model was a core. An SLS analysis was performed for first a concrete thickness of 300 mm and then a ULS analysis was performed. Thereafter, the core thickness was increased until the comfort criterion was fulfilled, and a ULS analysis was performed afterwords. An illustration of the 20-storey hybrid timber building with GLT columns and beams at the lowest two floors is presented in Figure 4.8.

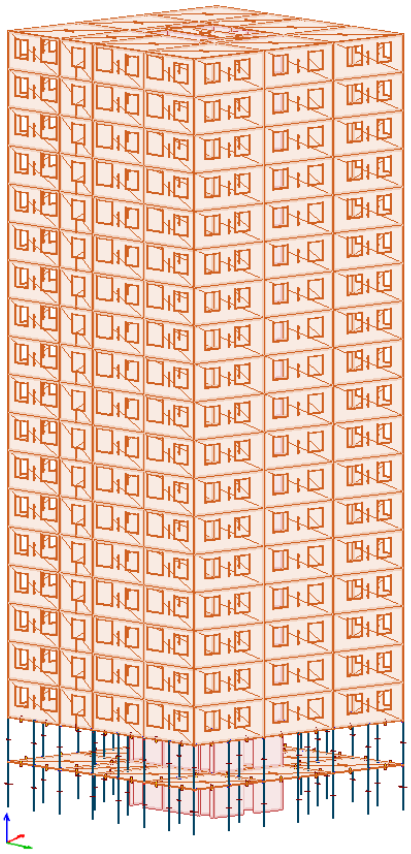

Figure 4.8: Hybrid timber building with GLT columns and beams at lowest two floors.

4.13 Analysis of Hybrid Timber Office Building

An additional analysis is performed on a hybrid timber model for an office building. The structural system is composed of glulam timber beams and columns of GL30c complemented with a concrete core in the center of the building built with concrete walls of concrete class C35/45. The CLT panels that were utilized for slabs are of type 280-7s which were used in previous analyses of the residential building model. Mechanical properties for glulam beams and columns are presented in Table 4.6. All parameters in the table below are given in the unit of MPa.

Table 4.6: Mechanical properties for glulam timber beam & column GL30c.

$E_{0.05}$	$G_{0.05}$	$f_{t,90,k}$	$f_{c,0,k}$	$f_{c,90,k}$	$f_{v,k}$	$f_{t,0,k}$	$f_{m,1,k}$	$f_{m,2,k}$
10800	540	0.50	24.50	2.50	3.50	20.07	30.88	33.00

The building model consists of 18 storeys and stands at a total height of 63 meters. Glulam timber beams and columns are utilized, featuring a rectangular cross-section measuring 215 x 450 mm. In the analysis, various thicknesses of concrete core walls

are examined to assess their impact on the building's eigenfrequency and mass. These variations result in changes to the maximum acceleration recorded within the building for a given analysis with a specific wall thickness. An illustration of the FE-model of the hybrid timber office building is presented in Figure 4.9.

The assumptions made in previous analyses remain applicable here, assuming that the building is constructed on a stiff foundation. Consequently, the columns on the first floor are considered to be clamped, implying a rigid connection between these columns and the foundation. For all subsequent floors above the first, the columns are modeled as simply supported, featuring hinged connections at both ends. Similarly, all beams in the model are assumed to be simply supported, with hinged connections at both ends.

Comprehensive analyses were conducted for SLS on two types of buildings of equal height, measuring 63 meters. The first was a 21-storey residential building, while the second was an 18-storey office building. Their respective floor heights were 3 meters and 3.5 meters. The analyses were performed for various concrete element thickness starting at 400 mm up to 650 mm. Different dynamic responses were recorded for both structures, leading to varying utilization ratios concerning the maximum allowable accelerations in the buildings.

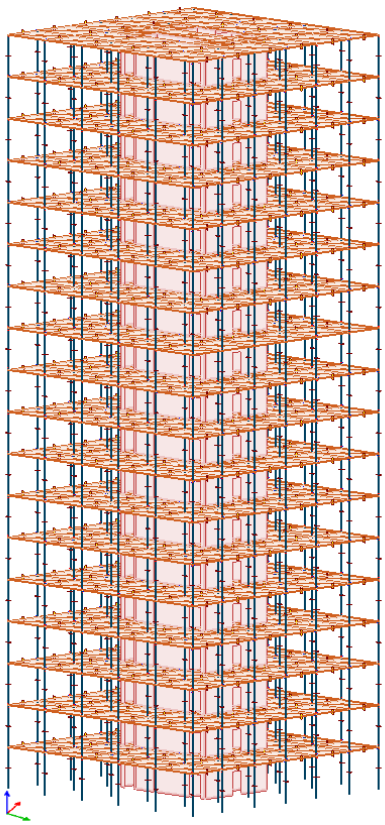

Figure 4.9: Hybrid timber building with glulam timber beam and column structural system with CLT slabs and a concrete core extending along the buildings height.

5
Results

The analyses were conducted for multiple types of buildings with different structural systems and usages. The analyses start with a pure timber building with 10 storeys, and the tallest hybrid building tested was a 40-story building with a concrete core and concrete slabs in the upper one-third of the building. Both the results of the ULS and SLS analyses are presented in the chapter. More detailed results can be found in appendix.

5.1 Timber Building with CLT Components

The initial building model utilized timber exclusively, incorporating Cross-Laminated Timber (CLT) elements. Both the CLT wall and slab elements consisted of 5 layers, amounting to a total thickness of 180 mm. The analysis resulted in a maximum acceleration of 0.049 m/s^2 for an 11-storey building with a height of 33 m. When the building increased by one floor, the wind-induced acceleration increased beyond the allowed limit for accelerations in residential buildings. The results can be observed in Figure 5.1. The ULS capacity was tested for the 12-storey building which did not fulfill the comfort criteria and the wall that had the largest utilization ratio was a shear wall in the core on the fourth floor of 29 % in the verification of tension. The second largest utilization ratio was compression with a value of 16 %. The building in this case will therefore not fulfill the comfort requirement before the maximum load-bearing capacity is reached.

The wall and plate elements in the building were changed to thicker CLT elements consisting of 7-layer elements with a total thickness of 280 mm in the pure timber building. The results show that two more storeys could be added and still fulfill the comfort criteria. The results are also shown in Figure 5.1. The utilization ratio for the ULS analysis in the shear wall decreased to 28% for the tension and 13 % for the compression. The wall with the largest utilization ratio was one on the fourth floor.

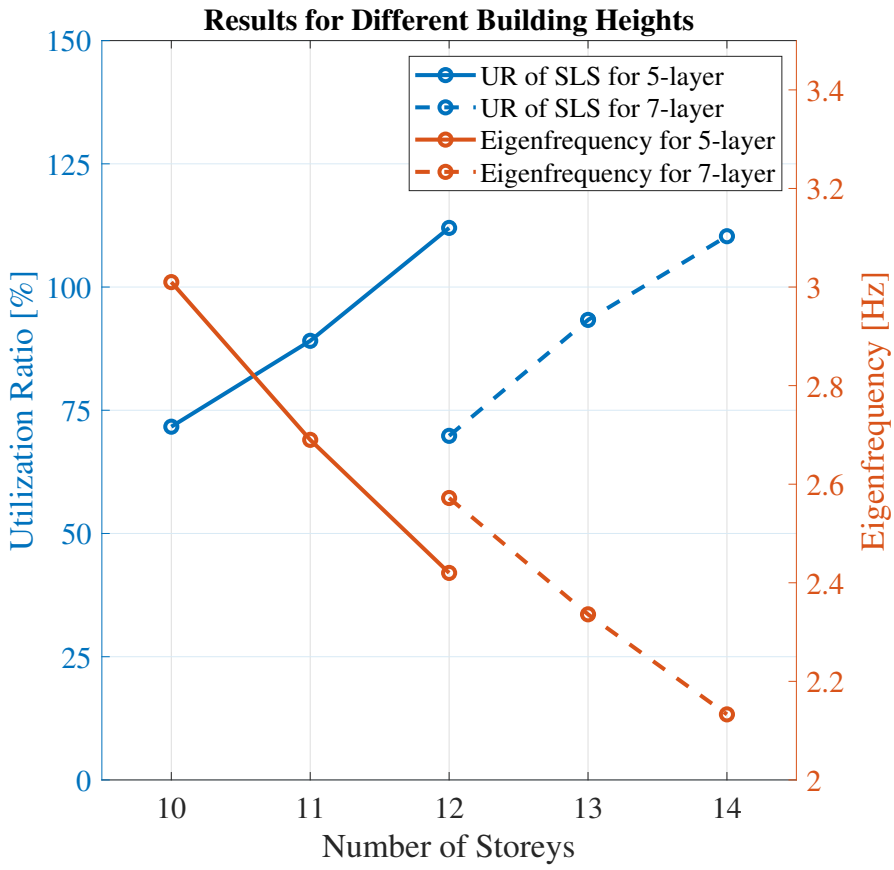

Figure 5.1: Results of different CLT buildings with different panel types.

The height of the building was then increased to observe how tall the building could become if the comfort criteria was disregarded. Here, the CLT wall and slab elements consisted of 5 layers, amounting to a total thickness of 180 mm. The ULS analysis resulted in a utilization ratio for the most loaded wall which was a shear wall in the core on floor 7 and the failing criteria was tension. The results from the analysis can be observed in Figure 5.2 and show that the maximum buildable height of the building consisting of CLT elements is 24 floors.

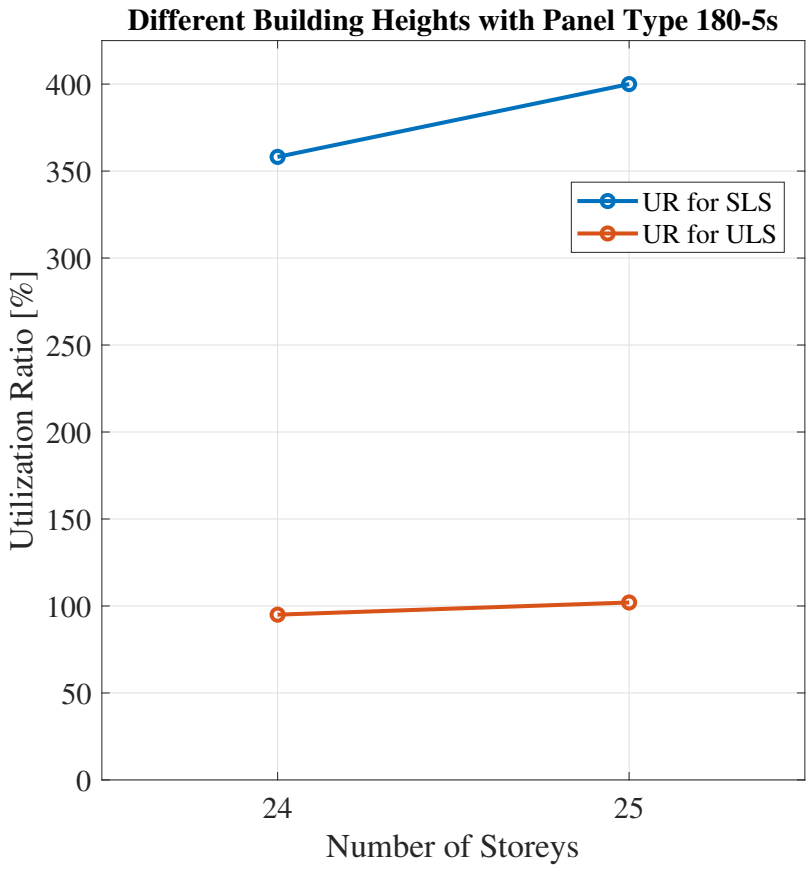

Figure 5.2: Results of a tall CLT building with panel type 180-5s.

5.2 Hybrid Timber Building with Concrete Floor Elements

The 12-storey building with 5 layers of CLT in Subsection 5.1 did not fulfill the comfort criteria. To address this issue, it was decided to convert the top floor into concrete to increase the equivalent mass of the building and therefore decrease the acceleration. The results from the analysis can be seen in Figure 5.3. The concrete floor would need to have a larger thickness than 400 mm to achieve an acceptable acceleration. A better design for the building would be having multiple floors on the uppermost third part of the building made out of concrete. Another observation is when the amount of concrete is increasing the fundamental frequency decreases.

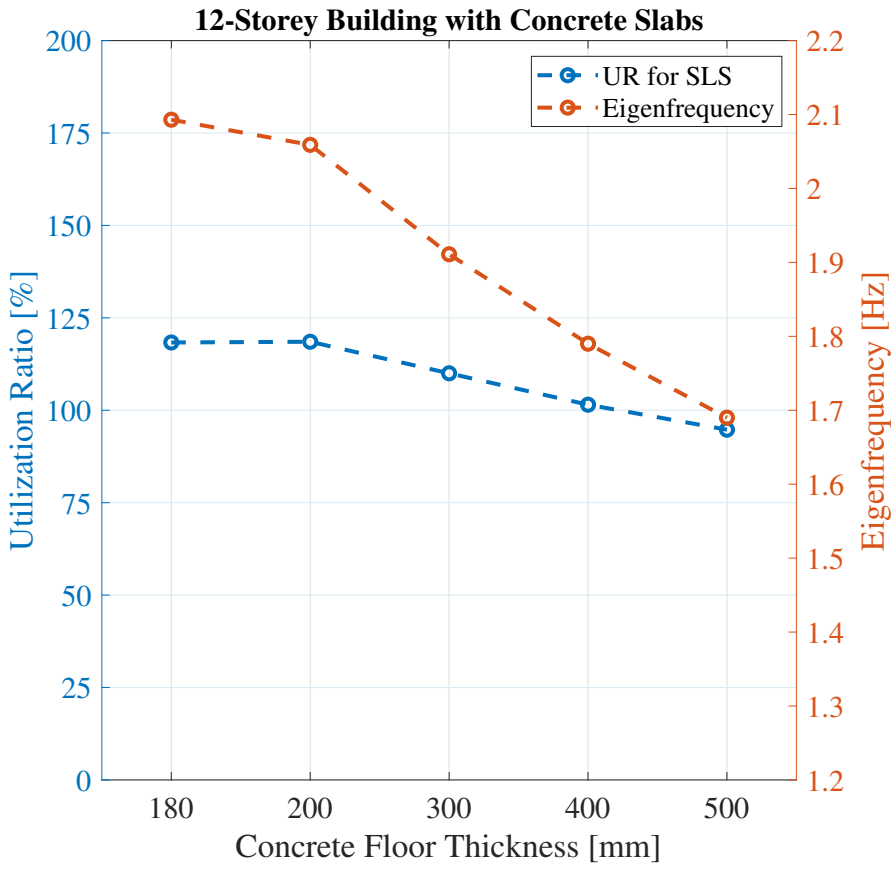

Figure 5.3: Results of a 12-storey hybrid building with 180 mm CLT elements and a varying concrete floor thickness on the uppermost floor.

Subsequently, a 20-storey building was then adopted, the CLT-floor elements on the upper sixth floors were replaced with concrete and the thickness was varied to see at which thickness the analysis resulted in acceptable acceleration values. The thickness for which the comfort requirement was fulfilled was 550 mm. The Ultimate limit state capacity was then tested for the slabs with 200 mm thickness and 550 mm. The failing wall was located in the core on the sixth storey for the 200 mm thick slabs and at first storey for the 550 mm thick slabs. The failure mode was tension for the thinner concrete slabs and compression for the thicker concrete slabs. The results can be observed in Figure 5.4. The wall with the largest utilization ratio was located on the sixth storey in the core where the largest stresses can be found in a corner. The failure criterion was tension and the utilization ratio increased from 75 % to 79 % as the added concrete thickness increased the wind load.

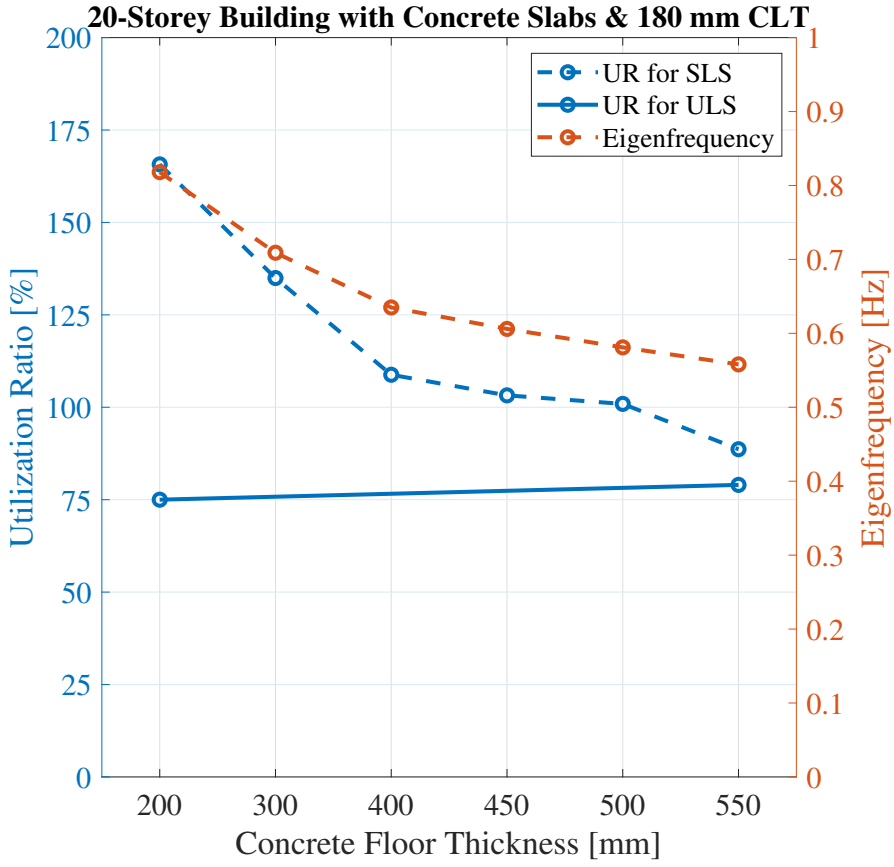

Figure 5.4: Results of a 20-storey building with varying concrete lfloor thickness and 180 mm CLT elements.

The structural performance of the same 20-storey building was reassessed using larger 7-layer elements. This analysis aimed to determine the extent to which the concrete thickness could be reduced while still meeting design requirements. The findings of this study are illustrated in Figure 5.5. The comfort criterion was achieved between a concrete thickness of 350 mm and 400 mm. Despite the reduction in concrete thickness, the building's ability to withstand the maximum loads was verified, where a maximum of utilization ratio in ULS of 52 % in tension obtained in the core wall at the sixth floor.

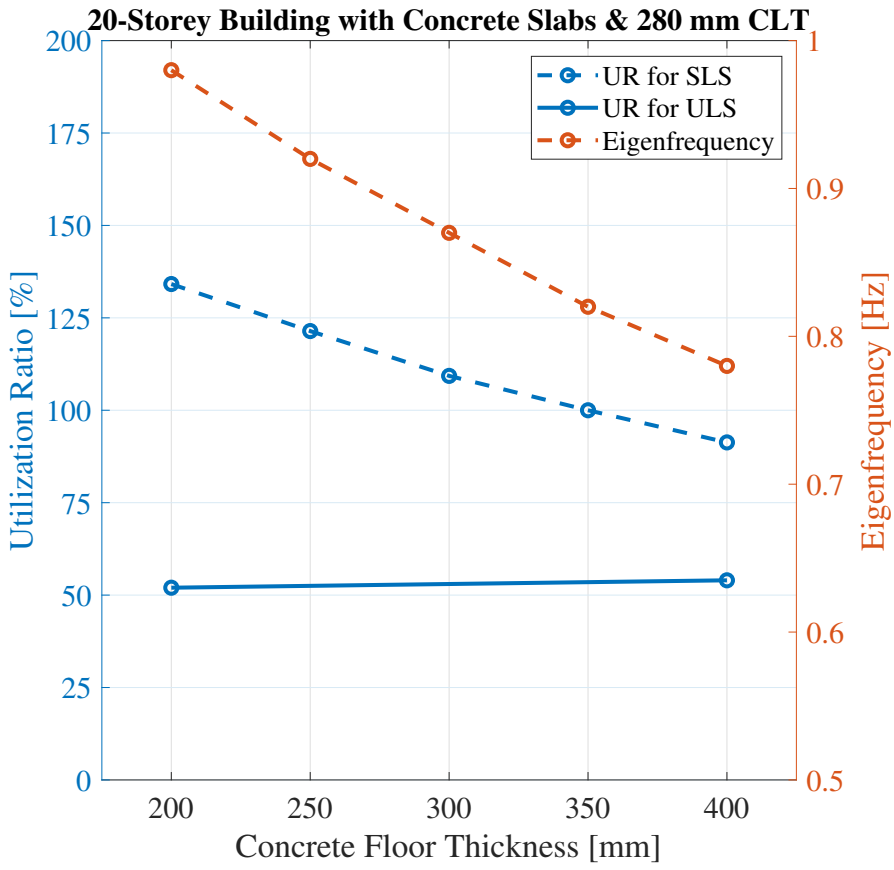

Figure 5.5: Results of a 20-storey building with varying concrete floor thickness and 280 mm CLT elements.

5.3 Hybrid Timber Building with Concrete Core.

Another 20-storey hybrid structure such where the CLT elements in the core are exchanged for prefabricated concrete elements was analysed. The benefit is both an added mass and stiffness which would contribute to better structural performance with regard to the SLS criteria. The thickness of the concrete walls was increased until the comfort criteria with regard to the maximum allowed acceleration were fulfilled. The results can be observed in Figure 5.6. The largest utilization ratio can be found on the first floor with the failing mode being compression. The increasing thickness of concrete walls resulted in a larger ULS utilization ratio. Here, it can also be observed that the fundamental frequency decreases with an increased amount of concrete.

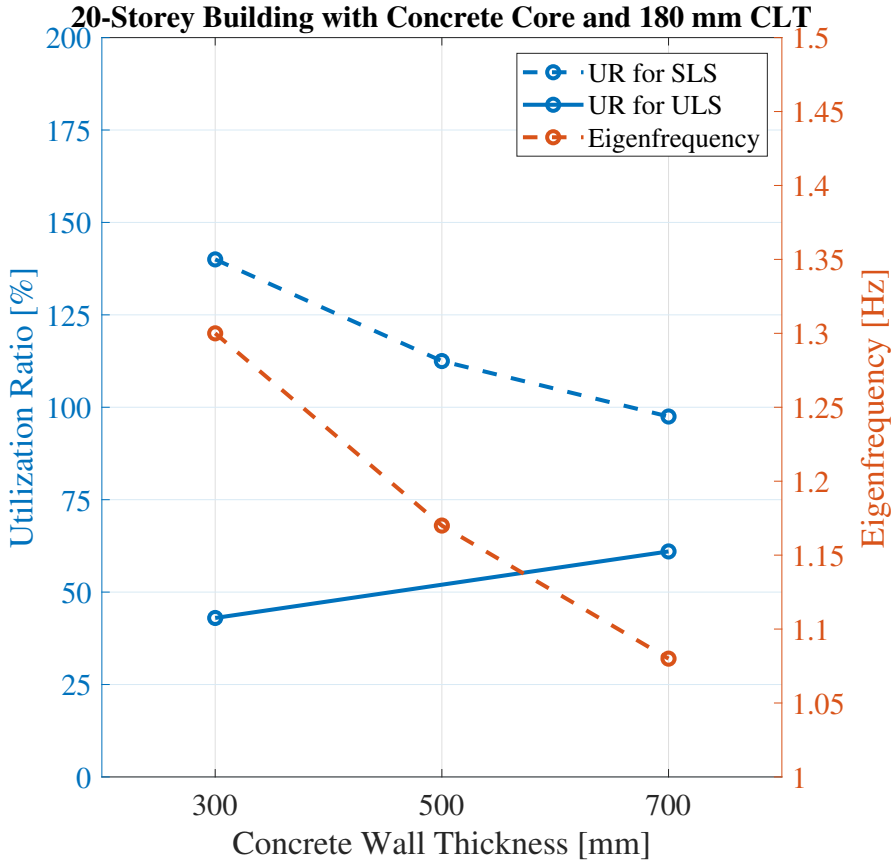

Figure 5.6: Results of a 20-storey hybrid building with concrete core and 180 mm CLT.

The 20-storey building was then analyzed with CLT elements with a total thickness of 280 mm and contained 7 layers to observe if the thickness of the concrete elements could be reduced as the added thickness would contribute to larger stiffness and mass to receive better SLS performance with regard to comfort. The results can be observed in Figure 5.7. The results show that the thickness of the concrete walls can be reduced with 300 mm. The thicker CLT walls resulted in a lower ULS utilization ratio as larger elements reduce the compression stresses in an element.

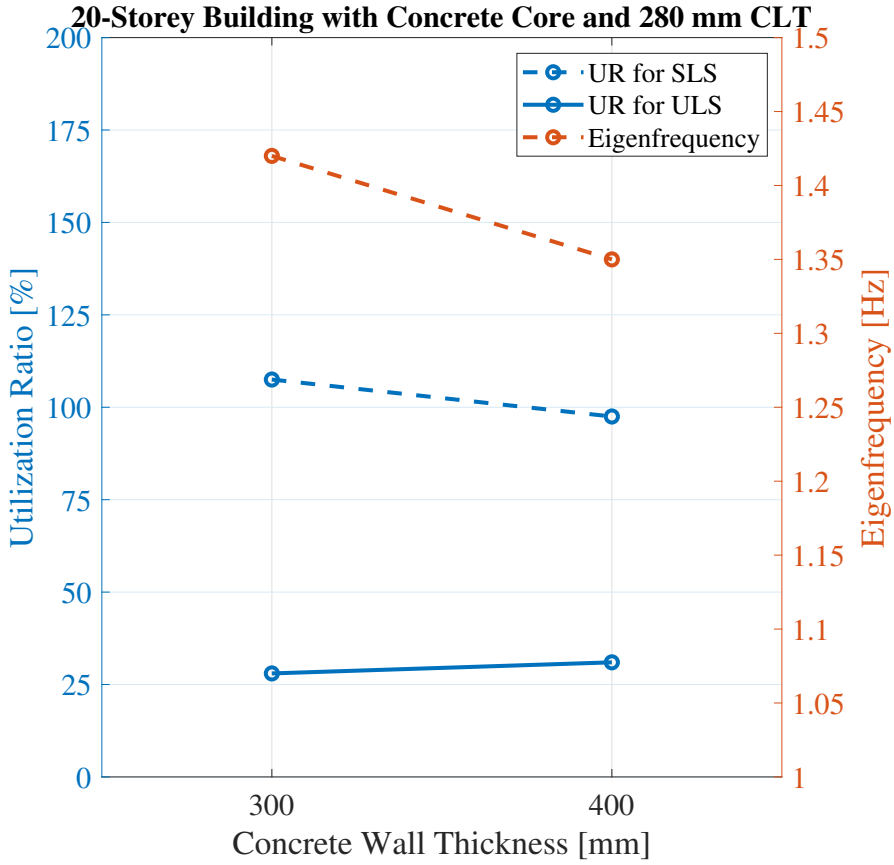

Figure 5.7: Results of a 20-storey hybrid building with a concrete core and 280 mm CLT.

Five new floors were added to the 20-storey building and the CLT elements were changed back to a thickness of 180 mm. To achieve the comfort criteria, the concrete wall thickness needs to be increased to over 900 mm which can be observed in Figure 5.8 and the building would fail in compression. Previous analyses have shown that the comfort criteria will govern the design, but in this case, the ultimate limit state was the designing criteria.

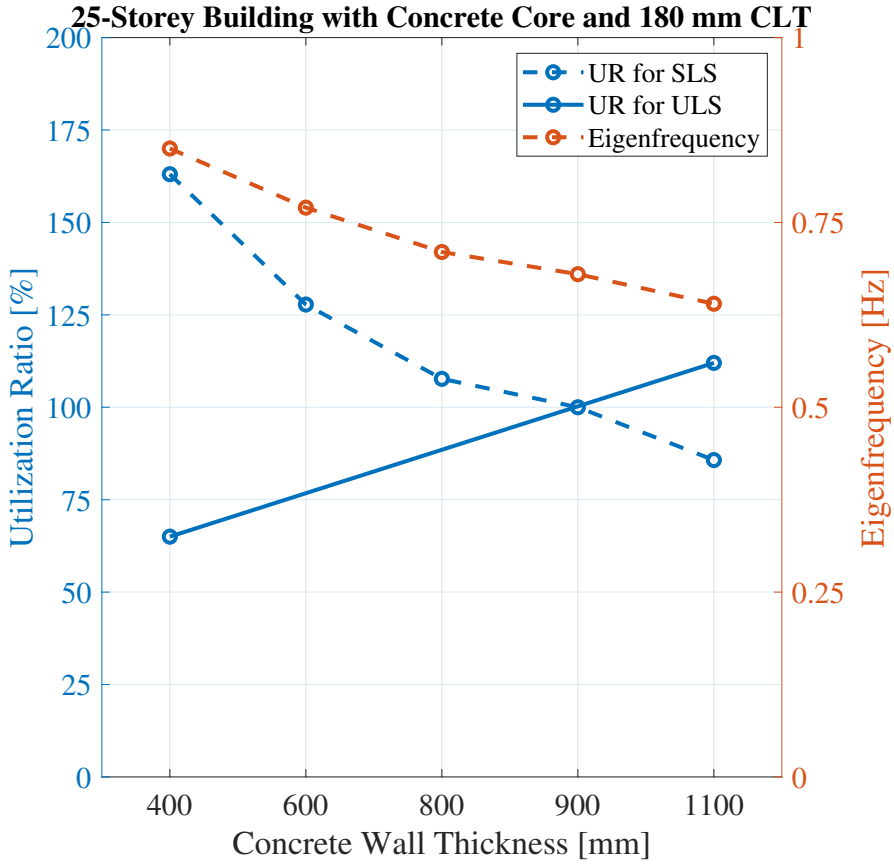

Figure 5.8: Results of a 25-storey hybrid building with a concrete core and 180 mm CLT.

The same 25-storey building was then analyzed with increased thickness for the CLT elements. The results can be observed in Figure 5.9. The Ultimate limit state capacity was then tested for both of the 400 mm thick wall and the 900 mm thick wall. The failure mode was compression. The increased CLT thickness resulted in a decrease in concrete thickness.

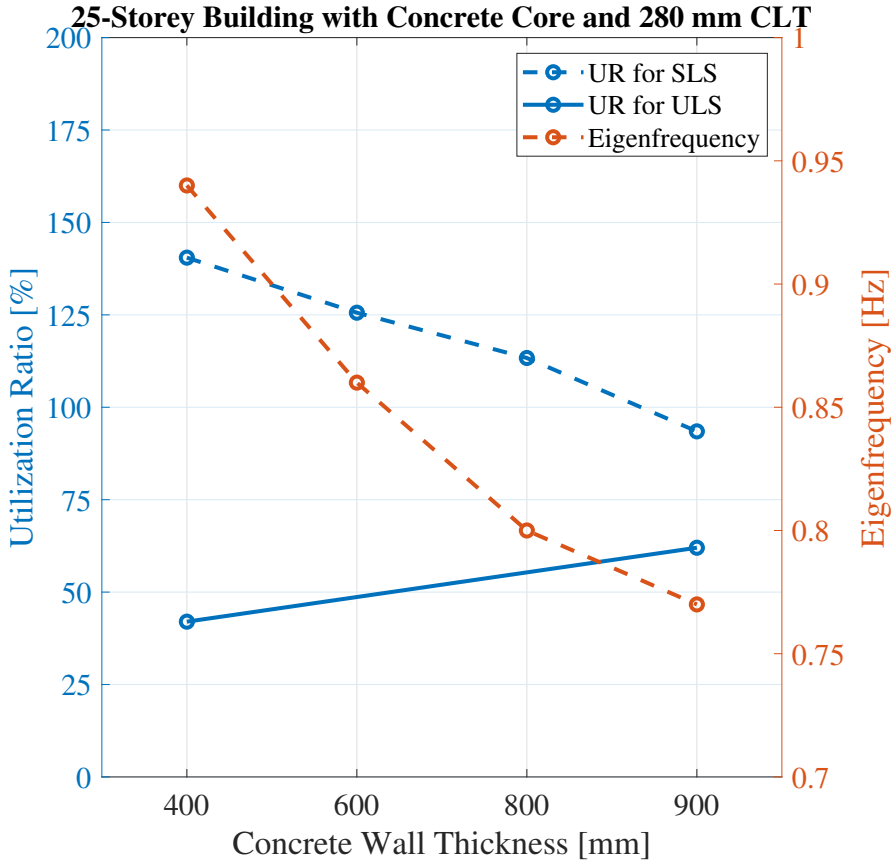

Figure 5.9: Results of a 25-storey hybrid building with a concrete core and 280 mm CLT.

5.4 Hybrid Timber Building with Concrete Core and Concrete Floors.

Analyses were then performed for a combination of the two hybrid structures from previous sections with a concrete core and concrete floors on the top third of the building. These analyses were performed as the thickness of the concrete could become large for the hybrid structure with a concrete core. The results from the 20-storey building can be seen in Figure 5.10, where the failure mode was compression on the first floor of a wall.

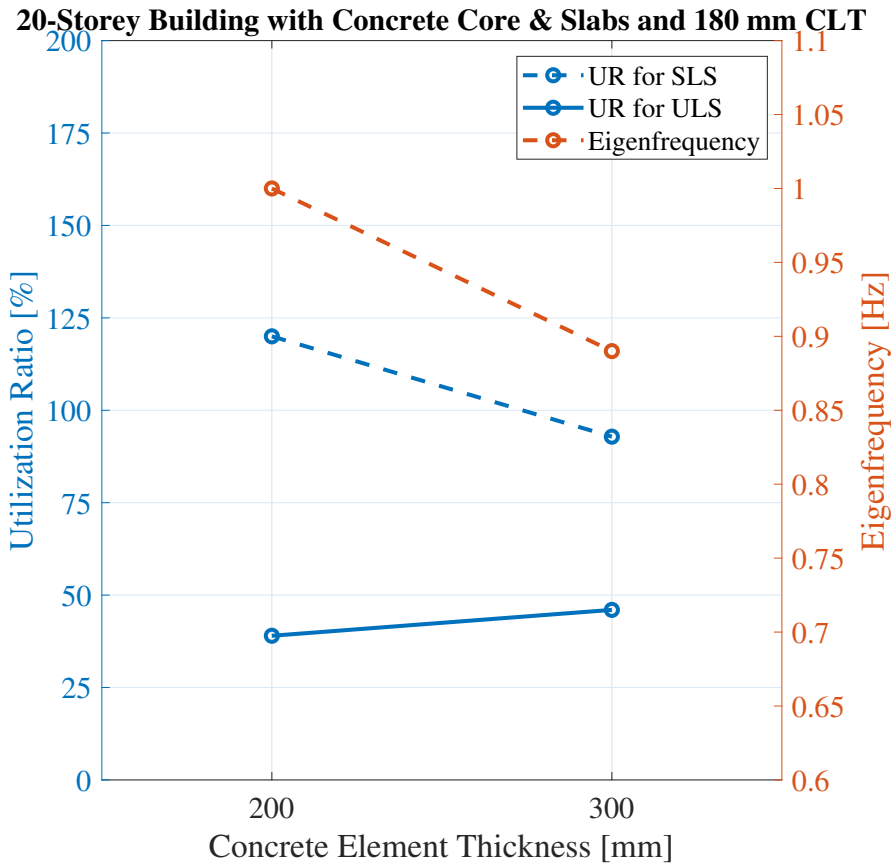

Figure 5.10: Results of a 20-storey hybrid building with a concrete core and slabs with 180 mm CLT.

A 25-storey building was then analyzed to observe the required concrete thickness where the comfort criterion is fulfilled. The increased concrete thickness would contribute to larger stresses in the CLT walls. The failure mode in the ULS analysis for the CLT walls is compression on the first floor. The results can be observed in Figure 5.11.

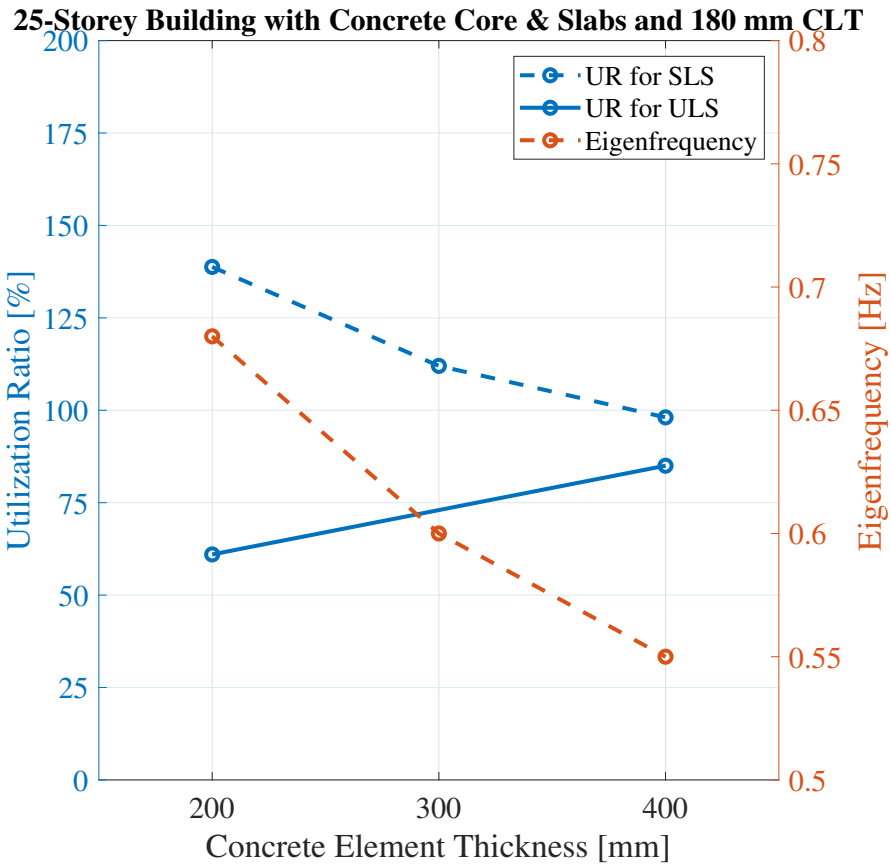

Figure 5.11: Results of a 25-storey hybrid building with a concrete core and slabs 180 mm CLT.

To achieve lower concrete volume the 180 mm CLT elements were changed to 7 layers and 280 mm thick. The changes will increase both the stiffness and mass of the building. The utilization ratio in ULS was also decreased as more material could be utilized. The results in Figure 5.11 show that the thickness of concrete could be decreased with 100 mm by using thicker CLT elements compared with results from Figure 5.12.

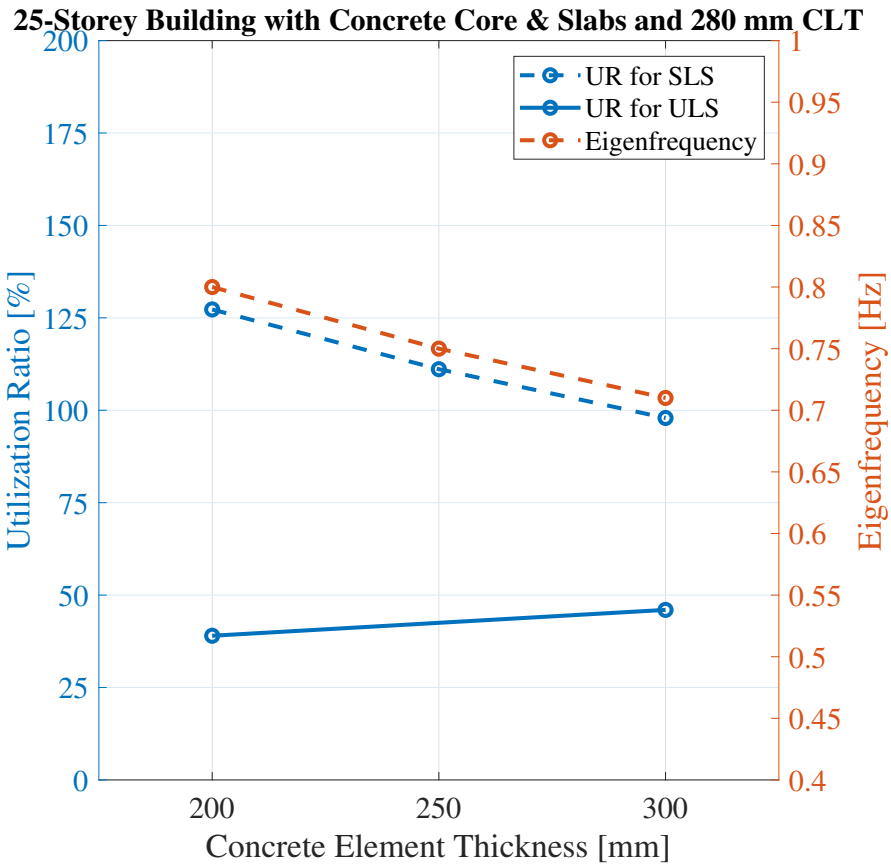

Figure 5.12: Results of a 25-storey hybrid building with a concrete core and slab and 280 mm CLT.

The building's height was increased to 30 floors to observe if the ULS capacity would be governing the design of the building. The results in Figure 5.13 show that with an increased height the concrete floors and walls need to be thicker compared to the 25-storey building to achieve acceptable accelerations. The stresses in the timber walls also increased, and the failure mode was compression.

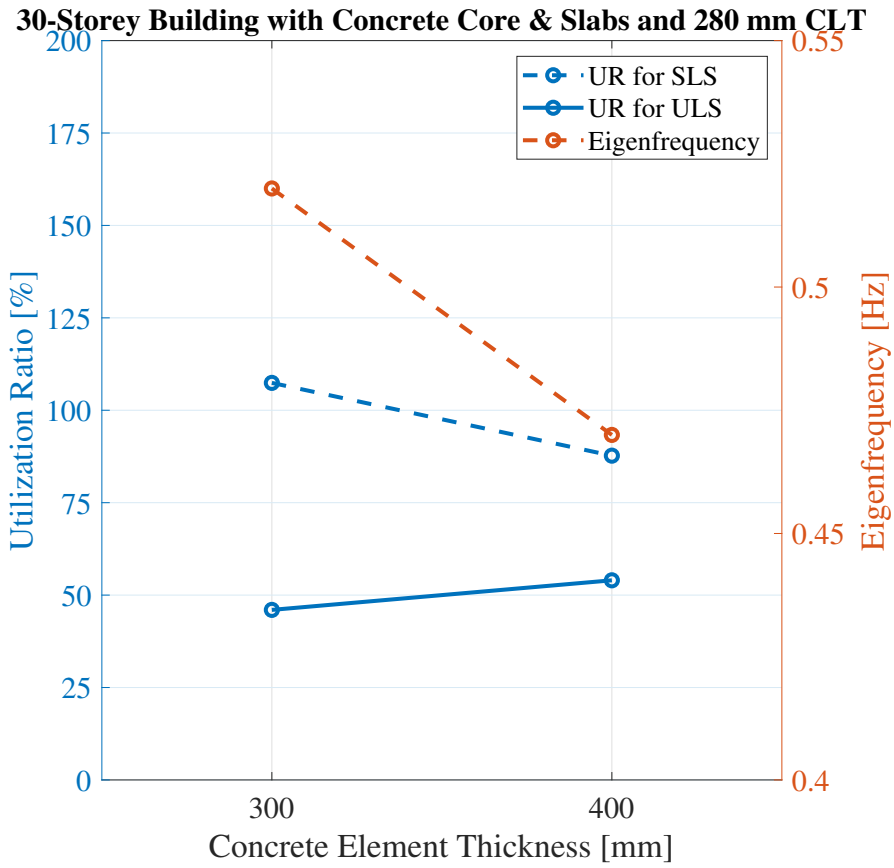

Figure 5.13: Results of a 30-storey hybrid building with concrete core and slabs and 280 mm CLT.

The building's height was further increased to 35 floors. The results in Figure 5.14 show that when the comfort criterion is achieved the building fails in ULS with failure mode compression.

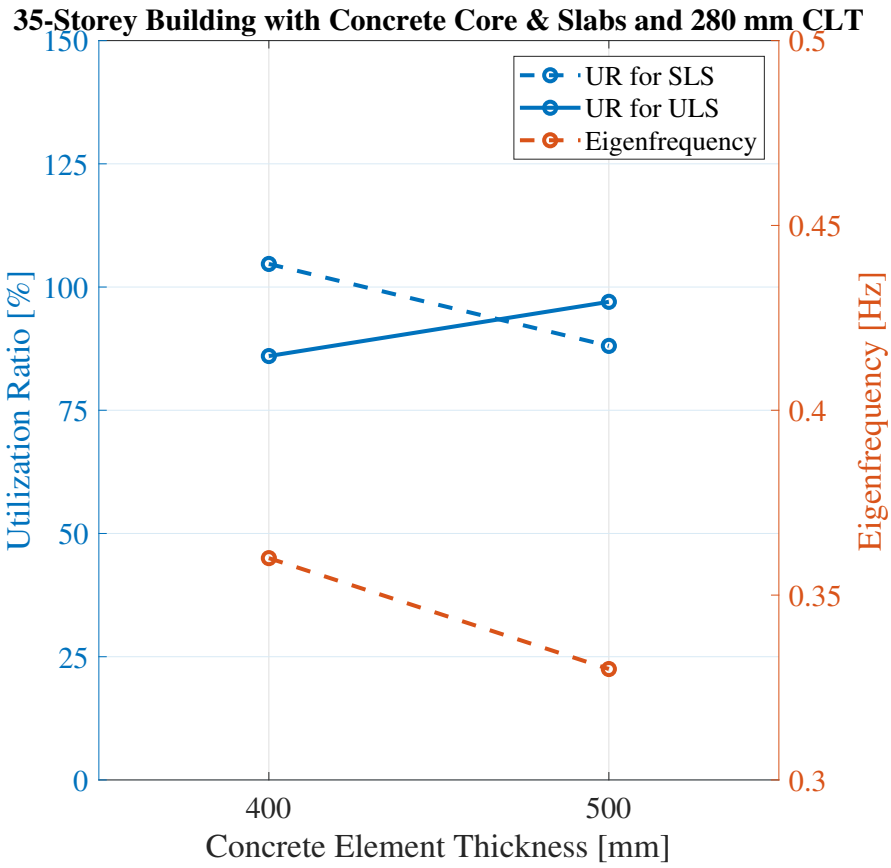

Figure 5.14: Results of a 35-storey hybrid building with concrete core and 280 mm CLT.

5.5 Hybrid Timber Building with the First Two Floors in Concrete

Usually, in buildings, it is common to have commercial spaces or basements on the first few floors. Therefore, analyses were also performed of a timber building with two floors at the bottom made out of concrete to see if the change would make a noticeable difference compared to previous results from the pure timber building. The results in Figure 5.15 show that the increase in concrete thickness had a negligible effect on the dynamic response of the building.

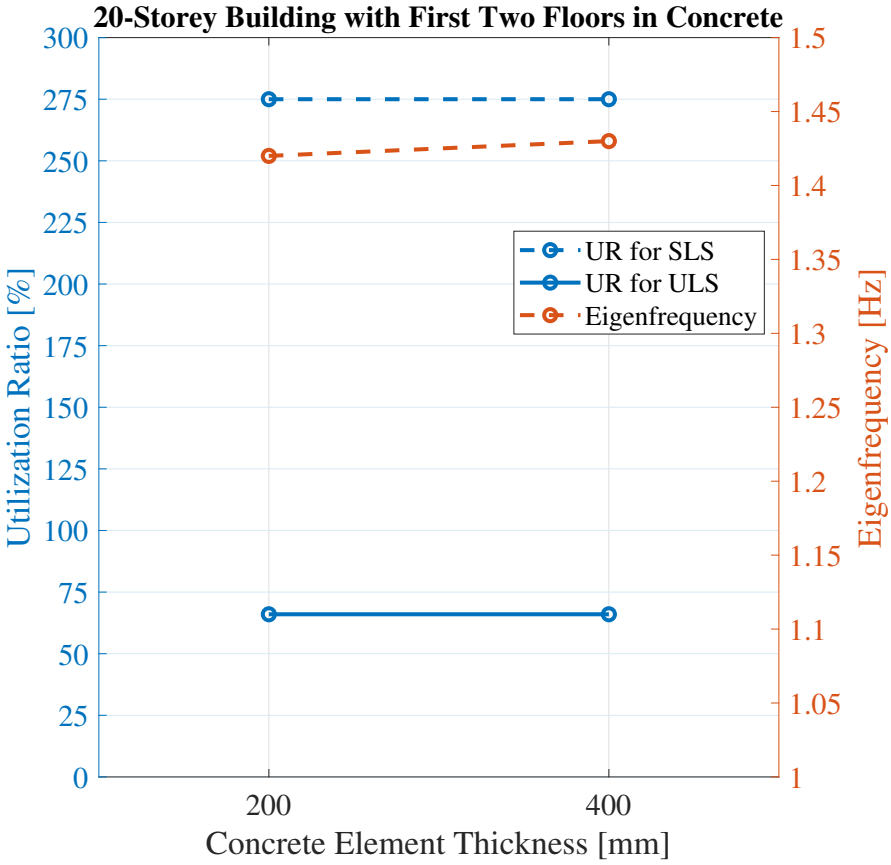

Figure 5.15: Results of a 20-storey hybrid building with the first two floor in concrete and 180 mm CLT elements.

5.6 Hybrid Timber Building with Multiple Floors in Concrete

The analysis of the hybrid timber-concrete building resulted in a lowered acceleration values for increased thickness of concrete elements. However, the response of the building in terms of maximum acceleration was affected by the change in thickness of concrete elements only when it led to the change of mass on the upper third part of the building and then the equivalent mass was also changed. The results of the analysis are given in Figure 5.16 for a 25-storey hybrid building with the lowest 8 storeys entirely made in concrete and the 17 above existing storeys are in CLT walls and slab with a concrete core extending along the entire height of the building.

A 13-storey pure timber building with 280 mm CLT elements depicted in Figure 5.1 can be exceeded in height, while still fulfilling the comfort criteria, by a mixed-use hybrid timber building. In the hybrid structure, a total of 17 storeys mainly consisting of timber, each with 280 mm CLT, can be constructed on top of 8 concrete storeys with 400 mm of cross-section for all concrete elements. Additionally, a concrete core is incorporated in the middle of the building, spanning its full length.

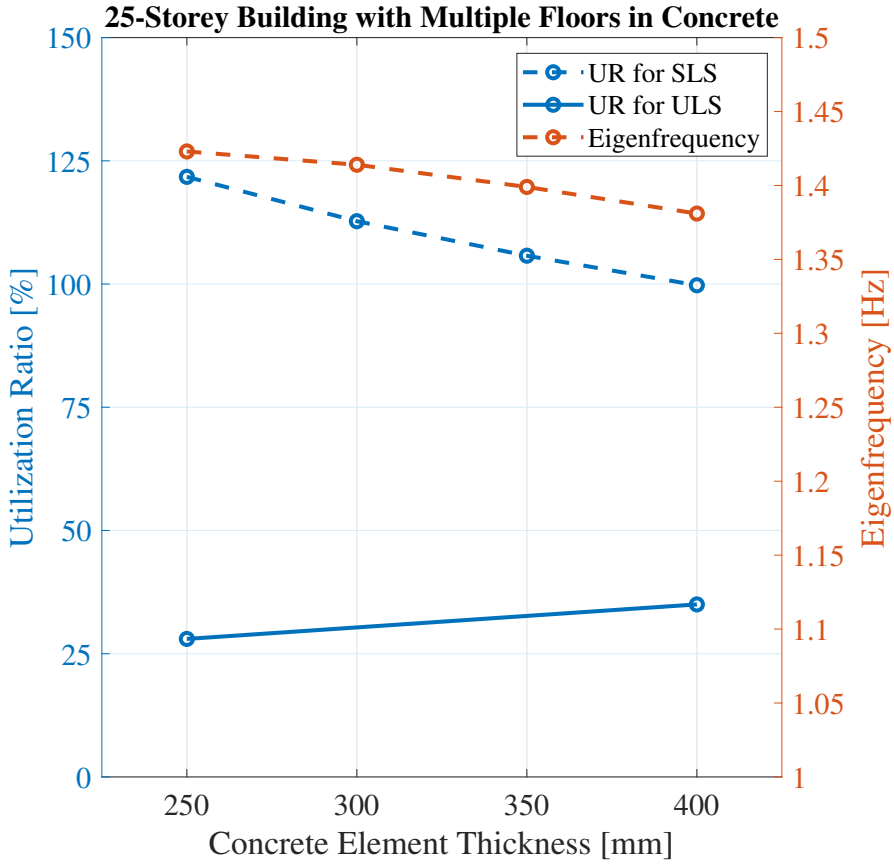

Figure 5.16: Results of a 25-storey hybrid building with concrete core and 280 mm CLT and the lowest 8 storeys entirely made of concrete.

5.7 Hybrid Timber Building with Commercial Areas

A 30-storey building was analysed with different concrete thicknesses. Instead of only incorporating storeys with residential usage, the top five storeys are commercial. The results are shown in Figure 5.17 and visualize that commercial storeys on top of residential buildings can allow a reduced concrete thickness and still fulfill both ULS and SLS. The ULS criteria that had the largest utilization ratio was compression on the first floor.

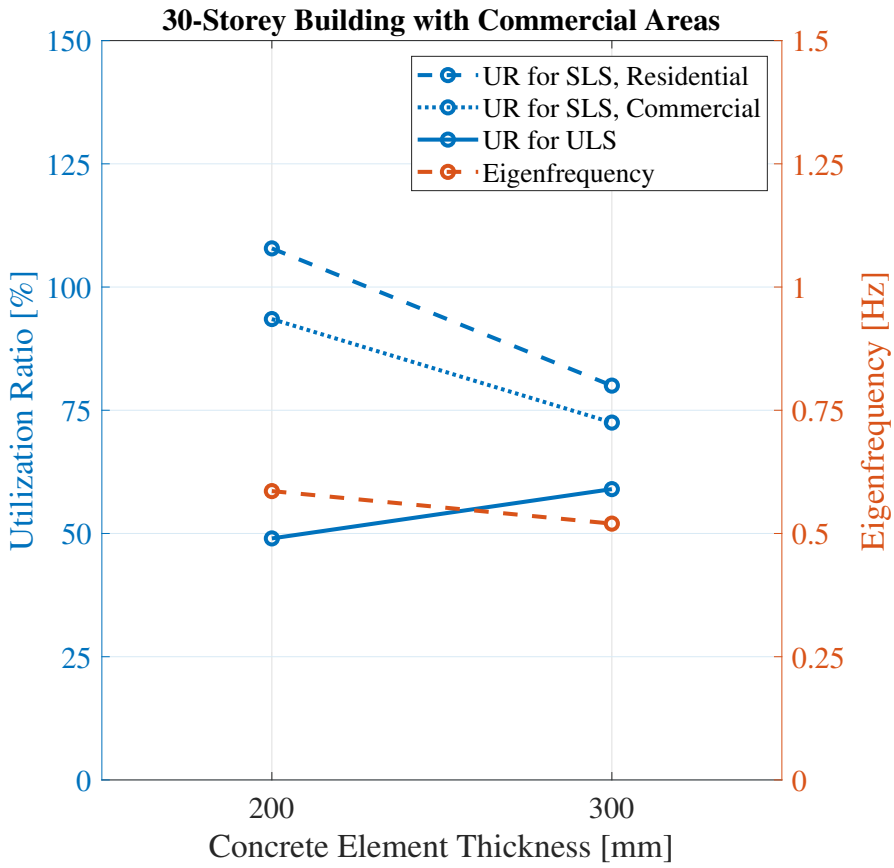

Figure 5.17: Results of a 30-storey hybrid building with commercial storeys on top of residential and a varying concrete floor and core wall thickness with 280 mm CLT.

The height of the building was then increased to 35 and 40 storeys and analyzed with an increasing concrete thickness. The results can be observed in Figure 5.18 and Figure 5.19. For these buildings the concrete slab and wall thickness needed to be increased. The ULS ratio increased as the building was subjected to an increased self-weight and the failing criterion was compression.

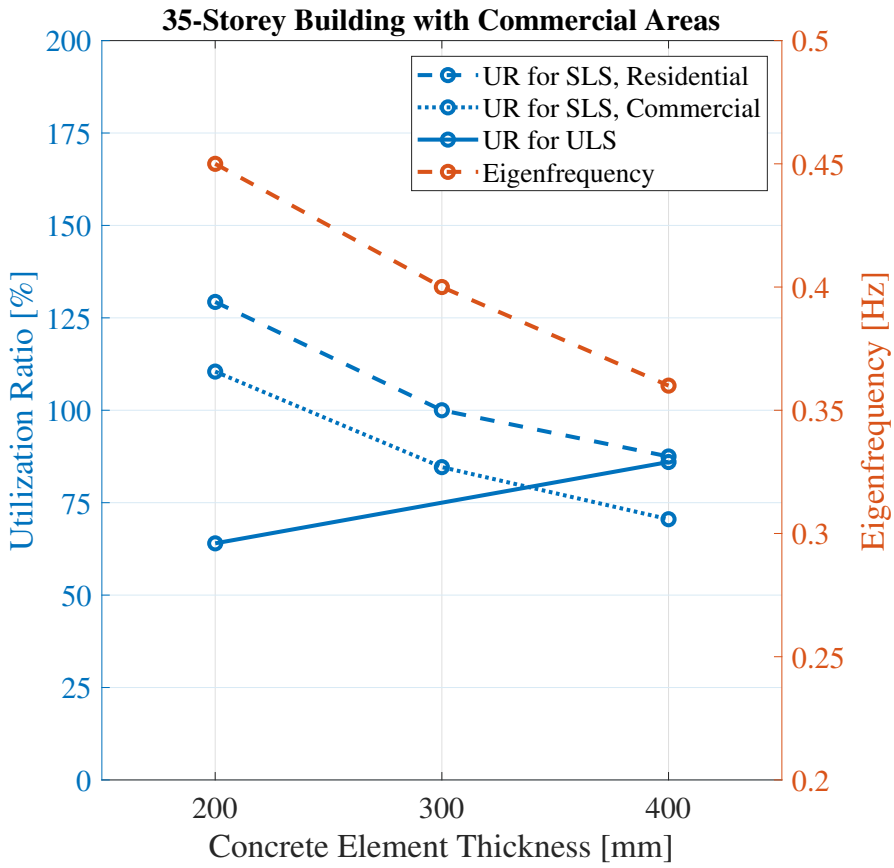

Figure 5.18: Results of a 35-storey hybrid building with concrete core and 280 mm CLT.

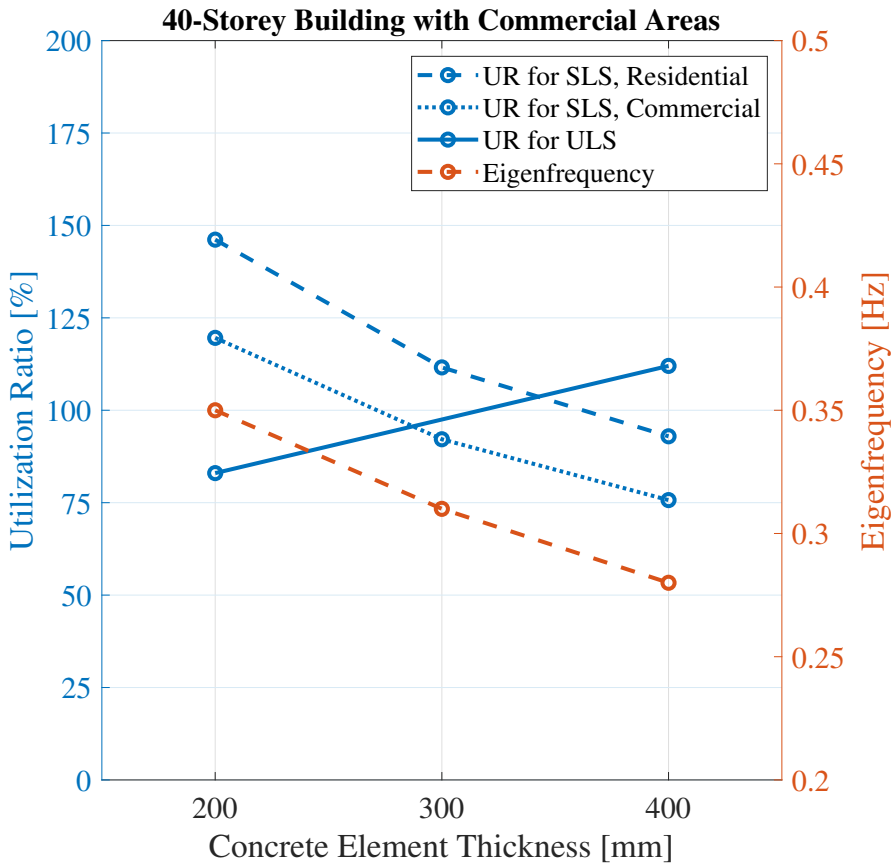

Figure 5.19: Results of a 40-storey hybrid building with concrete core and 280 mm CLT.

5.8 Reinforcing CLT Panels

The first building that was analyzed in this section was the 40-storey building with a concrete core and concrete slabs at the upper third part of the building with a thickness of 400 mm. Parts of the wall was replaced with a column connecting to the concrete core. The results can be observed in Table 5.1. The GLT column that replaced the walls had a utilization ratio of 63 % and therefore the comfort criterion would in this case also govern the design.

Table 5.1: ULS capacity for CLT elements for a 40-storey building with added columns.

	Number of storeys	Concrete thickness [mm]	UR in ULS for CLT [%]	failure criterion for CLT wall
Without columns	40	400	112	Compression
With columns	40	400	74	Compression

A previously analysed 25-storey hybrid building with a concrete core was analysed. To achieve acceptable accelerations, the core walls needed to be at least 900 mm thick and did not fulfill all the requirements in the Ultimate limit state. Parts of the CLT walls that connected to the core were changed to GLT columns. The results can be observed in Table 5.2. The utilization ratio decreased for the CLT wall. The GLT beams had a utilization ratio of 108 % which implies that the columns should be larger or contain a higher strength class.

Table 5.2: ULS capacity for CLT elements for a 25-storey building with added columns.

	Number of storeys	Concrete thickness [mm]	UR in ULS for CLT [%]	failure criterion for CLT wall
Without columns	25	1100	112	Compression
With columns	25	1100	58	Compression

5.9 Comparison Between ULS and SLS

A 25-story hybrid building with 300 mm thick core walls and slabs at the upper third building was modeled with a varying height. The results can be seen in Figure 5.20. It can be observed that the utilization ratio for SLS has a larger increase from 18 to 20 storeys and from 24 to 26 storeys compared to the others. The Utilization ratio for ULS increases at about the same rate. In this case it is also the SLS that governs the design.

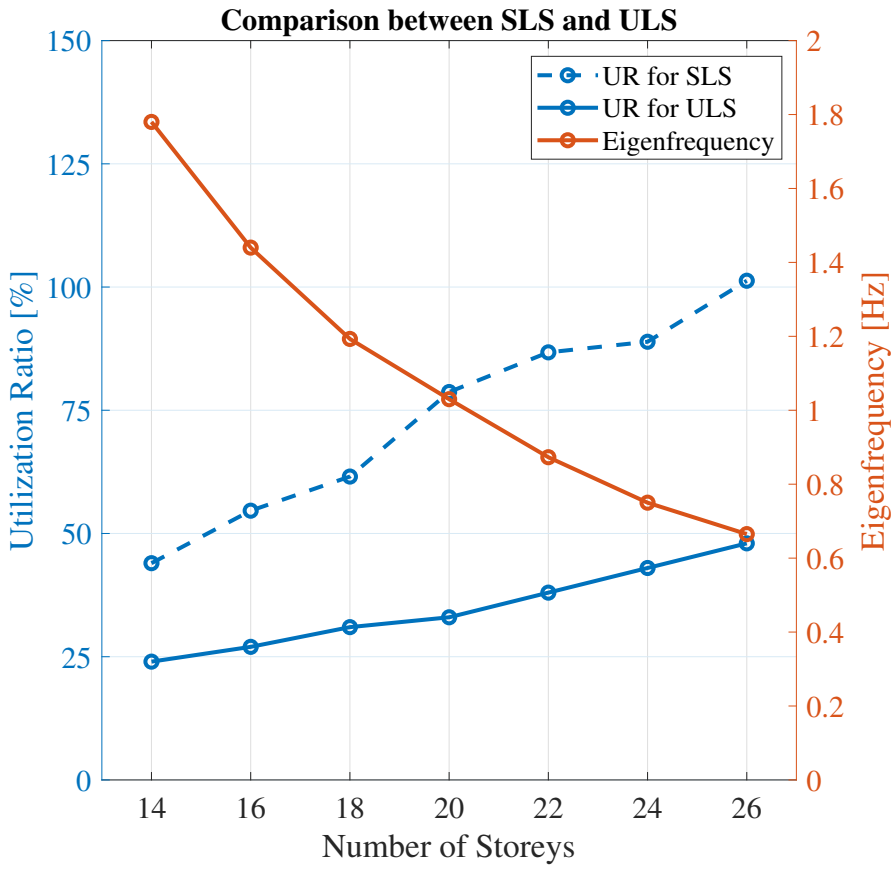

Figure 5.20: Results for various building heights comparing ULS with SLS with 300 mm concrete core and slabs and 280 mm CLT

5.10 Different Ratios of Usages for the Building

The 40-story building was modeled with a concrete core and concrete slabs at the upper third with a varying amount of commercial usage. Figure 5.21 shows the SLS utilization ratio of an increased concrete thickness where one storey at the top of the building is commercial. From the figure, it can be observed that there are large differences between the utilization ratios. The building fulfills both criteria at a thickness of 500 mm. A more optimal solution would be to have a more similar ratio between commercial and residential usage.

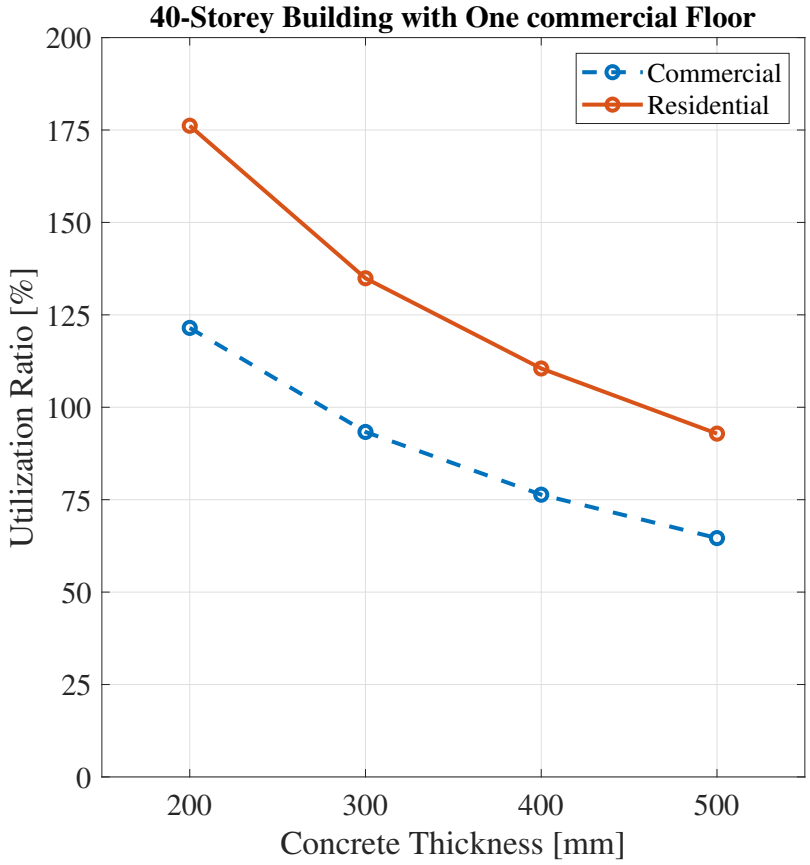

Figure 5.21: Comparison between UR for SLS for different usage of the buildings with one commercial floor.

The proportion of commercial areas was increased and a more optimal solution was obtained as shown in Figure 5.22 where the nine storeys at the top are commercial. It can be observed that the concrete thickness can be reduced by 200 mm on each concrete wall and slab, which still fulfills the comfort criteria. If the number of commercial storeys would further increase, there would not be benefits as the accelerations at the top of the building do not change.

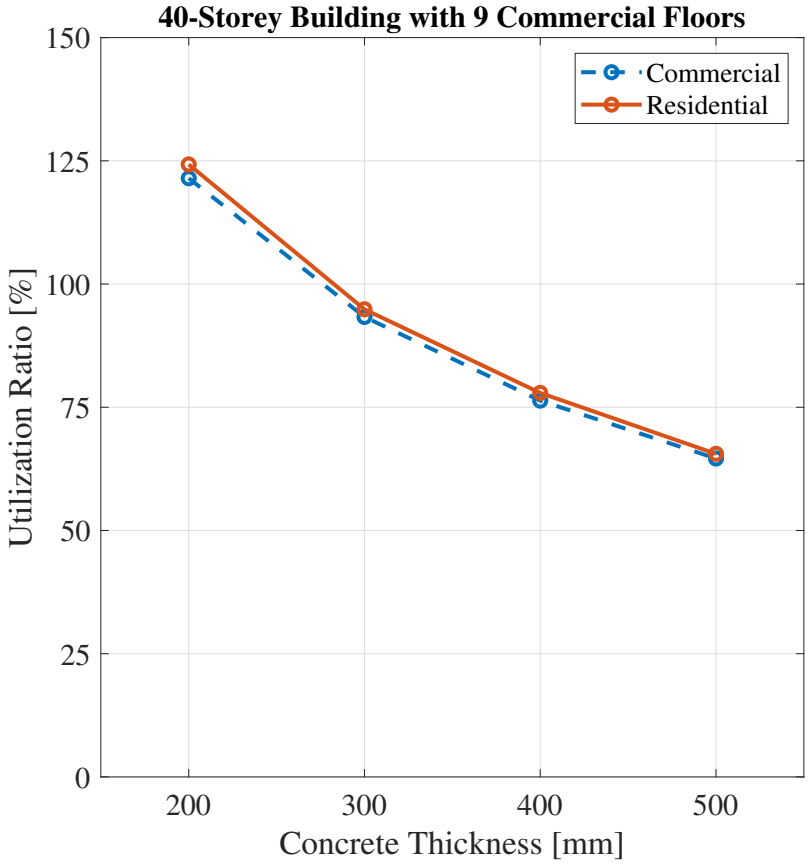

Figure 5.22: Comparison between UR for SLS for different usage of the buildings with 9 commercial floors.

The 40-storey building was then analysed with a fixed concrete slab thickness and a varying number of commercial storeys. The results in Figure 5.23 show a continuous decrease in utilization ratio for residential floors with an increased amount of commercial floors.

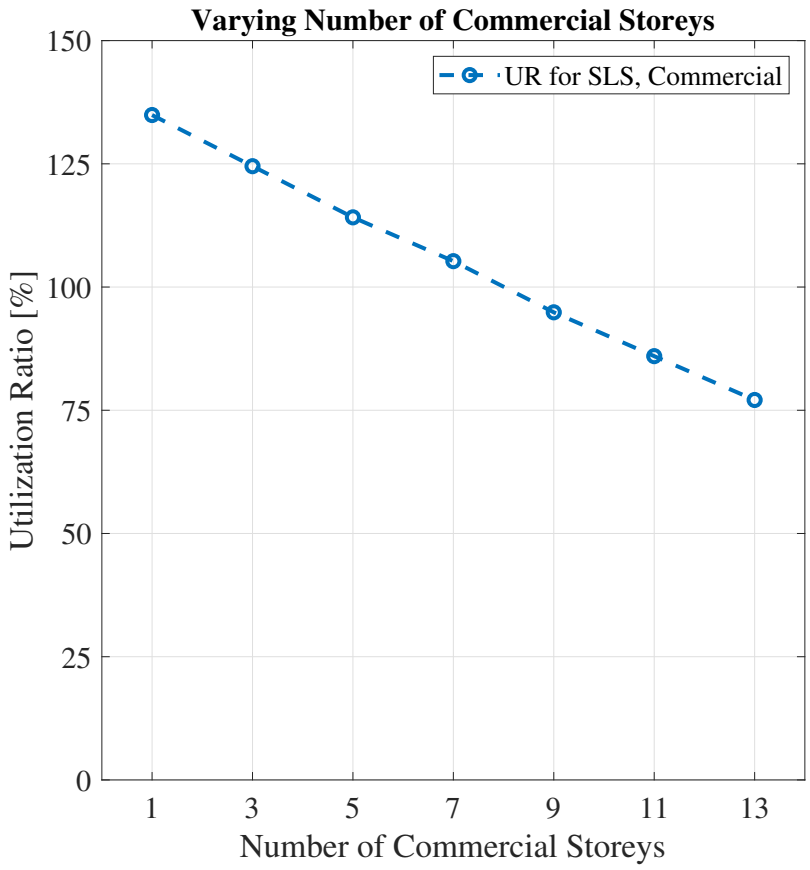

Figure 5.23: Results of a 40-storey building with a concrete core and slab thickness of 300 mm with a varying amount of commercial storeys.

5.11 Hybrid building with a Changed Structural System at the Bottom of the Building

The two lowest floors in a hybrid building with a concrete core was changed to a beam and column system for the 20-storey building was analysed. The results can be seen in Figure 5.24 and show that to meet the comfort criterion the concrete walls required a thickness of 800 mm which was 400 mm more than the hybrid building with a concrete core with CLT elements. The ULS analyses showed a utilization ratio of 70 % for the GLT elements and almost 100% for the CLT elements.

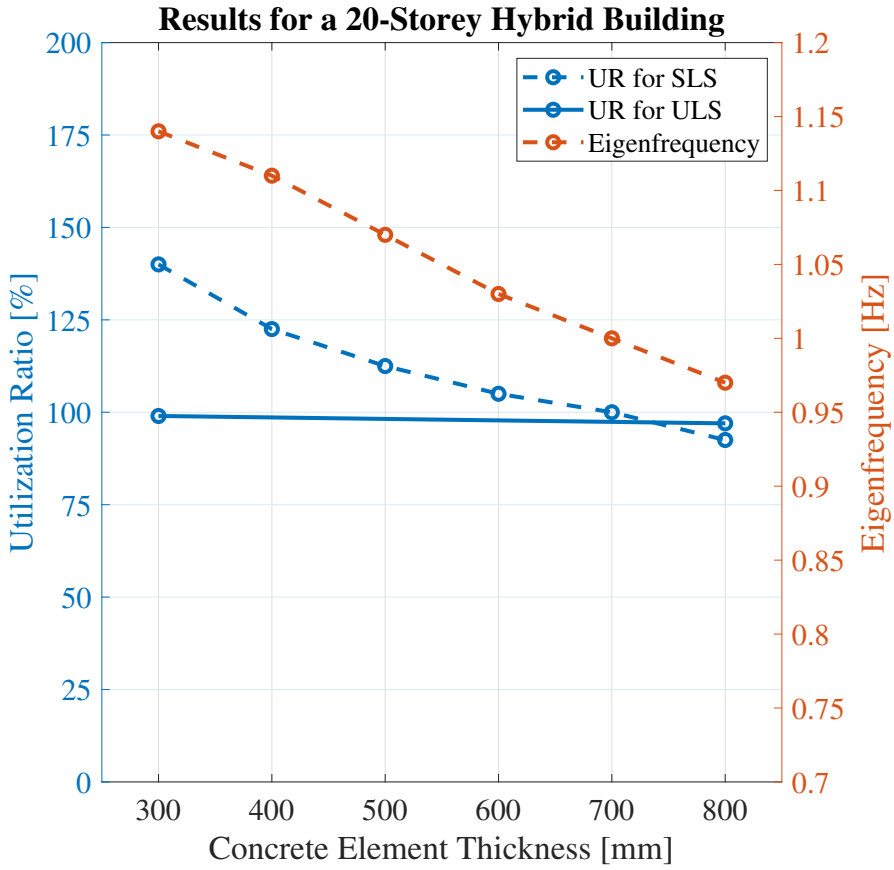

Figure 5.24: Results of a 20-storey hybrid building with a changed structural system at the lowest two floors with 280 mm CLT.

5.12 Hybrid Timber Office Building

The peak utilization ratio of the glulam timber columns reaches 71 %, primarily influenced by combined compression parallel to the fibers and flexural buckling around the weak axis. This phenomenon predominantly dictates the design considerations. Notably, the most vulnerable columns are situated on the second floor, featuring hinged connections at both ends and bearing the highest load.

Conversely, for the CLT slabs, the highest utilization ratio ranges between 54 % and 51 %, with a slight decrease observed as the concrete wall thickness in the building's core increases.

Regarding the SLS criteria, the maximum acceleration value experienced in the building is primarily influenced by the change in the thickness of the concrete walls in the building's core. It decreases to a value of 0.070 m/s² for a concrete wall thickness of 650 mm, where it just reaches the allowed limit for an eigenfrequency of 0.711 Hz. Results of a comparative study between a residential and an office building, both standing at a height of 63 meters, yet employing different structural

systems is illustrated in Figure 5.25. Maximum utilization ratio in ULS for column and slab in the office building and for a wall in the residential building are presented in Figure 5.26.

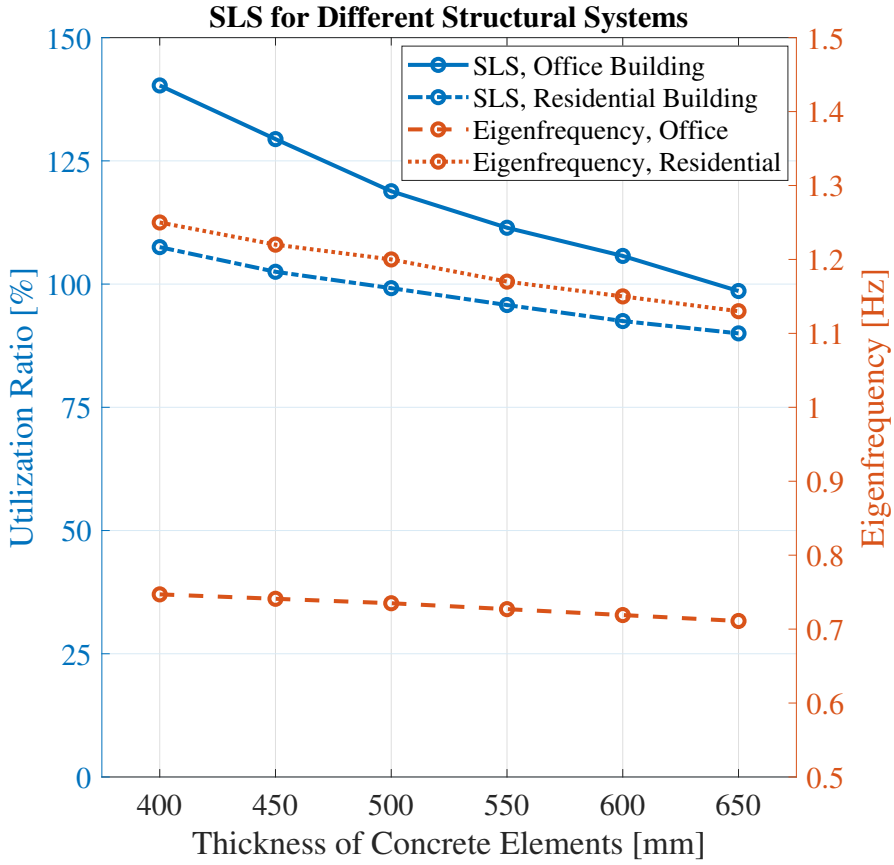

Figure 5.25: Results of a comparative study with regard to SLS, between a residential and an office building of the same height.

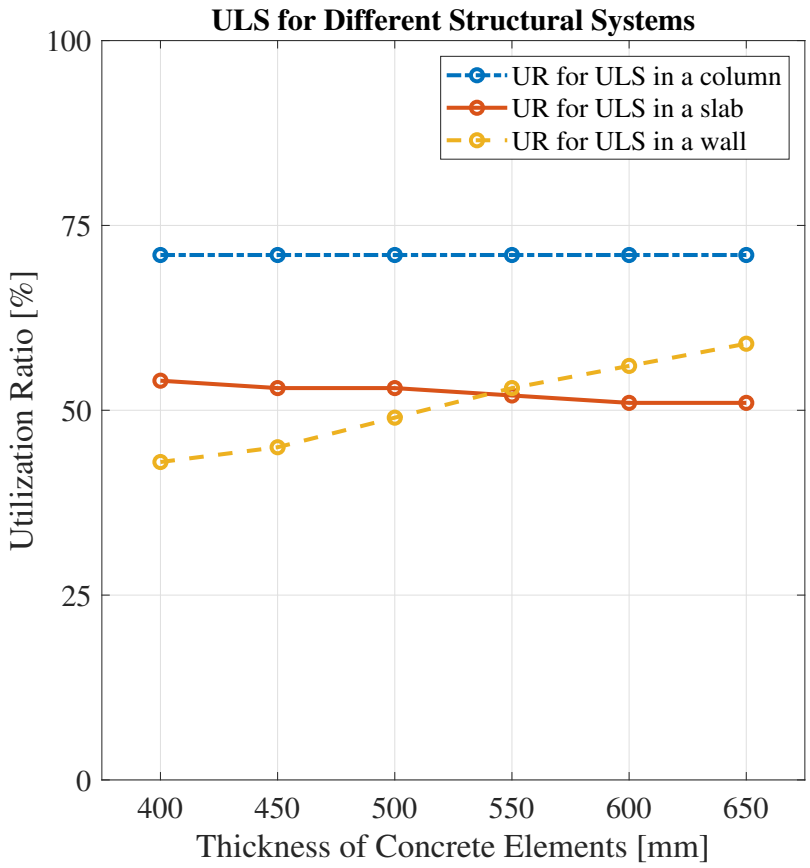

Figure 5.26: Results of maximum utilization ratio in ULS for column and slab in an office building and for a wall in a residential building.

6
Discussion

Several different parameters affect a building's dynamic and structural performance. In general, more stiffness and equivalent mass contribute to improved dynamic performance. However, the added mass have the opposite effect on the load-bearing capacity.

6.1 Changing the Type of CLT Panels

When changing the thickness and the number of layers for the CLT elements, the effect with regard to the dynamic performance was significant. For the tested building two more storeys could be added by increasing the thickness of the CLT panels with 100 mm. The thicker elements increase the fundamental frequency, but also the limit for allowable accelerations where there was a combined effect. The added thickness of the CLT contributed to an increased equivalent mass and stiffness which improved the dynamic performance. The largest ULS utilization ratio could be found in the core and it was through tension. It was localized to the corners close to the openings where the stress concentrations are large. The thicker elements contributed to a decreased utilization ratio as the stresses would spread out over a larger area compared to thinner CLT elements. For this type of building, it is the acceleration that limits the height due to the building failing in SLS while the CLT panels can resist more load. The maximum number of storeys for the tested building was considered to be 13 storeys.

6.2 Adding a Concrete Core

The concrete core has benefits both in the service limit state and ultimate limit state. The added concrete led to an increase in stiffness and mass which improved the dynamic performance and lowered the accelerations. The added height reduced the dynamic performance of the building as taller buildings have lower fundamental frequency. The different thicknesses of CLT panels also had an impact on the dynamic performance in the same way as for the pure timber building. The required concrete thickness to fulfill the comfort criteria decreased with 300 mm for the 20-storey building when the CLT panels were increased from 5 layers to 7 layers. 20 storeys of the analyzed residential building is possible to build with a concrete thickness of 400 mm, utilizing 7-layer CLT panels. When the height increases to 25 storeys, the concrete thickness needs to be 900 mm, which can be considered unreasonably large.

In terms of ULS analyses the most loaded CLT wall is not in the core as the previous timber walls were replaced with concrete, since reinforced concrete can sustain the tension forces. The most loaded wall is one on the bottom floor which sustains large compression forces. The compression criteria had the largest utilization ratio and the largest compression stresses in the panel where located in a corner connected to the concrete core. The utilization ratio also increases with increasing concrete thickness due to the stiffer wall taking more load which increases the stress concentration in the corner. The analyses have shown that the utilization ratio in the panels could be decreased by shortening the length of the wall and instead installing GLT columns. The CLT wall have a fiber direction that alternates with each layer. It means that for a 7-layer panel, only 4-layers would be in the main direction. The GLT columns have all the fibers in the same direction which means that more material could be utilized in the longitudinal direction of the element.

6.3 Adding Concrete Slabs

The concrete slabs have shown that the added mass at the top of the building improves the dynamic performance as the equivalent mass increases. If the concrete slabs had been added to the lower storeys of the building, the equivalent mass would not have been affected. The 20-storey building needed a concrete thickness of 550 mm for the thinner CLT walls at the upper third part of the building which is less thickness compared to the hybrid building with just a concrete core. The concrete slabs do have a larger volume compared to the building with a concrete core. However, for the thicker CLT walls used in the 20-storey building, the concrete element thickness needed was between 350 mm and 400 mm to fulfill the comfort criterion, which is comparable with the required thickness for the building containing the concrete core.

The compression forces increased with an increasing concrete slab thickness. The added weight increases the self-weight of the slabs and therefore the CLT walls need to sustain a higher load. The increasing compression forces increase the ULS utilization ratio and therefore the ULS and SLS counteract each other. When increasing the thickness of the slabs, the SLS performance increases, and the ULS utilization ratio also increases. For the tested building, it is the tension criterion that had the largest ULS utilization ratio. The ratio did not significantly increase with an increased concrete thickness as the wind load was approximately the same. These tension stresses were localized to corners in core walls. The analyses show that the utilization ratio for ULS is lower than for SLS and it is therefore SLS that is more critical in design compared to ULS.

6.4 Combination of Concrete Core and Concrete Slab

The combined effect of a concrete core and slabs contributed to an increased dynamic performance of the building. The 25-storey building needed a concrete thickness of 300 mm while a building with just a concrete core needed a thickness of 900 mm to fulfill the acceleration criterion. The combination makes it possible to build taller buildings.

The ULS utilization ratio is smaller compared to the those in SLS in most cases. The building should therefore be designed for acceleration where the ULS also would be fulfilled. When reaching 40 storeys the added weight and stiffness contribute to high utilization ratio in ULS. The ratio could be reduced by installing GLT columns which reinforce the CLT panels.

The fundamental frequency of the building decreases with an increasing amount of concrete as the mass increases. The acceleration also decreases with increasing concrete thickness and the limit for allowed acceleration increases with a decreasing fundamental frequency. When the height of a building increases the fundamental frequency decreases and the acceleration increases. The utilization ratio for SLS is both dependent on the acceleration and the corresponding limit. The limit for fundamental frequency between one and two hertz is constant while below one hertz the limit increases with a decreasing fundamental frequency. The results have shown that the utilization ratio increases more in the range between one and two hertz compared to when the fundamental frequency is below one hertz.

6.5 Different Usage of the Building

The limit for accelerations is dependent on two parameters which are the fundamental frequency and the use case of the building. A commercial use allows for higher accelerations compared to residential. It is therefore beneficial to have offices on the top floors of the building where the accelerations are the largest. The optimal number of office floors was nine where the SLS utilization for office and residential was approximately the same. However, in today's buildings, it is unusual to have office spaces on top of apartments. For a 30-storey building with the top five storeys used for commercial purpose, one could save 100 mm of concrete thickness. This way, even taller buildings are possible to build which makes it possible to build 40 storeys or even taller. Note that these analyses assume the same floor plan on each floor. A system with beams and columns would contribute to a lower fundamental frequency of the building as the elements are not as stiff compared to walls, which contributes to a decreased dynamic performance.

A more conventional building is to have commercial areas such as restaurants and stores or basements on the lower floors of the building. They are often made out

of concrete. When changing the two and eight bottom floors into concrete the observation was that the concrete were stiff and the 20-storey building with the two bottom storeys in concrete performed like an 18-storey timber building. The equivalent mass of the building does not increase when increasing the mass at the bottom of the building and therefore the improvement of the dynamic performance is limited.

The commercial areas often have a more open floor plan with a beam and column system. The decreased stiffness of the columns and beams resulted in a decreased SLS performance. The thickness of the concrete walls needed to be increased from 400 to 800 mm for the hybrid building with a concrete core when the bottom two storeys had the beam and column system. The columns below the CLT wall takes a large amount of load and there were high stress concentrations in the corner of the walls. The increased concrete thickness would in this case reduce the maximum utilization as the core walls would take more load. To reduce the large stresses, the GLT columns could extend along the height of the building.

6.6 Comparing Different Structural Systems

The performance of the hybrid building with the beam and column system became worse compared to the slab and wall hybrid system with a concrete core even though the limit for acceleration was increased for commercial usage. The main disadvantage is lower mass and stiffness. The elements that resist the lateral loads are the concrete core walls, while the residential buildings have CLT walls that can withstand horizontal actions. A way to improve the performance of the office building would be to install a bracing system. The utilization ratio for the office building in the ULS analysis was smaller compared to the SLS analysis. The increasing concrete core did not significantly affect the compression forces in the columns. The utilization ratio in ULS for the slabs in the office building, was slightly reduced as the core sustains more load with an increased concrete wall thickness. If concrete slabs had been incorporated the ratio would have significantly increased. In most cases, it has been compression that has been the failure criterion for ULS. In the case of the columns, the compression capacity needs to be reduced due to the risk of buckling.

6.7 Possible Sources of Error

One possible numerical error was noticed during the convergence analyses. When the design check was performed on a load-bearing element the maximum stresses are chosen. They were commonly located towards an edge or a corner. When the mesh size was reduced these stresses were increased. The stresses in these areas did not entirely converge and they are therefore dependent on the mesh.

Another possible source of error is the structural damping of the building. The choice of the parameter was based on recommendations from SS-EN 1991-1-4 (2005). The value of the damping ratio had a large impact on the results for accelerations. The

recommendations were based on a timber structure. If the parameter had been based on a concrete tower the dynamic performance of the building would decrease.

The geometry of the building was set early in the project. The dimensions of the building would affect its dynamic performance. The surroundings were assumed to be with a terrain category of three. Several additional parameters were assumed at an early stage, which would affect the ULS and SLS performance of the building.

The horizontal wind loads were approximated through the maximum wind pressure on top of each storey and distributed on each storey. This is conservative as the wind pressure increases logarithmically over the height of the building. The wind pressure is dependent on the fundamental frequency, which resulted in a factor that increased wind pressure to be more conservative.

The approximation of equivalent mass, as introduced in SS-EN 1991-1-4 (2005), was to calculate the average mass of the top third part of the building. A more general expression that contains an integration of the mass and the mode function would capture a more realistic behavior of the structure.

Almost all the connections in the model are assumed to be hinged, but a more realistic behavior of a connection would be somewhere in between clamped and hinged. The connections on the first floor are assumed to be fixed between the walls or columns and the foundation, but this might be difficult to achieve on the construction site.

7
Conclusion

7.1 Summary

There are several different parameters that influence the dynamic performance of a building. The analyses have shown that the main parameters that affected the accelerations were the height, the mass, and the stiffness of the building.

The dynamic performance of the building decreases with increasing height. The main reason is the decreased fundamental frequency. To improve performance, increasing concrete volume has proven to result in better SLS performance. Both by adding a concrete core and slabs at the top third of the building. Another way to improve the dynamic performance of the building is to increase the thickness of the timber elements. Large improvements were observed for an increased thickness of 100 mm for the CLT walls and slabs. The ULS utilization ratio for the CLT panels increased with an increasing concrete volume for the residential building. The analyses have shown that in almost all cases it is the SLS criterion will govern the design of the building. When the concrete thickness becomes unreasonably large or when the building reaches 40 storeys the ULS criteria will govern the design. The challenges with ULS capacity of the CLT wall elements can be fixed by installing GLT columns in critical areas.

The main objective of the thesis was to conclude how tall a just timber and hybrid timber structure can be. For the studied floor plan of a residential building, the maximum number of storeys for a pure timber building with CLT elements is 13 storeys while for a hybrid building with a concrete core with a thickness of 400 mm, the limit was up to 20 storeys. When the upper third slabs also are made of concrete the height could be increased to 30 storeys. The height could even further be increased with top storeys considered to obtain a commercial use, up to 40 storeys, namely a 120 m high building could be built. From a structural engineering point of view a hybrid building is a direct competitor to a concrete building up to at least 30 storeys or 90 meters. If the structural system would change to a system with less mass and stiffness, for example a beam and column system for the whole building or for a couple of storeys, the dynamic performance of the building would significantly decrease.

7.2 Further Studies

Some examples are listed below of possible research areas is presented that are based on the findings in the thesis:

In the report, SLS is referred to as the comfort criterion. In many cases SLS is a wider concept. For example, no long-term effects such as creep or a design against fire have been considered.

Regarding structural systems, no system with bracing was tested. The system with the columns and beams would benefit from bracing as it would increase the stability of the building.

The analyzed building had a square footprint. Other proportions of the building and different sizes would have an impact on the dynamic performance of the building. A larger footprint would have a larger stiffness and mass which can impact the performance positively.

In tall buildings, dampers are used to improve the dynamic performance. These would make it possible to build taller buildings. Taller buildings have proven in the thesis to have a larger utilization ratio for ULS.

In a building, there are several amount of connections that need to be designed. In the FE-model, the connections have not been included. It would therefore be a reasonable research area to design connections for a tall hybrid building.

In the project, the foundation has been modeled as fully stiff. A more realistic behavior would be to model spring elements, which could impact the dynamic performance of the building.

Bibliography

Abrahamsson, T. (2019). Structural dynamics and linear systems-compute, test, calibrate and validate.

Abu-zidan, Y., Mendis, P., Gunawardena, T., Mohotti, D., & Fernando, S. (2022). Wind design of tall buildings: The state of the art. *Electronic Journal of Structural Engineering*, *22*(01), 53–71.

Al-Emrani, M., Engström, B., Johansson, M., & Johansson, P. (2013). *Bärande konstruktioner, del 1*. Institutionen för Bygg- och miljöteknik.

Barcelo, L., Kline, J., Walenta, G., & Gartner, E. (2014). Cement and carbon emissions. *Materials and structures*, *47*(6), 1055–1065.

Boverket. (1997). *Boverkets handbok om snö- och vindlast*. Accessed 2024-02-05.

Boverket. (2021). *Boverkets föreskrifter och allmänna råd (2011:10) om tillämpning av europeiska konstruktionsstandarder (eurokoder)*. https://www.boverket.se/sv/lag--ratt/forfattningssamling/gallande/eks---bfs-201110/ Accessed 2024-02-05.

Cavicchia, R. (2021). Are green, dense cities more inclusive? densification and housing accessibility in oslo. *Local Environment*, *26*(10), 1250–1266.

Cermak, J. E. (1977). Wind-tunnel testing of structures. *Journal of the Engineering Mechanics Division*, *103*(6), 1125–1140. https://doi.org/10.1061/JMCEA3.0002301

Craig Jr, R. R., & Benzley, S. E. (1982). Structural dynamics, an introduction to computer methods.

Dahlén, J., & Niemi-Impola, J. (2023). Dynamic optimization of high rise timber-hybrid buildings a fem study of the effect on the dynamic response of combining timber and concrete in a high rise building.

Engström, B. (n.d.). Distribution of horizontal load on bracing elements.

Gagg, C. R. (2014). Cement and concrete as an engineering material: An historic appraisal and case study analysis. *Engineering Failure Analysis*, *40*, 114–140.

Iqbal, A. (2021). Developments in tall wood and hybrid buildings and environmental impacts. *Sustainability*, *13*(21), 11881.

Kallmén, S. (2022). Trä som byggnadsmaterial.

Kappos, A. (2001). *Dynamic loading and design of structures*. CRC Press.

Landel, P. (2022). *Wind-induced vibrations in tall timber buildings: Design standards, experimental and numerical modal analyses* [Doctoral dissertation, Linnaeus University Press].

Larsson, C. (2023). *Timber-concrete hybrid structural systems: Examples, long and short-term dynamic monitoring, and numerical analysis* [Doctoral dissertation, Linnaeus University Press].

Latterini, F., Mederski, P. S., Jaeger, D., Venanzi, R., Tavankar, F., & Picchio, R. (2023). The influence of various silvicultural treatments and forest operations on tree species biodiversity. *Current Forestry Reports*, *9*(2), 59–71.

Mario, P., & Young, H. K. (2019). Structural dynamics: Theory and computation.

Mendis, P., Ngo, T., Haritos, N., Hira, A., Samali, B., & Cheung, J. (2007). Wind loading on tall buildings. *Electronic Journal of Structural Engineering*.

Saemundsson, Á. F. (2007). Wind effects on high rise buildings.

Smith, B. S., & Coull, A. (1991). *Tall building structures: Analysis and design*. John Wiley Sons.

SS-EN 1991-1-1. (2002). *Eurocode 1: Actions on structures - part 1-1: General action - densities, self-weight, imposed loads for buildings*. Svenska institutet för standarder, Stockholm.

SS-EN 1991-1-4. (2005). *Eurocode 1: Actions on structures - part 1-4: General action - wind actions*. Svenska institutet för standarder, Stockholm.

SS-ISO 10137. (2008). *Bases for design of structures: Serviceability of buildings and walkways against vibration*. Svenska institutet för standarder, Stockholm.

Strømmen, E. (2010). *Theory of bridge aerodynamics*. Springer Science & Business Media.

Swedish Wood. (2019). *The clt handbook: Clt structures - facts and planning*.

Swedish Wood. (2022). *Design of timber structures - structural aspects of timber construction*.

Tapia, C., & Aicher, S. (2023). A new concept for column-to-column connections for multi-storey timber buildings—numerical and experimental investigations. *Engineering Structures*, *295*, 116770. https://doi.org/https://doi.org/10.1016/j.engstruct.2023.116770

Tedesco, J., McDougal, W. G., & Ross, C. A. (2000). *Structural dynamics*. Pearson Education London, UK.

Van Den Einde, L., Zhao, L., & Seible, F. (2003). Use of frp composites in civil structural applications. *Construction and building materials*, *17*(6-7), 389–403.

Williams, M. (2016). *Structural dynamics*. CRC Press.

A

Appendix

A.1 Detailed results from convergence studies

Table A.1: Results of the convergence study from the model with CLT-panel.

	Seed size 3 m	Seed size 2 m	Seed size 0.8 m	Seed size 0.6 m	Seed size 0.5 m	Seed size 0.4 m	Seed size 0.3 m
1 [kNm/m]	0.87	0.87	0.84	0.82	0.82	0.82	0.82
2 [kNm/m]	1.04	1.04	1.08	1.08	1.08	1.08	1.08
3 [kNm/m]	8.14	7.83	8.20	8.20	8.20	8.20	8.20
4 [kNm/m]	12.95	12.05	12.03	12.33	12.20	12.20	12.20
5 [kN/m]	4.23	4.73	4.31	4.59	4.59	4.59	4.59
6 [kN/m]	7.40	7.28	7.09	7.29	7.29	7.29	7.30
7 [kN/m]	42.91	42.95	42.28	41.02	42.74	42.42	42.61
8 [kN/m]	36.08	36.15	37.61	36.36	36.46	36.46	36.90
9 [kN/m]	154.57	154.52	159.22	158.273	158.01	157.90	158.33
10 [kN/m]	173.10	173.19	181.60	179.37	179.42	179.68	179.78
11 [Hz]	1.282	1.281	1.274	1.268	1.264	1.262	1.259
12 [kN/m]	99.42	99.65	156.17	158.21	162.00	143.86	141.64

A.2 Detailed results for analyzed pure CLT building

Table A.2: Maximum attainable height with a pure timber building with 5-layer CLT elements.

No. of storeys	Building's height [m]	Eigenfreq. [Hz]	Total mass [ton]	Acceleration [m/s^2]
10	30	3.01	937	0.043
11	33	2.69	1034	0.049
12	36	2.42	1130	0.056

Table A.3: Maximum attainable height with a pure timber building with 7-layer CLT elements.

No. of storeys	Building's height [m]	Eigenfreq. [Hz]	Total mass [ton]	Acceleration [m/s^2]
12	36	2.57	1603	0.037
13	39	2.34	1739	0.042
14	41	2.13	1875	0.046

Table A.4: Analysis for a tall CLT building with an increasing height when the comfort criterion is disregarded.

No. of storeys	Building's height [m]	Eigenfreq. [Hz]	Total mass [ton]	Acceleration [m/s^2]	Max Utilization degree ULS [%]
24	72	0.98	2289	0.154	95
25	75	0.92	2385	0.164	102

A.3 Detailed results for analyzed CLT timber building with concrete floors

Table A.5: Accelerations with a varying concrete floor thickness at top floor for the 12-storey hybrid building.

Building's height [m]	Thickness of concrete floor [mm]	Eigenfreq. [Hz]	Equivalent mass [ton/m]	Acceleration [m/s^2]
36	180	2.09	42.7	0.050
36	200	2.06	44.5	0.049
36	300	1.91	54.0	0.044
36	400	1.79	63.4	0.041
36	500	1.69	73.2	0.038

Table A.6: Results from a 20-storey building with a varying concrete slab thickness with 5-layer CLT elements.

Thickness of concrete floor [mm]	Eigenfreq. [Hz]	Equivalent mass [ton/m]	Acceleration [m/s²]	Max utilization ratio in ULS [%]
200	0.82	86	0.073	75
300	0.71	118	0.062	
400	0.64	150	0.053	
450	0.61	167	0.052	
500	0.58	178	0.051	
550	0.056	199	0.047	79

Table A.7: Results from a 20-storey building with a varying concrete slab thickness with 7-layer CLT panels.

Thickness of concrete floor [mm]	Eigenfreq. [Hz]	Equivalent mass [ton/m]	Acceleration [m/s²]	Max utilization ratio in ULS [%]
200	0.98	93	0.055	52
250	0.92	109	0.051	
300	0.87	126	0.047	
350	0.82	142	0.044	
400	0.78	158	0.042	54

A.4 Detailed results for analyzed CLT building with concrete core

Table A.8: Results from a 20-storey building with a varying wall thickness of concrete core. The thickness of CLT-elements are 180 mm.

Thickness of concrete elements [mm]	Eigenfreq. [Hz]	Total mass [ton]	Acceleration [m/s²]	Max utilization ratio in ULS [%]
300	1.30	4019	0.056	43
500	1.17	5570	0.045	
700	1.08	7122	0.039	61

Table A.9: Results from a 20-storey building with a varying wall concrete core thickness. The thickness of CLT elements are 280 mm.

Thickness of concrete elements [mm]	Eigenfreq. [Hz]	Total mass [ton]	Acceleration [m/s²]	Max utilization ratio in ULS [%]
300	1.42	4686	0.043	28
400	1.35	5461	0.039	31

Table A.10: Results from a 25-storey building with a varying concrete core thickness and 180 mm thick CLT elements.

Thickness of concrete elements [mm]	Eigenfreq. [Hz]	Total mass [ton]	Acceleration [m/s²]	Max utilization ratio in ULS [%]
400	0.85	6000	0.075	65
600	0.77	7939	0.063	
800	0.71	9879	0.056	
900	0.68	10848	0.054	
1100	0.64	12788	0.048	112

Table A.11: Results from a 25-storey building with a varying concrete core thickness and 280 mm CLT elements.

Thickness of concrete elements [mm]	Eigenfreq. [Hz]	Total mass [ton]	Acceleration [m/s²]	Max utilization ratio in ULS [%]
400	0.94	6834	0.059	42
600	0.86	8773	0.054	
800	0.80	10712	0.051	
900	0.77	11682	0.043	62

A.5 Detailed results for analyzed CLT timber building with concrete core and floors

Table A.12: Results from a 20-storey building with a varying concrete floor and core wall thickness and 180 mm thick CLT elements.

Thickness of concrete elements [mm]	Eigenfreq. [Hz]	Equivalent mass [ton/m]	Acceleration [m/s²]	Max utilization ratio in ULS [%]
200	1.00	107	0.048	39
300	0.89	151	0.039	46

Table A.13: Results from a 25-storey building with a varying concrete floor and core wall thickness and 180 mm thick CLT elements.

Thickness of concrete elements [mm]	Eigenfreq. [Hz]	Equivalent mass [ton/m]	Acceleration [m/s²]	Max utilization ratio in ULS [%]
200	0.68	109	0.069	61
300	0.60	155	0.056	
400	0.55	201	0.051	85

Table A.14: Results from a 25-storey building with a varying concrete floor and core wall thickness and 280 mm thick CLT elements.

Thickness of concrete elements [mm]	Eigenfreq. [Hz]	Equivalent mass [ton/m]	Acceleration [m/s²]	Max utilization ratio in ULS [%]
200	0.80	115	0.056	39
250	0.75	138	0.050	
300	0.71	161	0.047	46

Table A.15: Results from a 30-storey building with a varying concrete floor and core wall thickness and 280 mm thick CLT elements.

Thickness of concrete elements [mm]	Eigenfreq. [Hz]	Equivalent mass [ton/m]	Acceleration [m/s²]	Max utilization ratio in ULS [%]
300	0.52	172	0.058	46
400	0.47	222	0.050	54

Table A.16: Results from a 35-storey building with a varying concrete floor and core wall thickness and 280 mm thick CLT elements.

Thickness of concrete elements [mm]	Eigenfreq. [Hz]	Equivalent mass [ton/m]	Acceleration [m/s²]	Max utilization ratio in ULS [%]
400	0.36	211	0.067	86
500	0.33	258	0.059	97

A.6 Detailed results for analyzed CLT timber building with concrete core and floors at the lowest two storeys

Table A.17: Results from a 20-storey building with the two lowest storeys consisting of concrete elements and 180 mm thick CLT elements.

Thickness of concrete elements [mm]	Eigenfreq. [Hz]	Equivalent mass [ton/m]	Acceleration [m/s²]	Max utilization ratio in ULS [%]
200	1.42	30	0.11	66
400	1.43	30	0.11	66

A.7 Detailed results for analyzed CLT timber building with concrete core and floors at the lowest 8 storeys

Table A.18: Results from a 25-storey building with 8 storeys in concrete at bottom of building with a varying concrete floor and core wall thickness and 280 mm thick CLT elements

Thickness of concrete elements [mm]	Eigenfreq. [Hz]	Equivalent mass [ton/m]	Acceleration [m/s^2]	Max utilization ratio in ULS [%]
250	1.42	68	0.049	28
300	1.41	74	0.045	30
350	1.40	80	0.042	33
400	1.38	86	0.040	35

A.8 Detailed results for analyzed CLT timber building with commercial and residential usage

Table A.19: Results from a 30-storey building with five commercial storeys on top of residential and a varying concrete floor and core wall thickness and 280 mm thick CLT elements.

Thickness of concrete elements [mm]	Eigenfreq. [Hz]	Equivalent mass [ton/m]	Acceleration C [m/s^2]	Acceleration R [m/s^2]	Max utilization ratio in ULS [%]
200	0.59	122	0.072	0.055	49
300	0.52	172	0.058	0.044	59

Table A.20: Results from a 35-storey building with five commercial storeys on top of residential and a varying concrete floor and core wall thickness and 280 mm thick CLT elements.

Thickness of concrete elements [mm]	Eigenfreq [Hz]	Equivalent mass [ton/m]	Acceleration C [m/s²]	Acceleration R [m/s²]	Max utilization ratio in ULS [%]
200	0.45	118	0.095	0.075	64
300	0.40	164	0.077	0.061	
400	0.36	211	0.067	0.056	86

Table A.21: Results from a 40-storey building with five commercial storeys on top of residential and a varying concrete floor and core wall thickness and 280 mm thick CLT elements.

Thickness of concrete elements [mm]	Eigenfreq. [Hz]	Equivalent mass [ton/m]	Acceleration C [m/s²]	Acceleration R [m/s²]	Max utilization ratio in ULS [%]
200	0.35	119	0.116	0.095	83
300	0.31	166	0.094	0.077	
400	0.28	213	0.081	0.066	112

A.9 Detailed results for analyzed GLT beam and column system with a concrete core

Table A.22: Results for a 20-storey building with a beam and column system at the two first storeys, a varying concrete thickness and 280 mm thick CLT elements.

Thickness of concrete elements [mm]	Eigenfreq. [Hz]	Total mass [ton]	Acceleration [m/s²]	Max utilization ratio in ULS [%]
300	1.14	78	0.056	99
400	1.11	91	0.049	
500	1.07	104	0.045	
600	1.03	117	0.042	
700	1.00	127	0.040	
800	0.97	143	0.037	97

A.10 Detailed results for analyzed office GLT beam and column timber building with concrete core and floors

Table A.23: Results from an 18-storey office building with a varying concrete element thickness and 280 mm thick CLT elements.

Thickness of concrete elements [mm]	Eigenfreq. [Hz]	Equivalent mass [ton/m]	Acceleration [m/s^2]	slab [%]	Max utilization ratio in ULS [%]
400	0.75	73	0.094	54	71
450	0.74	79	0.088	53	71
500	0.74	85	0.082	53	71
550	0.73	91	0.078	52	71
600	0.72	97	0.074	51	71
650	0.71	103	0.070	51	71

A.11 Detailed results for analyzed residential CLT timber building with concrete core and floors

Table A.24: Results from a 21-storey residential building with a varying concrete element thickness and 280 mm thick CLT elements.

Thickness of concrete elements [mm]	Eigenfreq. [Hz]	Equivalent mass [ton/m]	Acceleration [m/s^2]	Max utilization ratio in ULS [%]
400	1.25	91	0.043	43
450	1.22	98	0.041	45
500	1.20	104	0.03967	49
550	1.17	110	0.0383	53
600	1.15	117	0.037	56
650	1.30	123	0.036	59

Calculations of Wind Dynamics for SLS and ULS

Input data:

$v_b := 25\ \frac{m}{s}$	Reference wind velocity Assuming Terrain category III
$z_0 := 0.3\ m$	Roghness length dependent on terrain category
$c_o := 1$	Topography factor
$h := 75\ m$	Height of the building
$b := 21.8\ m$	Width of the building
$h_{ref} := 10\ m$	Reference height of the building
$z_{max} := 200\ m$	Maximum height
$\rho := 1.25\ \frac{kg}{m^3}$	Air density
$n_{1.x} := 0.602\ Hz$	Fundamental frequency of the building
$c_{pe} := 1.3$	Pressure coefficient for external pressure
$c_{f.0} := 2.1$	Force coefficient without free-end flow
$T := 600\ s$	The reference time for the mean wind velocity
$\psi_\lambda := 0.64$	Reduction factor for elements with end effects
$\psi_r := 1$	Reduction factor for rounded corners
$T_a := 2$	Time period
$z := 1\ m, 2\ m .. h$	Height above ground surface
$z_{0.ll} := 0.05\ m$	Terrain parameter associated with terrain category 2
$z_{min} := 5\ m$	Terrain parameter associated with terrain category III

$\delta_s := 0.09$

Decrement of structural damping for timber, EC.

Ultimate Limit State:

$$I_v(z) := \frac{1}{c_o \cdot \ln\left(\frac{z}{z_0}\right)}$$

Turbulence intensity

$I_v(h) = 0.181$

$$k_r := 0.19 \cdot \left(\frac{z_0}{z_{0.ll}}\right)^{0.07} = 0.215$$

Terrain factor

$$c_r := \begin{cases} \text{if } h \le z_{min} \\ \quad k_r \cdot \ln\left(\frac{z_{min}}{z_0}\right) \\ \text{else} \\ \quad k_r \cdot \ln\left(\frac{h}{z_0}\right) \end{cases} = 1.189$$

Roughness factor

$$v_m := c_r \cdot c_o \cdot v_b = 29.732 \ \frac{m}{s}$$

Characteristic mean wind velocity

$$y_c := \frac{150 \cdot n_{1.x}}{v_m} \cdot m = 3.037$$

Non-dimensional frequency

$$F := \frac{4 \cdot y_c}{\left(1 + 70.8 \cdot {y_c}^2\right)^{\frac{5}{6}}} = 0.055$$

Karmans wind energy spectrum

$$\phi_h := \frac{1}{1 + \frac{2 \cdot n_{1.x} \cdot h}{v_m}} = 0.248$$

Size factor concerning the height of the building

$$\phi_b := \frac{1}{1 + \frac{3.2 \cdot n_{1.x} \cdot b}{v_m}} = 0.415$$

Size factor concerning the width of the building

$$m_e := 155 \cdot 1000 \cdot \frac{kg}{m} = \left(1.55 \cdot 10^5\right) \frac{kg}{m}$$ Eqvivalent mass

$$c_f := c_{f.0} \cdot \psi_r \cdot \psi_\lambda = 1.344$$ Force coefficient

$$z_s := \begin{cases} \text{if } 0.6 \cdot h \geq z_{min} \\ \quad 0.6 \cdot h \\ \text{else} \\ \quad z_{min} \end{cases} = 45\ m$$ Reference height

$$c_{rz} := \begin{cases} \text{if } z_s \leq z_{min} \\ \quad k_r \cdot \ln\left(\frac{z_{min}}{z_0}\right) \\ \text{else} \\ \quad k_r \cdot \ln\left(\frac{z_s}{z_0}\right) \end{cases} = 1.079$$ Roughness factor

$$v_{mz} := c_{rz} \cdot c_o \cdot v_b = 26.981 \frac{m}{s}$$ Characteristic mean velocity for reference height zs

$$\delta_{az} := \frac{c_f \cdot \rho \cdot b \cdot v_{mz}}{2 \cdot n_{1.x} \cdot m_e} = 0.005$$ Average decrement of damping

$$R := \sqrt[2]{\frac{2 \cdot \pi \cdot F \cdot \phi_b \cdot \phi_h}{\delta_s + \delta_{az}}} = 0.609$$ Resonance response

$$B := \sqrt[2]{\exp\left(\begin{array}{l} -0.05 \cdot \left(\frac{h}{h_{ref}}\right) + \left(1 - \frac{b}{h}\right) \\ \cdot \left(0.04 + 0.01 \cdot \left(\frac{h}{h_{ref}}\right)\right) \end{array}\right)} = 0.864$$ Background response

$$v := n_{1.x} \cdot \frac{R}{\sqrt[2]{B^2 + R^2}} = 0.347 \frac{1}{s}$$ Up-crossing frequency

$$k_p := \sqrt[2]{2 \cdot \ln\left(v \cdot T\right)} + \frac{0.6}{\sqrt[2]{2 \cdot \ln\left(v \cdot T\right)}} = 3.451$$ Peak factor

$q_b := 0.5 \cdot \rho \cdot {v_b}^2 = 390.625\ \boldsymbol{Pa}$

Reference mean velocity pressure

$q_p(z) := \left(1 + 2 \cdot k_p \cdot I_v(z)\right) \cdot \left(k_r \cdot \ln\left(\frac{z}{z_0}\right) \cdot c_o\right)^2 \cdot q_b$

$q_p(h) = 1.243\ \boldsymbol{kPa}$

Characteristic peak wind pressure

$q_{p2}(z) := \left(1 + 2 \cdot 3 \cdot I_v(z)\right) \cdot \left(k_r \cdot \ln\left(\frac{z}{z_0}\right) \cdot c_o\right)^2 \cdot q_b$

Characteristic peak wind pressure when kp is three

$q_f(z) := \frac{q_p(z)}{q_{p2}(z)}$

Coefficient to determine the pressure difference

$A_{ref} := b \cdot h$

Reference area

$I_{vz} := \frac{1}{c_o \cdot \ln\left(\frac{z_s}{z_0}\right)} = 0.2$

Turbulence intensity at reference height zs

$c_s c_d := \frac{1 + 2 \cdot k_p \cdot I_{vz} \cdot \sqrt[2]{B^2 + R^2}}{1 + 6 \cdot I_{vz}} = 1.117$

Structural factor

$Z := \frac{h}{b} = 3.44$

$y_1 := -0.7 \qquad y_0 := -0.5$

$x_1 := 5 \qquad x_0 := 1$

Interpolating the external pressure coefficient

$svar := y_0 + \left(Z - x_0\right) \cdot \frac{\left(y_1 - y_0\right)}{\left(x_1 - x_0\right)} = -0.622$

$1.5 \cdot c_s c_d \cdot 1.15 \cdot svar = -1.199$

$1.5 \cdot c_s c_d \cdot 1.15 \cdot 0.8 = 1.542$

Final coefficients for loads in FEM-Design

Service Limit State:

$$v_s := 0.75 \cdot v_b \cdot \sqrt[2]{1 - 0.2 \cdot \ln\left(-1 \cdot \ln\left(1 - \frac{1}{T_a}\right)\right)} = 19.425 \ \frac{m}{s}$$

$$v_{s5} := v_s = 19.425 \ \frac{m}{s}$$ Five years' wind velocity

$$v_{ms5} := c_r \cdot c_o \cdot v_{s5} = 23.102 \ \frac{m}{s}$$ Characteristic mean wind velocity

$$y_{cs} := \frac{150 \cdot n_{1.x}}{v_{ms5}} \cdot m = 3.909$$ Non-dimensional frequency

$$F_s := \frac{4 \cdot y_{cs}}{\left(1 + 70.8 \cdot {y_{cs}}^2\right)^{\frac{5}{6}}} = 0.0463$$ Karmans wind energy spectrum

$$\phi_{hs} := \frac{1}{1 + \frac{2 \cdot n_{1.x} \cdot h}{v_{ms5}}} = 0.204$$ Size factor concerning the height of the building

$$\phi_{bs} := \frac{1}{1 + \frac{3.2 \cdot n_{1.x} \cdot b}{v_{ms5}}} = 0.355$$ Size factor concerning the width of the building

$$v_{mzs} := c_{rz} \cdot c_o \cdot v_{s5} = 20.964 \ \frac{m}{s}$$ Characteristic mean velocity for reference height zs

$$\delta_{azs} := \frac{c_f \cdot \rho \cdot b \cdot v_{mzs}}{2 \cdot n_{1.x} \cdot m_e} = 0.004$$ Average decrement of damping

$$R_s := \sqrt[2]{\frac{2 \cdot \pi \cdot F_s \cdot \phi_{bs} \cdot \phi_{hs}}{\delta_s + \delta_{azs}}} = 0.473$$ Resonance response

$$I_{v1} := \frac{1}{c_o \cdot \ln\left(\frac{h}{z_0}\right)} = 0.181$$ Turbulence intensity for the entire height of the building

$$q_{ms} := 0.5 \cdot \rho \cdot {v_{ms5}}^2 = 333.55\ \boldsymbol{Pa}$$

$$\phi_{1.x}(z) := \left(\frac{z}{h}\right)^{1.5}$$

Mode shape function

$$\sigma_x(z) := \frac{3 \cdot I_{v1} \cdot R_s \cdot q_{ms} \cdot b \cdot c_f \cdot \phi_{1.x}(z)}{m_e}$$

Standard deviation of acceleration

$$\sigma_x(h) = 0.016\ \frac{\boldsymbol{m}}{\boldsymbol{s}^2}$$

$$X_{max}(z) := k_p \cdot \sigma_x(z)$$

Maximum acceleration

$$X_{max}(h) = 0.05587\ \frac{\boldsymbol{m}}{\boldsymbol{s}^2}$$

Limits for acceleration:

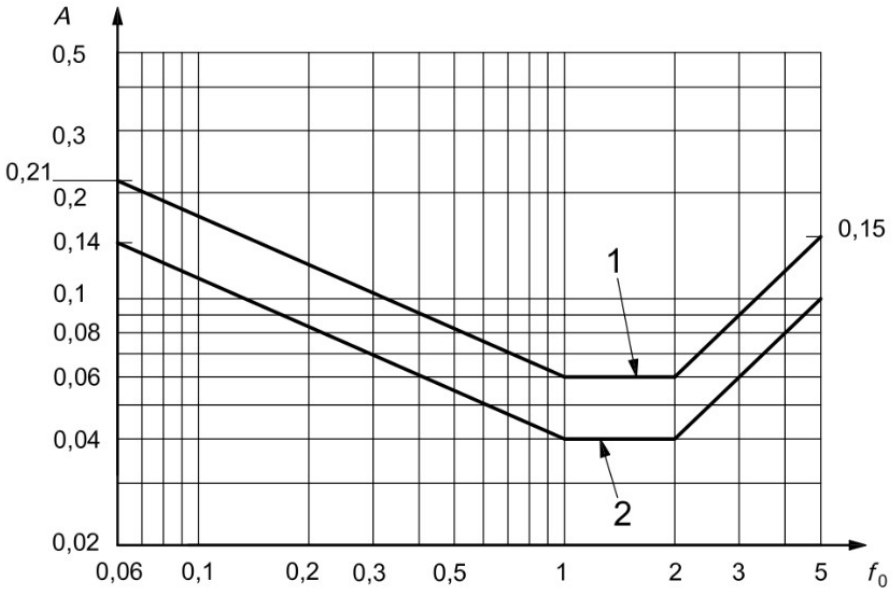

Plots:

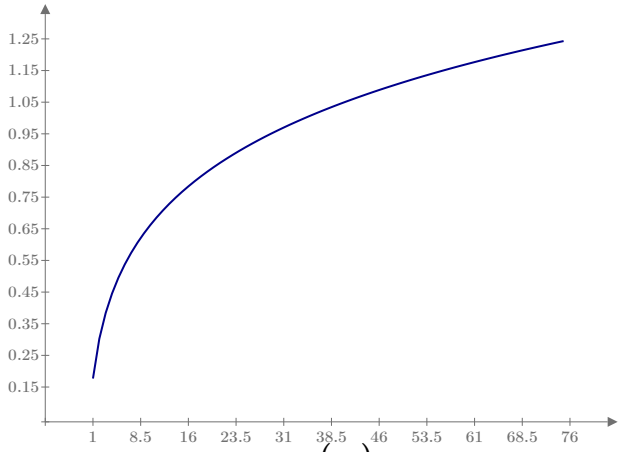

$q_p(z)\ (kPa)$

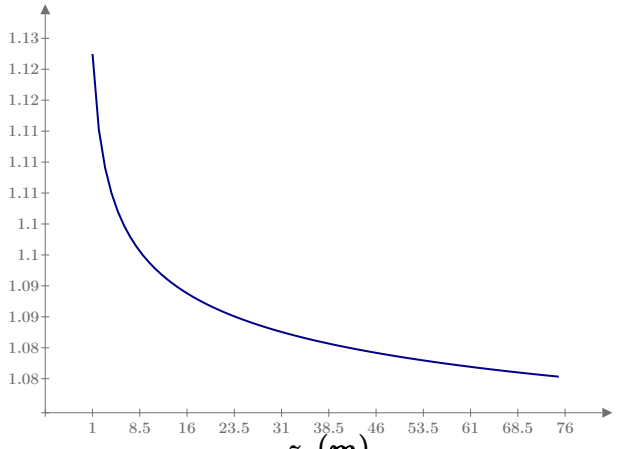

$q_f(z)$

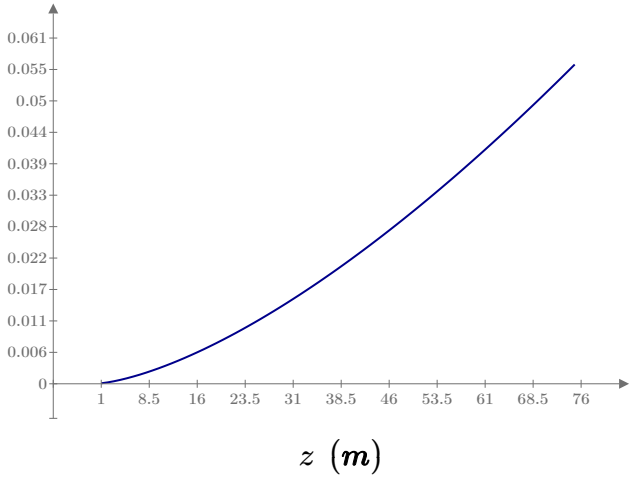

$X_{max}(z)\ \left(\frac{m}{s^2}\right)$

TP.32
Maximum of load combinations

Project		Scale	
Description		File name	
Designer		Date/Time	
Signature		Comments	

Geometry

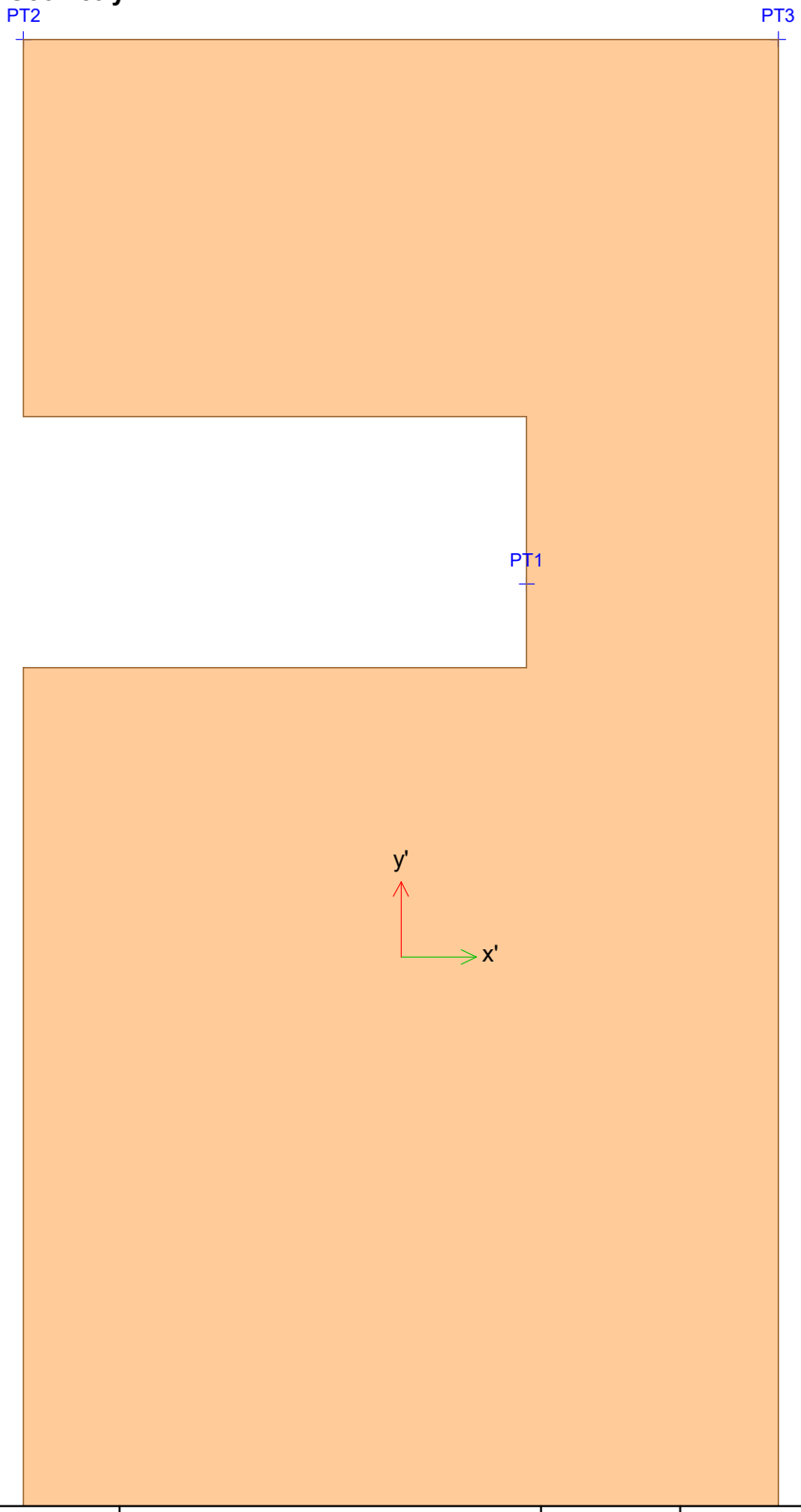

Maximum nodes:
PT1 (6.00, 16.67, 2.00) [m]
PT2 (6.00, 14.50, 0.00) [m]
PT3 (6.00, 14.50, 3.00) [m]

Node numbers:
PT1: 272868
PT2: 264705
PT3: 264785

Panel type:
280-7s

Total thickness:
t = 280.00 mm

Project		Scale	
Description		File name	
Designer		Date/Time	
Signature		Comments	

Panel properties

Service class: 1, $\gamma_{M,ult.}$ = 1.25, $\gamma_{M,acc./seis.}$ = 1.00, k_{sys} = 1.00

No	Material	Thickness [mm]	Θ [°]	ρ [kg/m^3]
1	C24	40	0	420
2	C14	40	90	350
3	C24	40	0	420
4	C14	40	90	350
5	C24	40	0	420
6	C14	40	90	350
7	C24	40	0	420

Mechanical properties

No	$E_{0,mean}$ [N/mm^2]	$E_{90,mean}$ [N/mm^2]	v_{xy} [-]	$G_{xy,mean}$ [N/mm^2]	$G_{xz,mean}$ [N/mm^2]
1	11000	0	0.00	690	690
2	7000	0	0.00	440	440
3	11000	0	0.00	690	690
4	7000	0	0.00	440	440
5	11000	0	0.00	690	690
6	7000	0	0.00	440	440
7	11000	0	0.00	690	690

No	$G_{yz,mean}$ [N/mm^2]
1	69
2	44
3	69
4	44
5	69
6	44
7	69

Mechanical properties - 5% quantile values

No	$E_{0,05}$ [N/mm^2]	$E_{90,05}$ [N/mm^2]	$G_{xy,05}$ [N/mm^2]	$G_{xz,05}$ [N/mm^2]	$G_{yz,05}$ [N/mm^2]
1	9240	0	580	580	58
2	5880	0	370	370	37
3	9240	0	580	580	58
4	5880	0	370	370	37
5	9240	0	580	580	58
6	5880	0	370	370	37
7	9240	0	580	580	58

Limit stresses

No	$f_{m,0,k}$ [N/mm^2]	$f_{m,90,k}$ [N/mm^2]	$f_{t,0,k}$ [N/mm^2]	$f_{t,90,k}$ [N/mm^2]	$f_{c,0,k}$ [N/mm^2]	$f_{c,90,k}$ [N/mm^2]
1	24.0	24.0	14.5	0.400	21.0	2.50
2	14.0	14.0	7.20	0.400	16.0	2.00
3	24.0	24.0	14.5	0.400	21.0	2.50
4	14.0	14.0	7.20	0.400	16.0	2.00
5	24.0	24.0	14.5	0.400	21.0	2.50
6	14.0	14.0	7.20	0.400	16.0	2.00
7	24.0	24.0	14.5	0.400	21.0	2.50

No	$f_{xy,k}$ [N/mm^2]	$f_{v,k}$ [N/mm^2]	$f_{vR,k}$ [N/mm^2]	$f_{tor,k}$ [N/mm^2]
1	4.00	4.00	2.00	2.50
2	3.00	3.00	1.50	2.50
3	4.00	4.00	2.00	2.50
4	3.00	3.00	1.50	2.50
5	4.00	4.00	2.00	2.50
6	3.00	3.00	1.50	2.50
7	4.00	4.00	2.00	2.50

Tension and bending, x - 6.2.3

Panel: 'TP.32.1', Layer: '2', LC: 'ULS 1', k_{mod} = 0.90, PT1

$$\frac{\sigma_{t,0,d}}{f_{t,0,d}} + \frac{|\sigma_{m,0,d}|}{f_{m,0,d}} = \frac{0.73}{5.18} + \frac{|-0.00|}{10.08} = 0.14 \leq 1.00 \quad (6.17) - OK$$

Tension and bending, y - 6.2.3

Not relevant

Compression and bending, x - 6.1.4, 6.2.4

Panel: 'TP.32.1', Layer: '1', LC: 'ULS 1', k_{mod} = 0.90, PT2

$$\frac{|\sigma_{c,0,d}|}{f_{c,0,d}} = \frac{|-10.42|}{15.12} = 0.69 \leq 1.00 \quad (6.2) - OK$$

$$\left(\frac{\sigma_{c,0,d}}{f_{c,0,d}}\right)^2 + \frac{|\sigma_{m,0,d}|}{f_{m,0,d}} = \left(\frac{-10.42}{15.12}\right)^2 + \frac{|0.00|}{17.28} = 0.48 \leq 1.00 \quad (6.19) - OK$$

Compression and bending, y - 6.1.4, 6.2.4

Not relevant

Shear, xy - 6.1.7

Panel: 'TP.32.1', Layer: '1', LC: 'ULS 1', k_{mod} = 0.90, PT2

$$\frac{|\tau_{xy,d}|}{f_{xy,d}} = \frac{|-1.26|}{2.88} = 0.44 \leq 1.00 \quad (6.13) - OK$$

Shear, xz - 6.1.7

Panel: 'TP.32.1', Layer: '4', LC: 'ULS 1', k_{mod} = 0.90, PT3

$$\frac{|\tau_{xz,d}|}{f_{v,d}} = \frac{|-0.02|}{2.16} = 0.01 \leq 1.00 \quad (6.13) - OK$$

Shear, yz - 6.1.7

Panel: 'TP.32.1', Layer: '3', LC: 'ULS 1', k_{mod} = 0.90, PT3

$$\frac{|\tau_{yz,d}|}{f_{R,d}} = \frac{|-0.02|}{1.44} = 0.01 \leq 1.00 \quad (6.13) - OK$$

Shear interaction

Panel: 'TP.32.1', Layer: '1', LC: 'ULS 1', k_{mod} = 0.90, PT2

$$\left(\frac{\tau_{xy,d}}{f_{xy,d}}\right)^2 + \left(\frac{\tau_{xz,d}}{f_{v,d}}\right)^2 = \left(\frac{-1.26}{2.88}\right)^2 + \left(\frac{0.00}{2.88}\right)^2 = 0.19 \leq 1.00 - OK$$

Tension and shear

Panel: 'TP.32.1', Layer: '3', LC: 'ULS 1', k_{mod} = 0.90, PT3

$$\frac{\sigma_{t,90,d}}{f_{t,90,d}} + \frac{|\tau_{yz,d}|}{f_{R,d}} = \frac{0.00}{0.29} + \frac{|-0.02|}{1.44} = 0.01 \leq 1.00 \text{ - OK}$$

Compression and shear

Panel: 'TP.32.1', Layer: '3', LC: 'ULS 1', k_{mod} = 0.90, PT3

$$\frac{|\sigma_{c,90,d}|}{f_{c,90,d}} + \frac{|\tau_{yz,d}|}{f_{R,d}} = \frac{|0.00|}{1.80} + \frac{|-0.02|}{1.44} = 0.01 \leq 1.00 \text{ - OK}$$

Buckling

Not relevant

Torsion

Not relevant

Summary

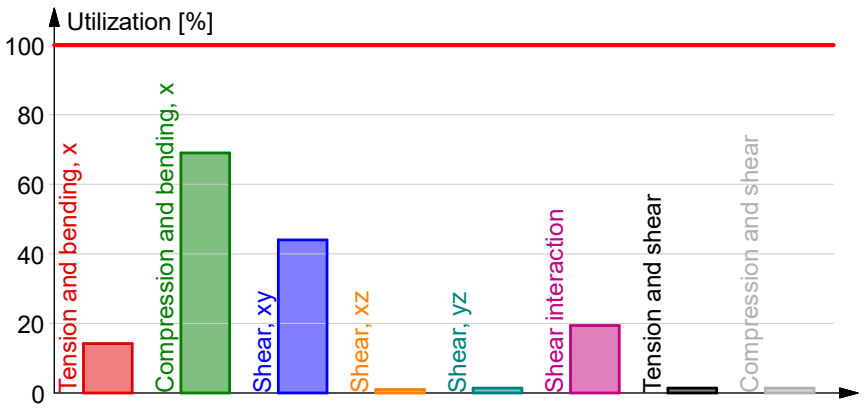

Project		Scale	
Description		File name	
Designer		Date/Time	
Signature		Comments	

C.38.1
Maximum of load combinations

GL 30c

(Glued laminated), Service class 1

$E_{0,05}$	=	10800 N/mm^2	$f_{t,90,k}$	=	0.50 N/mm^2
$G_{0,05}$	=	540 N/mm^2	$f_{c,0,k}$	=	24.50 N/mm^2
γ_M	=	1.25	$f_{c,90,k}$	=	2.50 N/mm^2
$\gamma_{M,acc./seis.}$	=	1.00	$f_{v,k}$	=	3.50 N/mm^2
k_{sys}	=	1.00			

Glulam 215x450

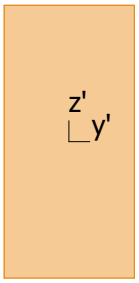

A	=	96750 mm^2	$f_{t,0,k}$	=	20.07 N/mm^2
W_1	=	7.256e+06 mm^3	$f_{m,1,k}$	=	30.88 N/mm^2
W_2	=	3.467e+06 mm^3	$f_{m,2,k}$	=	33.00 N/mm^2
i_1	=	130 mm			
i_2	=	62 mm			
I_2	=	3.727e+08 mm^4			
I_t	=	1.043e+09 mm^4			

Combined bending and axial tension - 6.2.3

Not relevant

Combined bending and axial compression - 6.1.4, 6.2.4

LC: 'ULS 2', k_{mod} = 0.90, x = 0.00 mm

$$\frac{\sigma_{c,0,d}}{f_{c,0,d}} = \frac{10.92}{17.64} = 0.62 \leq 1.00 \quad (6.2) \text{ - OK}$$

$$\left(\frac{\sigma_{c,0,d}}{f_{c,0,d}}\right)^2 + \frac{\sigma_{m,1,d}}{f_{m,1,d}} + k_m \frac{\sigma_{m,2,d}}{f_{m,2,d}} =$$

$$= \left(\frac{10.92}{17.64}\right)^2 + \frac{0.00}{22.23} + 0.70\,\frac{0.00}{23.76} = 0.38 \leq 1.00 \quad (6.19) \text{ - OK}$$

$$\left(\frac{\sigma_{c,0,d}}{f_{c,0,d}}\right)^2 + k_m \frac{\sigma_{m,1,d}}{f_{m,1,d}} + \frac{\sigma_{m,2,d}}{f_{m,2,d}} =$$

$$= \left(\frac{10.92}{17.64}\right)^2 + 0.70\,\frac{0.00}{22.23} + \frac{0.00}{23.76} = 0.38 \leq 1.00 \quad (6.20) \text{ - OK}$$

Combined shear and torsion - 6.1.7, 6.1.8

LC: 'ULS 1', k_{mod} = 0.90, x = 0.00 mm

$\tau_d = 0.00\ N/mm^2 \leq f_{v,d} = 2.52\ N/mm^2$ (6.13) - OK

Flexural buckling around axis 1 - 6.3.2

LC: 'ULS 2', k_{mod} = 0.90, x = 0.00 mm

$\beta_c = 0.1$ (6.29)

$$\lambda_1 = \frac{l_0}{i_1} = \frac{3500}{130} = 26.94$$

$$\lambda_{rel,1} = \frac{\lambda_1}{\pi}\sqrt{\frac{f_{c,0,k}}{E_{0,05}}} = \frac{26.94}{\pi}\sqrt{\frac{24.50}{10800}} = 0.408 \quad (6.21)$$

$$k_1 = 0.5\left(1 + \beta_c\left(\lambda_{rel,1} - 0.3\right) + \lambda_{rel,1}^{\ 2}\right) =$$

$$= 0.5\left(1 + 0.1\left(0.408 - 0.3\right) + 0.408^2\right) = 0.589 \quad (6.27)$$

$$k_{c,1} = \frac{1}{k_1 + \sqrt{k_1^{\ 2} - \lambda_{rel,1}^{\ 2}}} = \frac{1}{0.589 + \sqrt{0.589^2 - 0.408^2}} = 0.987 \quad (6.25)$$

$$\frac{\sigma_{c,0,d}}{k_{c,1} \cdot f_{c,0,d}} + \frac{\sigma_{m,1,d}}{f_{m,1,d}} + k_m \cdot \frac{\sigma_{m,2,d}}{f_{m,2,d}} =$$

$$= \frac{10.92}{0.987 \cdot 17.64} + \frac{0.00}{22.23} + 0.70 \cdot \frac{0.00}{23.76} = 0.63 \leq 1.00 \quad (6.23) \text{ - OK}$$

Flexural buckling around axis 2 - 6.3.2

LC: 'ULS 2', k_{mod} = 0.90, x = 0.00 mm

β_c = 0.1 (6.29)

$$\lambda_2 = \frac{l_0}{i_2} = \frac{3500}{62} = 56.39$$

$$\lambda_{rel,2} = \frac{\lambda_2}{\pi}\sqrt{\frac{f_{c,0,k}}{E_{0,05}}} = \frac{56.39}{\pi}\sqrt{\frac{24.50}{10800}} = 0.855 \quad (6.22)$$

$$k_2 = 0.5\left(1 + \beta_c\left(\lambda_{rel,2} - 0.3\right) + \lambda_{rel,2}^{\ 2}\right) =$$

$$= 0.5\left(1 + 0.1\left(0.855 - 0.3\right) + 0.855^2\right) = 0.893 \quad (6.28)$$

$$k_{c,2} = \frac{1}{k_2 + \sqrt{k_2^{\ 2} - \lambda_{rel,2}^{\ 2}}} = \frac{1}{0.893 + \sqrt{0.893^2 - 0.855^2}} = 0.868 \quad (6.26)$$

$$\frac{\sigma_{c,0,d}}{k_{c,2} \cdot f_{c,0,d}} + k_m \cdot \frac{\sigma_{m,1,d}}{f_{m,1,d}} + \frac{\sigma_{m,2,d}}{f_{m,2,d}} =$$

$$= \frac{10.92}{0.868 \cdot 17.64} + 0.70 \cdot \frac{0.00}{22.23} + \frac{0.00}{23.76} = 0.71 \leq 1.00 \quad (6.24) \text{ - OK}$$

Lateral torsional buckling - 6.3.3

Not relevant

Bending at apex - 6.4.3

Not relevant

Tension at apex - 6.4.3

Not relevant

Summary

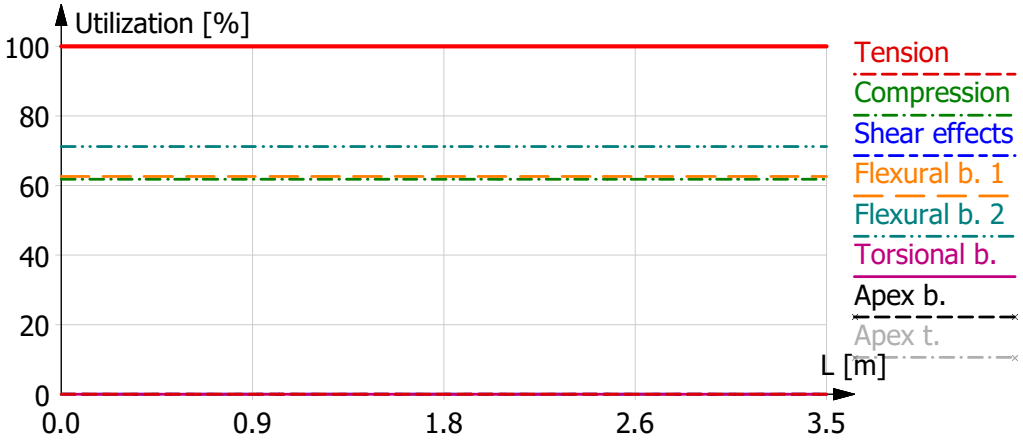

Project		Scale	
Description		File name	
Designer		Date/Time	
Signature		Comments	

DEPARTMENT OF ARCHITECTURE AND CIVIL ENGINEERING
CHALMERS UNIVERSITY OF TECHNOLOGY
Gothenburg, Sweden 2024
www.chalmers.se

CHALMERS
UNIVERSITY OF TECHNOLOGY